A STRIPLINE ANTENNA FOR RADIATED IMMUNITY TESTING

Francisçus Jozua van Dam

EWI
TELECOMMUNICATION ENGINEERING

EXAMINATION COMMITTEE
Prof. Dr. Ir. ing. F.B.J. Leferink
Dr. Ir. M.J. Bentum
Ir. J. Schipper

THALES

UNIVERSITY OF TWENTE.

27-10-2011

Summary

The use of different radiating structures for radiated susceptibility test Electromagnetic Compatibility (EMC)is a field of ongoing research. Especially with relative long wave lengths for frequencies between 2-30 MHz in the confined space of an anechoic chamber which is used to test for radiated susceptibility it is not easy to generate a strong and uniform electric field for large pieces of equipment. The main question in this research was to see whether it was possible to build a large stripline antenna for the testing of pieces of equipment of roughly 2.0m high, combined with a high field strength of 200 V/m when using a 2.5kW amplifier.

Small stripline antennas have been internationally standardized for EMC testing for small components or wire bundles in the automotive industry in the ISO 11452-5. In this research available literature has been studied and stripline antennas have been simulated with computational electromagnetics software. Furthermore experiments with scale models in an anechoic chamber have been performed. Stripline antenna impedance depends heavily on the width/height. In order to keep the stripline antenna physically realizable with in the anechoic chamber, stripline antennas for input impedances greater than 50Ω have been simulated and tested in practice.

Impedances of 200Ω and 100Ω have been transformed to 50Ω using ferrite core based unbalanced to unbalanced transmission line transformers of the Ruthroff type.

Results of these experiments have led to a possible solution in the form of a wire stripline antenna with an impedance of 100Ω. The S11 parameter is -10 dB or better over a frequency range from 2 to 30 MHz.

Samenvatting

Het gebruik van verschillende structuren voor het doen van testen met betrekking tot de stralingsgevoeligheid binnen de Elektromagnetische Compatibiliteit is een veld van continu onderzoek. De lange golflengten voor de lage frequenties in het gebied van 2 tot 30 MHz in de beperkte ruimte van een semi anechoische ruimte welke gebruikt wordt voor het doen van stralingsgevoeligheid maken het lastig om een sterk en uniform elektrisch veld te genereren. De hoofdvraag voor dit onderzoek was of het mogelijk is om een grote stripline antenne te bouwen voor apparatuur met een hoogte van 2.0m in combinatie met een veldsterkte van 200 V/m waarbij een 2.5 kW versterker wordt gebruikt.

Kleine stripline antennes zijn internationaal gestandaardiseerd voor het testen van kleine componenten of draadbundels in de auto-industrie in de ISO 11452-5 standaard. In dit onderzoek is de aanwezige literatuur bestudeerd en zijn stripline antennes gesimuleerd met speciale software welke geschikt is voor het berekenen van elektromagnetische velden. Verder zijn experimenten gedaan met schaalmodellen in de anechoische ruimte.
Gezien de afhankelijkheid van de hoogte en breedte verhoudingen voor de antenne impedantie zijn er testen gedaan met impedanties van 50Ω, 100 Ω en 200 Ω welke zijn gesimuleerd en getest in de praktijk.

Impedanties van 200Ω en 100Ω zijn getransformeerd naar een impedantie van 50Ω doormiddel van ongebalanceerde transmissielijn transformatoren met ferriet kernen van het Ruthroff type.

Resultaten van deze experimenten hebben geleid tot een mogelijke oplossing in de vorm van een stripline antenne met een impedantie van 100Ω of 200Ω. De reflectiecoëfficiënt van de ontworpen 100Ω stripline antenne is beter of gelijk aan -10dB in het frequentiegebied van 2 tot 30 MHz.

Table of contents

Table of figures

List of abbreviations

AWG	American Wire Gauge, measure for the diameter of wire
Balun	Balanced to unbalanced impedance transformer for transmission lines
BEM	Boundary Element Method, a method used to solve Maxwell's equations.
CEM	Computational Electromagnetics, solving Maxwell's equations in a numerical manner with the help of software.
ECC	Environmental Competence Centre, shock, climate and EMC testing department at Thales Hengelo.
EMC	Electromagnetic Compatibility, the ability of equipment to function satisfactorily in its electromagnetic environment without introducing intolerable electromagnetic disturbances to other equipment in that environment
EMI	Electromagnetic Interference
EUT	Equipment Under Test
FEM	Finite Element Method, a way to solve differential equations
MoM	Method of Moments, also known as Boundary Element Method.
RF	Radio Frequency, range between 30 kHz and 300 GHz.
RS	Radiated Susceptibility
R&S	Rohde & Schwarz
SAE	Society of Automotive Engineers in the United States
SEC1	Semi anechoic chamber with a conducting ground plane
SEC2	Fully anechoic chamber with an isolated groundplane
SLA	Stripline Antenna
TEM cell	Transverse Electromagnetic waveguide used to perform EMC measurements.
TL	Transmission Line
TLT	Transmission Line Transformer
VNA	Vector Network Analyzer

Unun	Unbalanced to unbalanced impedance transformer for transmission lines
Wdg	Windings
W.E.	Würth Elektronik

Chapter 1 Introduction

In this chapter the context of this thesis project is presented: “A stripline antenna for radiated susceptibility”. Next the stripline antenna is given its place in the environment which is electromagnetic compatibility testing. Second the need for radiated susceptibility testing is explained. Subsequently the requirements for the electric field that is to be generated with the stripline antenna are presented. Finally the structure of this thesis can be found in the last paragraph.

1.1 Stripline antennas

A stripline antenna is a radiating transmission line structure. The stripline antenna functions in such a way that the electromagnetic (EM) waves that are being send trough the transmission line produce a strong electric field. This field stands between the two different planes of the stripline antenna. Because the stripline is a Transverse Electromagnetic transmission line the magnetic and the electric field are orthogonal in phase and the amplitude difference is 120π (377)Ω. So if the the electric field strength in known, the magnetic field is also defined. Therefor the electric field will be used in the further discussion. In Fig 1.1 it can be seen that the upper plane is the actual radiator from where electric field is radiated to the bottom plane which is the ground plane.

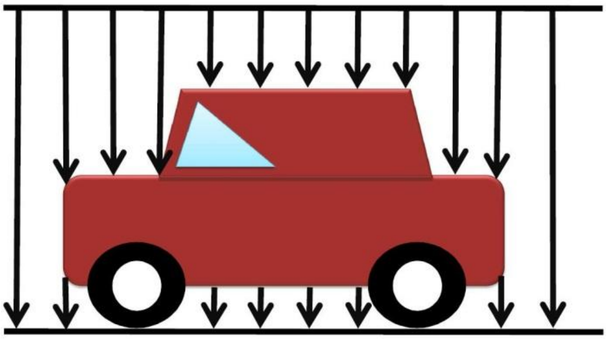

Fig 1.1, Radiated electric field

This electric field can be used to test the ability of electronic equipment to withstand strong electric fields. These electric fields are radiated by all kinds of transmitters e.g. radio stations, radar systems, or cell phones.
Most of the energy that is sent to the stripline antenna from the generator is actually passing through the stripline antenna and then fed into a dummy load to absorb the transmitted power.

1.2 About electromagnetic compatibility

Nearly every piece of equipment used these days is somehow controlled by electronic circuits or embedded computers. All these systems interact with their surroundings.
One of the ways they can interact in an unwanted manner is by picking up electromagnetic emissions from other equipment. An example of this is the pulsating noise made by a cellular phone that is audible through speakers pulsing in the rhythm of the transmissions.

The science of the way in which electronic systems interact with each other in an unwanted manner is called Electromagnetic Compatibility (EMC).
This field of electrical and electronic engineering came up after World War II and continues today to make sure that military equipment keeps working under wartime conditions with enemy action in mind.
Since 1996 the EC in Europe also places EMC requirements on nearly every electronic device for consumers or industrial applications that brought on the market.
Within EMC there are four distinguished types in which systems can interact:

1. Conducted Emission: The signals that are coming from electronic equipment through the connecting cables in Fig 1.2.

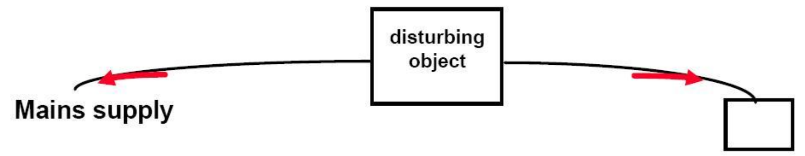

Fig 1.2, Conducted Emission

2. Conducted Susceptibility: The signals that are influencing electronic equipment are transmitted through the connected cables in Fig 1.3.

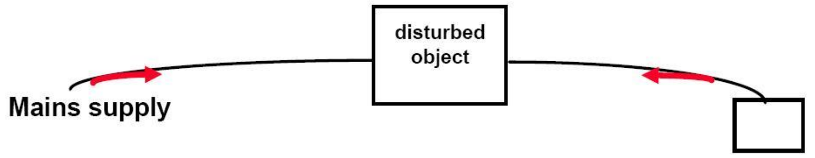

Fig 1.3, Conducted Susceptibility

3. Radiated Emission: Unwanted emission of electromagnetic waves coming from electronic equipment radiating outwards to other equipment or the environment in Fig 1.4.

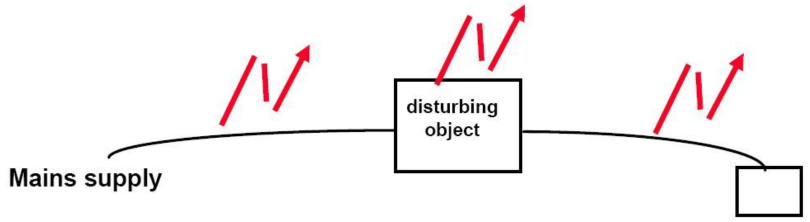

Fig 1.4, Radiated Emission

4. Radiated Susceptibility (RS): Unwanted electromagnetic waves entering the equipment from the outside in Fig 1.5.

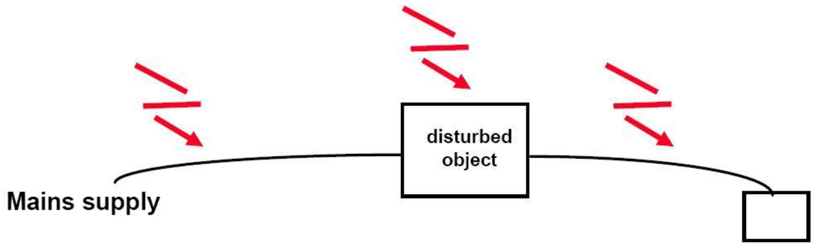

Fig 1.5, Radiated Susceptibility

A way to make sure that equipment functions as intended is by testing the equipment in an open air test site or and anechoic chamber without any other source of interference nearby.

1.3 The need for radiated susceptibility testing

There are two names for radiated susceptibility testing, the other commonly used term is radiated immunity testing. The first name is mainly seen in American and Military documents [**1**], the latter is more common in European EMC directives [**2**].

As already mentioned in 1.2, radiated susceptibility testing is done to check whether the device under test keep functioning when a strong electromagnetic field is radiated onto the device.
One of the main reasons this testing for commercial purposes is done is to make sure that the customer can use equipment bought in a shop inside their homes without any interference from other devices.
In the light of new electric cars and more and more electronic sensors and equipment in cars one can understand the necessity to test cars since no one would want a car to cause harm to other traffic when it would increase speed, break or veer of track when a nearby transmitter is activated.

1.4 Requirements for the generated electric field

One of the challenges in radiated susceptibility testing is to create an electric field that is both uniform in shape and has a field strength of 200 V/m for the frequency range 2-30 MHz with relative low power.
The antenna currently used at the ECC to test EUT’s for the frequency range between 2-30 MHz is the AT3000 from Amplifier Research.
This antenna has a width of 1.90m and uses coils to lengthen the antenna from an electromagnetic point of view.
In order to be able to test equipment wider than 1.90m wide the electric field generator currently used at the ECC is for the frequency range 2- 30 MHz is not sufficient to test the whole piece of equipment under test (EUT) at once.
If the equipment can’t be tested in one run the EUT has to be tested from multiple positions this can be seen in Fig 1.6
When these multiple positions are used it is not guarantee the high strength of the electromagnetic field at all instances.

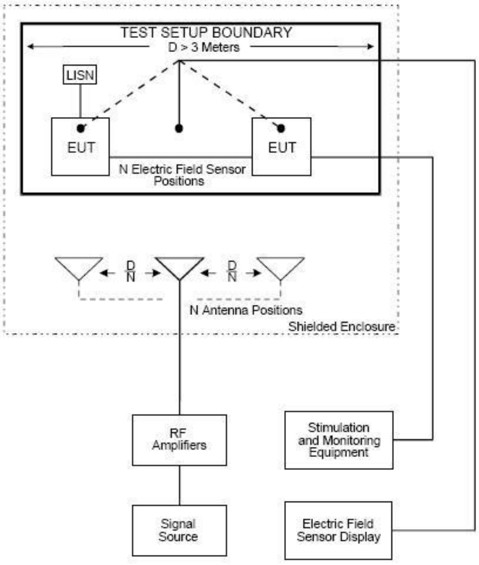

Fig 1.6, Testing with multiple antenna positions [1]

Testing with multiple antennas is not only cumbersome from a time point of view but also poses the hazard of equipment that might fail when exposed to strong electromagnetic fields over the entire device at the same time.

A normal half wavelength dipole antenna would have a length of 75m at a frequency of 2 MHz or a length of 5m at 30 MHz both are impractically large for indoor testing and would require adaptation with changing frequencies.
Other, broader band, transmission line like solutions that exist for radiated susceptibility testing are TEM-cells, Tri-plates and stripline antennas.
Each of these three have their different strengths and drawbacks which can be found in chapters 2 and 3.
The stripline antenna has been used in the past for EMC internationally standardized testing in the automotive industry to test cable bundles and small components.
Several manufacturers of EMC test equipment also claim to produce stripline antenna like devices for EMC testing which require up to 5 or 10 kW of power fed into the stripline antenna to reach an electric field strength of 200 V/m.
In the light of these findings the research question for a stripline antenna (SLA) for large EUT's was posed as follows:

"Can a sufficient radiating stripline antenna be built such that it produces a uniform electric field with the limits of the applicable standard of 200 V/m over the frequency range of 2 – 30 MHz with the input from a 2.5 kW amplifier output?
If so, is it possible to test EUT's with a height up to 2.0m high and what are the best dimensions for such a device?"

Fig 1.7, EUT under a stripline antenna

1.5 Structure of this thesis

The outline of this thesis is as follows. First the behavior of the electromagnetic field and TEM cells and Tri-plates is described in Chapter 2.
The stripline antenna theory and literature study comprise Chapter 3, Impedance Matching is found in Chapter 4, Computational Electromagnetics and stripline antenna model used in the simulations in and verification are found in Chapter 5. Experiments and measurements with stripline antenna antennas can be found in chapter 6-9. The conclusion and recommendations can be found in Chapter 10.

Chapter 2 Electromagnetic waves and transmission lines

In this chapter propagation of electromagnetic waves (EM) in TM, TE, TEM and Quasi-TEM modes is quickly reviewed for rectangular waveguides, cavity modes. and transmission lines. After this the scattering parameters, the reflection coefficient, the standing wave ratio and the return loss are explained which are used to estimate stripline antenna (SLA) performance. In the last two paragraphs TEM cells and Tri-plates are treated, these are in some cases comparable to SLA's and also used to perform Radiated Susceptibility (RS) tests.

One important aspect to keep in mind is that a lot of the behavior of EM waves depends on the wavelength. The formula for the free space wavelength λ in m is:

$$\lambda = \frac{c}{f} \tag{2.1}$$

Where c is equal to speed of light in free space $c = 2.998 \times 10^8$ m/s, f is the frequency in Hertz.

2.1 TM and TE waves

Electromagnetic waves can propagate in three different ways, by TE, TM, TEM and Quasi-TEM mode. The derivations of these electromagnetic wave properties can be found in many different books such as [**3**].
Quasi-TEM is transmission mode that looks like TEM in its behavior but is actually has very small E and H components in the direction of propagation.
These small E and H components make that the pure TEM solution does not exist but that the solution is a hybrid of TE and TM modes [**3**].
For a TEM mode at least two conductors are required, for TE and TM mode a single conductor like a waveguide can be sufficient [**3**].

2.2 Transmission Line Parameters and TEM propagation

Transmission Lines are made up of two conductors where current and voltage waves propagate between both conductors. The simplest of these consists of two parallel wires with a length of Δz.

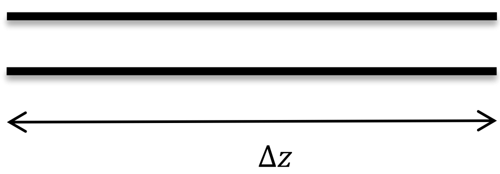

Fig 2.1, Simple Transmission Line

For short pieces of transmission line the properties of the transmission line can be given in lumped element which are an inductor, capacitor, resistor and a conductor each with their respective unit per meter such is shown in Fig 2.2.

The resistor R and the conductor G represent the ohms resistance and admittance.

The L and C components represent the inductive L and capacitive properties C of the transmission line which are the cause of the impedance of a transmission line at high frequencies.

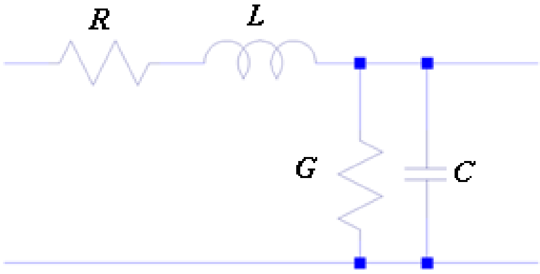

Fig 2.2, Lumped transmission line model

All properties from R, L, G and C are here in their respective unit length parameters.
With Kirchoff's law [**3**] these parameters can again be expressed in wave equations for Voltage $V(z)$and Current waves $I(z)$in both the positive and negative z direction.

$$V(z) = V_0^+ e^{-\gamma z} + V_0^- e^{\gamma z} \tag{2.4}$$

$$I(z) = I_0^+ e^{-\gamma z} + I_0^- e^{\gamma z} \tag{2.5}$$

Here the $V_0^+ e^{-\gamma z}$and $V_0^- e^{-\gamma z}$ represent the voltage wave on the $z^+$and z^-direction on the transmission line.
The parameter γ is a complex constant which represents the attenuation due to resistive losses from R and G and frequency dependent losses due to L and C.

$$\gamma = \alpha + j\beta \tag{2.6}$$

The frequency dependent part β can also be expressed as a combination of the L, C and ω.

$$\beta = j\omega\sqrt{LC} \tag{2.7}$$

The R and G parameter are independent of frequency and the inductance of L and the reactance of C are given as impedances.

$$X_L = j\omega L \tag{2.8}$$

$$X_c = \frac{1}{j\omega C} \tag{2.9}$$

The expressions for and the characteristic impedance can be given in terms of the lumped element or as ratio of voltage and current waves like in Ohms law.

$$Z_0 = \sqrt{\frac{R + j\omega L}{G + j\omega C}} = \sqrt{\frac{V_0^+}{I_0^+}} = \sqrt{-\frac{V_0^-}{I_0^+}} \tag{2.10}$$

When not taking into account the very low losses due to the R and G parameters the characteristic impedance can be expressed as the squared ratio of $L$and C.

$$Z_0 \approx \sqrt{\frac{L}{C}} \tag{2.11}$$

2.3 Scattering parameters and the reflection coefficient.

The voltage waves from paragraph 2.3 can also be used to express the difference between incoming and outgoing waves on a transmission line. This ratio is standardized in the form of scattering parameters.
Scattering parameters as can be found in [**3**] and are used to express a relation for currents and voltages at a given port of a network of passive elements like transmission lines and antennas.

$$S_{ij} = \frac{V_i^-}{V_j^+} \tag{2.12}$$

Here V_i^+ is the incident wave sent into the transmission line or device and V_i^-represents the wave reflected by the transmission line.

Fig 2.3, S21 schematic view

The S_{11} parameter is also known as the reflection coefficient Γ [**3**] which describes the amount of the energy that is send through the input port is reflected back to the same input port the and difference between the source impedance Z_0 and the load impedance Z_L.

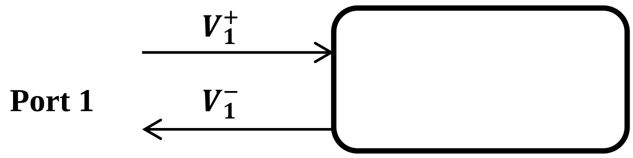

Fig 2.4, S11 Schematic view

$$S_{11} = \Gamma = \frac{V_0^-}{V_0^+} = \frac{Z_L - Z_0}{Z_L + Z_0} \tag{2.13}$$

The difference between the Z_0 and Z_L is also measured as the Voltage Standing Wave Ratio ($VSWR$) or Standing Wave Ratio(SWR).
This $VSWR$ is usually expressed in terms of the reflection coefficient Γ.

$$VSWR = \frac{1 - |\Gamma|}{1 + |\Gamma|} \tag{2.14}$$

When designing transmission lines it is important to keep the S_{11} parameter as small as possible and S_{21} which represents the transferred energy as high as possible.
The proportion of power lost due to reflections is expressed as the return loss RL [**3**].

$$RL = -20\log(\Gamma) \tag{2.15}$$

The return loss represents the amount of the signal that is lost due to the fact that signals are reflected from the one end of the transmission line back to the amplifier.

2.3.1 Limiting the S11 and S21 coefficients

In the scope of the following chapters an S11 coefficient is considered good if the S11 is -10dB or lower than -10 dB e.g. -12 dB or -30 dB. The dB implies that a logarithmic scale is used for the ratio between the forward and backward travelling voltage waves.

$$S_{ij}\ [dB] = 20 \cdot log_{10}(S_{ij}\ lin) \tag{2.16}$$

An S11 of -10 dB means that from the energy that is sent into the SLA only 10% of the energy is reflected back to the transmitter. The main reason for building the SLA is to radiate onto EUT's below the SLA and not to build a lossless high frequency transmission line such as a coaxial cable or a waveguide.

For the very short connections we accept a transmission loss of -1 to -1.5 dB, this accounts for a throughput of 79 to 70 percent of the energy that is transmitted.
For installations with SLA's transmission losses between -4 to -6 dB are realistic, with these losses only 40 to 25 percent of the energy arrives on the other end of the SLA.

2.4 TEM cells

TEM cells are relatively small compared to anechoic chambers and are usually used to test smaller pieces of electronic equipment.
TEM cells are used to test radiated susceptibility electronic equipment which is relatively small over a frequency range from DC to a few hundred MHz for a TEM cell [**4**] or from DC up to 1 GHz for the GTEM cell [**5**].

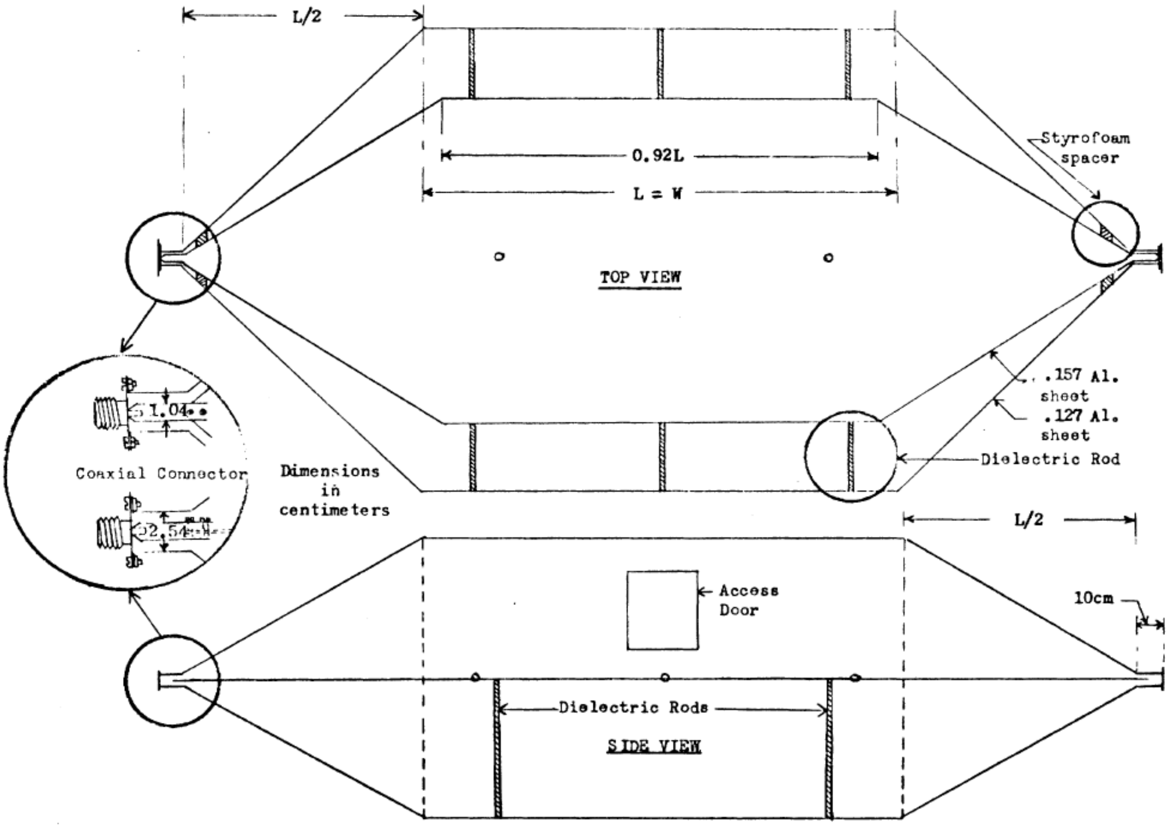

Fig 2.5, Design picture of a TEM cell [4]

A GTEM cell looks similar to a TEM cell but is in fact only the first half of a TEM cell with one wall lined with absorber to prevent cavity resonances at very high frequencies.

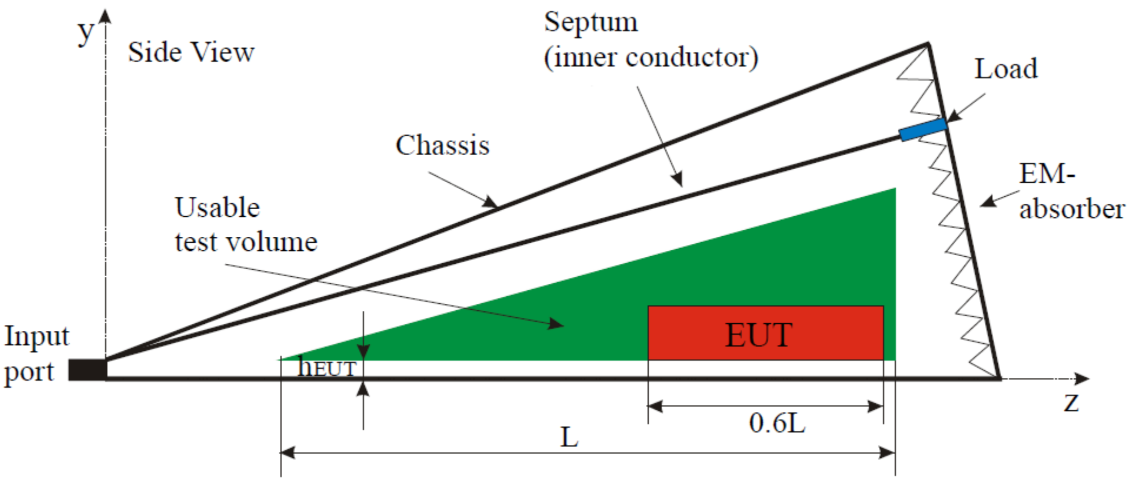

Fig 2.6, GTEM cell side view [6]

2.4.1 Advantages of a TEM cell

A TEM cell is relative broadband over a frequency range from about DC up to 1 GHz for the GTEM cell. In case of a closed TEM cell all electromagnetic radiation stays within the TEM cell so that no anechoic chamber is needed.

2.4.2 Disadvantages of a TEM cell

The height of the septum in a TEM cell decreases the height effective height of the TEM cell as can be seen in Fig 2.6.
The amplitude of the electric field in a TEM cell can vary over a wide range of frequencies in positive and negative manner with wide variations.

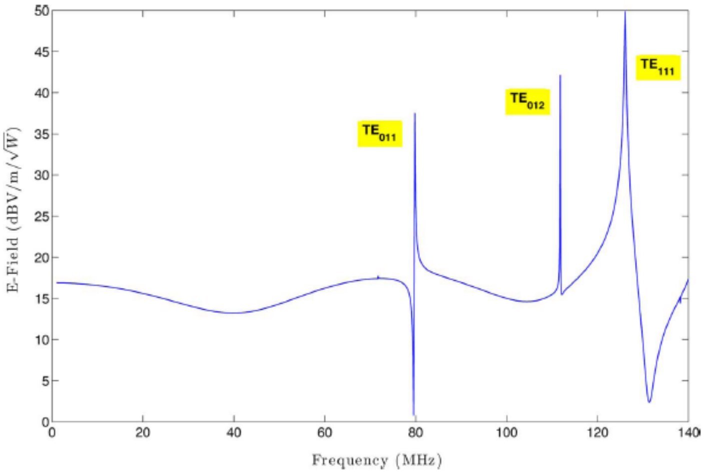

Fig 2.7, Total electric field from a model of the DSTO TEM cell [7]

This behavior is due to resonances for different TE and TM propagation modes in the TEM [7] or GTEM cell [5]. In order to solve the resonances inside TEM cells several experiments have been done but these have not yielded the results needed [8].

2.5 Tri-plates

Tri-plate lines are often named TEM cells
Tri-plates were used in several papers [**9**], [**10**] and [**11**] referring all to the withdrawn SAE J1113/25 standard from the Society of Automotive Engineers in the United States, the standard was cancelled in October 2002 by the SAE.

A Tri-plate has a similar construction to a TEM cell with the differences that it is open from the sides and with a septum conductor through the middle.

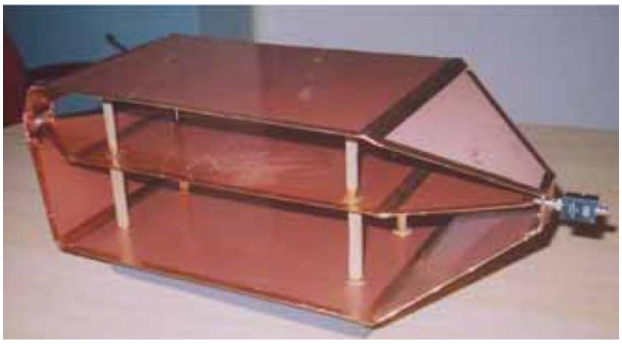

Fig 2.8, Photograpph of the prototype of the open TEM cell [12**]**

Tri-plates have as an advantage that they have less modes in their field field than TEM cells.
The modes that still exist in Tri-plate give no lesser fluctuations than TEM-cells.

Chapter 3 Stripline antenna properties from the literature

This chapter is used to describe all the useful properties from stripline antennas that were found in the literature available. First the microstrip transmission line whose properties closely resemble the SLA is described. Second the stripline antenna properties from the literature are treated.

3.1 Microstrip Transmission Lines

Microstrip Transmission lines are a relatively old and well known type of transmission lines.
In terms of theory these microstrip transmission lines are very similar to stripline antennas that are used for radiated susceptibility (RS) or radiated immunity testing.
Microstrip transmission lines are generally used to guide rf-signals for very high frequencies in the GHz range where they have lower losses than coaxial cable.

The equations for the impedance of a microstrip transmission line as can be found in [**3**] and have been derived by making use of elliptic functions and conformal mapping as can be found in [**13**].

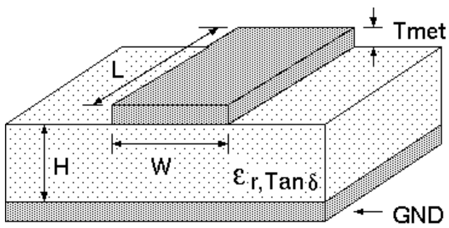

Fig 3.1, Microstrip Transmission Line [14**]**

The effective dielectric constant and impedance equations as have been given in [**3**] are as follows:

$$\varepsilon_e = \frac{\varepsilon_r + 1}{2} + \frac{\varepsilon_r - 1}{2} \frac{1}{\sqrt{1 + 12\frac{H}{W}}} \tag{3.1}$$

For $\frac{W}{H} \leq 1$ the following formula is valid:

$$Z_0 = \frac{60}{\sqrt{\varepsilon_e}} ln\left(\frac{8H}{W} + \frac{W}{4H}\right) \tag{3.2}$$

For $\frac{W}{H} \geq 1$ the following formula is valid:

$$Z_0 = \frac{120\pi}{\sqrt{\varepsilon_e\left[\frac{W}{H} + 1.393 + 0.667\ln(\frac{W}{H} + 1.444)\right]}} \tag{3.3}$$

The changing of width in a TEM transmission lines can be used to match different transmission line impedances and is called tapering.

Different tapers like the Exponential taper, the Triangular taper and Klopfenstein taper can match over a large frequency range but are to long for our application [**3**].

3.2 Stripline antenna properties

Stripline antennas for radiated susceptibility have first been described in an experimental setup in [**15**] in 1965.
More recent experiments were published in [**16**] [**17**] [**18**] and [**19**] which without exception referenced [**20**] for the specification of sizes E-field strength and impedance formula.

3.2.1 Electric Field Strength

The electric field strength is defined in V/m which can be found in [**3**].
The standard equation 3.4 has been given for the strength of the electric field E in Volts per meter, P is the power delivered to the antenna from the generator in Watts, Z is the impedance of the stripline antenna in ohms, and h is the height in meters above the conducting ground plane.

$$|E| = \frac{\sqrt{P \times Z}}{h} \tag{3.4}$$

As can be derived from this formula, a higher impedance would require less power to generate an equal amount of electric field strength.
The required power for the SLA has here been given in Fig 3.2 and Table 3.1 to show the transmitted power necessary to create an electric field of 200 V/m at a certain height.

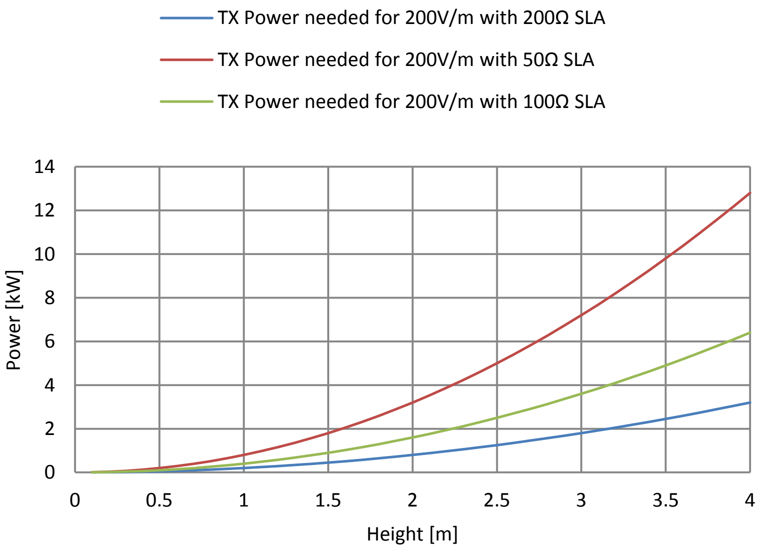

Fig 3.2, Height needed versus power for different impedances

Impedance in ohms	P [kW] 2.0m high	P [kW] 3.0m high	P [kW] 4.0m high
50 Ω	3.20 kW	7.20 kW	12.80 kW
100 Ω	1.60 kW	3.60 kW	6.40 kW
200 Ω	0.80 kW	1.80 kW	3.20 kW

Table 3.1, Power needed for a 200 V/m electric field

With the data from Table 3.1 it is possible to conclude that less power at the input is needed if a higher impedance is used to feed the SLA. For the amplifier that is currently used at Thales with an output of 2.5 kW it is impossible to generate an electric field of 200 V/m at a height of 2.0m with an impedance of 50Ω.

3.2.2 Stripline antenna Impedance

The only equation that was found for the impedance of a stripline antenna for EMC measurements was given in the ISO 11452-5 [**20**] and here displayed as equation 3.6. The ISO 11452-5 is a standard for testing electric components against narrowband electromagnetic interference which uses a predefined narrowband signals in combination with a broadband stripline antenna for a whole frequency range.
As can be seen in equation 3.6 which was given in [**20**] the impedance is mainly dependent on the ratio between height and width of the stripline antenna.

$$Z = \frac{120 \times \pi}{\frac{b}{h} + 2.42 - 0.44 \times \frac{h}{b} + \left(1 - \frac{h}{b}\right)^6} \tag{3.6}$$

Z = the characteristic impedance of the strip-line in Ohms
b = the width of the active conductor above the ground plane
h = the height of the active conductor above the ground plane

As with equation 3.2 and 3.3 for a microstripline which are both valid for a different w/h ratio, equation 3.6 is only valid if the ratio of b/h < 1, which limits the maximum impedance to 126 Ω.
The outcome of the impedance from equation 3.3 and 3.6 is the same when an $\varepsilon_r = 1$ for air is used for equation 3.1 to fill in equation 3.3.

Equation 3.3 was been derived by Wheeler in 1965 [**21**] for the impedance of a microstrip transmission line has been based on simplifications and conformal mapping [**13**].
The formula for an h/b ratio < 1was found in [**18**] and is the same as the formula 3.2 for a microstrip transmission line with $\varepsilon_e = 1$. A graph that combines both equation 3.2 and 3.6 in one graph is show in Fig 3.3. It can be seen that both equation 3.2 and 3.6 seamlessly cover the entire width/height ratio range.

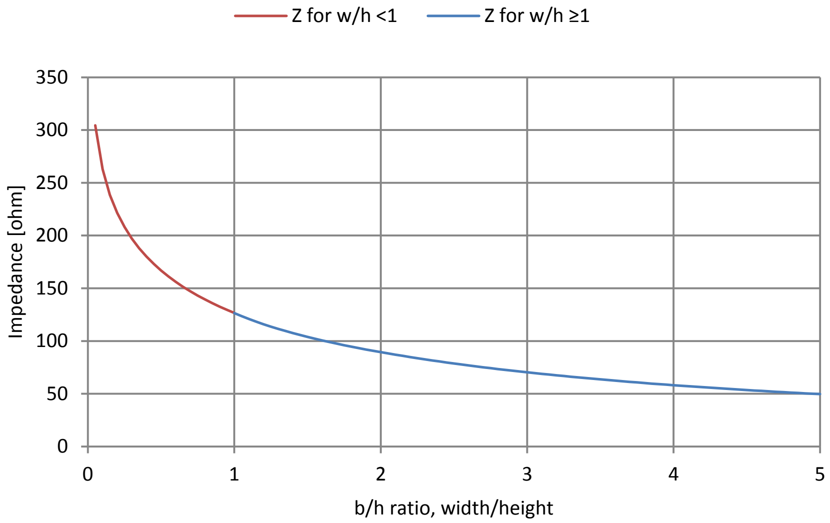

Fig 3.3, Impedance as a function of the width/height ratio

As can be suspected from the graph in Fig 3.3, the width versus height ratio is important when designing a stripline antenna (SLA). It is not always possible to pick a height versus width ratio as one would like to.

When designing a practical SLA for EMC the desired volume under the SLA and the available space in the anechoic chamber need to be considered.
If a minimum height of 2.0m is taken, the width over height ratio of the SLA which is stated in formula 3.6 and Fig 3.3 give width for a given height and a wanted impedance in table Table 3.2 here below.

	50 Ω	**100 Ω**	**112.5 Ω**	**200 Ω**
Height[m]	Width [m]	Width [m]	Width [m]	Width [m]
2.0	9.90	3.23	2.56	0.57
2.5	12.37	4.04	3.19	0.72
3.0	14.85	4.85	3.83	0.86
3.5	17.33	5.66	4.47	1.00
4.0	19.80	6.47	5.10	1.14
4.5	22.28	7.29	5.74	1.29
w/h ratio	4.95	1.62	1.28	0.286

Table 3.2, Width over height ratio

This means that to create a SLA with an impedance of 50Ω and a height of 2m a width of more than 10m is needed.

The anechoic semi chamber where the SLA might be used is 7m wide, 13m long and 5.6 m high.
The walls are covered with ferrite tiles and blue pyramid shaped absorbers that absorb electromagnetic waves to prevent reflections from the walls of the semi anechoic chamber.

Fig 3.4, The semi anechoic chamber with a conducting floor.

It is also required in [**1**] that the antenna stays at least 1m away from the walls of the anechoic chamber and the EUT. Since the anechoic chamber is only 7m wide an SLA with a 50Ω impedance cannot fit in the semi anchoic chamber (SEC1). Therefor the impedance needs to be changed and matched to 50Ω as will be described in chapter 4.

Chapter 4 Impedance matching

For a correct working stripline antenna a good reflection coefficient and impedance matching are crucial. As described in 2.3 transmitted energy is lost when an impedance mismatch occurs. In case of mismatch a lot of power from the amplifier is not generating an E-field but is reflected back to the amplifier. From Table 3.2 it is clear that it is impossible to fit a 50Ω stripline antenna of 2m high in the anechoic chamber. Therefor a closer look at different impedances and ways to match these impedances to 50Ω is necessary.

4.1 Lumped element matching

One of the simplest ways to match different impedances is to use capacitive and inductive lumped elements.
This can make a suitable match but has a very limited bandwidth due to the Bode Fano-limit [**3**].

$$\int_0^{\infty} ln \frac{1}{|\Gamma(\omega)|} d\omega \leq \frac{\pi}{RC} \tag{4.1}$$

The schematic that belongs to formula 4.1 is a parallel RC network from Fig 4.1 which can be attached to match a load to a network.

Fig 4.1, Parallel RC network

$$\Delta\omega \; ln \frac{1}{\Gamma_m} \leq \frac{\pi}{RC} \tag{4.2}$$

One of the conclusions of the Bode-Fano limit in equation 4.2 is that for certain load it is only possible to achieve a broader match at the cost of a higher loss due to a higher reflection coefficient in the pass band.
Lumped element matching is too narrow banded and unsuitable for the SLA which is a broadband transmission line.To make broadband impedance matches there are two other options, transmission line transformers (TLT) which are also known as impedance transformers and antenna tuners.

4.2 Baluns and transmission line transformers on ferrite and Iron powder cores

Transmission line transformers (TLT) have first been described in 1944 by Gunella [**22**] where a 960 Ω tube amplifier output was matched to a 60Ω transmission line using a 1:16 TLT. Later in 1959 Ruthroff [**23**]described a number of different configurations among which was the unbalanced to unbalanced transmission line transformer. This so called unun has been used in this work used to match coax cable to the stripline antenna. A fine reference work on TLT's was written by Jerry Sevick [**24**] with a more recent article published in 2008 [**25**]. There exist two distinct types of transmission line transformers, the balun which matches a balanced to an unbalanced line or load and ununs which match a unbalanced to and unbalanced line or load. Amongst licensed amateur radio operators a set of often used transmission line transformers consists of baluns which are used to match the coaxial unbalanced 50Ω in- and output of transceivers to different kinds of balanced antennas and transmission lines. These baluns can be wound on ferrite or iron powder cores or consist of a serial wound coil of coaxial cable close to the antenna. A basic description of broad band matching and baluns can be found in the ARRL Antenna Book [**26**]

4.2.1 Guanella 1:1 and 1:n^2 balun Transmission Line Transformers

The basic idea of a Transmission Line Transformer was described in 1944 by Guanella [**22**]. The basic schematic of a 1:1 Guanella balun can be seen in Fig 4.2.

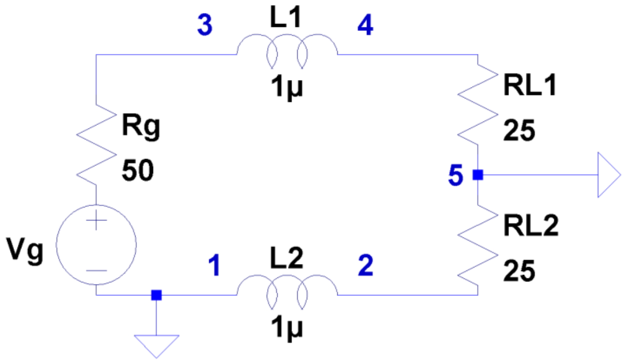

Fig 4.2, The Guanella 1:1 balun

The TLT in Fig 4.2 consists of a transmission line consisting of two parallel coils between 3 and 4 and between 1 and 2. The coils L1 and L2 are bifilar wound which means that the windings are laid in parallel. In this case the TLT is wound either with or without a core. Each coil should have a reactance which should be large enough that the coils are not seen as a short circuit from R_g to R_L. This reactance is necessary to prevent common mode currents which could else flow in parallel from 1 to 2 and from 3 to 4 over the transmission line (TL) which consists of the coils L1 and L2. By connecting different TL's in series and from other sides in parallel different impedance ratios can be obtained in 1:n^2 manner where n is a integer number of TL's.

4.2.2 Ruthroff ununs 1:4, 1:2.25 and 1:2

Ruthroff ununs are based on the concept of adding up the direct and the delayed voltage from different TL's. Since the delay of the voltage is directly dependent on the length of the TL in the TLT as could also be seen in formula 2.7 where β part the equation is related to the maximum usable working frequency of the TLT. For the simplest Ruthroff unun which is the 1:4 unun from Fig 4.3 the formula's for the transfer are derived in [**23**] using transmission line equations.

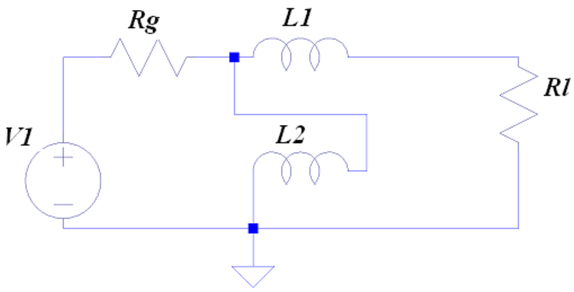

Fig 4.3, A Ruthroff 1:4 impedance unun

In this TLT the maximum transfer of power occurs when $R_L = 4R_g$.
With Ruthroff ununs it is also possible to build TLT's that are capable of other transfomation ratio's than 1:n^2. An example of these TLT's is the 1:2.25 or 1:2 TLT's that have been described in Chapter 7 in [**23**]. The 1:2.25 unun consists of tree parallel wound (trifilair) coils and are connected as in Fig 4.4. For a 1:2 unun it is necessary to make a tap on $L1$ and connect this to Rl this can be seen in Fig 4.5.

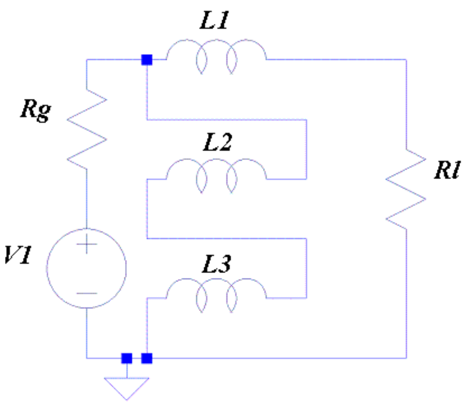

Fig 4.4, A Ruthroff 1:2.25 unun

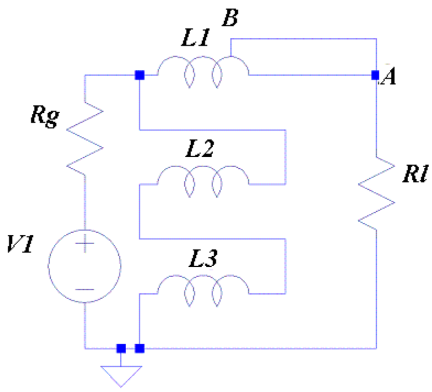

Fig 4.5, A 1:2 Ruthroff unun

4.2.3 Ferrite and Iron Powder cores

In order to build a good wide band TLT the TL has to be as short as possible while still obtaining the impedance necessary to build a functioning TLT. Instead of only winding the TL of the TLT as inductances with air as a core material, a core material that increase the impedance per winding is used. From different descriptions of TLT's in [**27**], [**28**] and [**24**] it was possible to find material descriptions for different purposes and different cores. Frequently used core materials are ferrite and iron powder.
The inductance of coils wound on different core materials can roughly be calculated using the following formulas:

$$L = \frac{N^2 \mu_r \mu_0 A}{l} \tag{4.3}$$

Here is L the selfinduction in Henry, N the number of windings, $\mu_r\mu_0$ is the permeability of the core material where μ_r is a material specific constant and μ_0 equals $4\pi \cdot 10^{-7}$.
The values of A which is the core cross section in m^2 and l, the length of the magnetic path in m. Both values depend on the size of the core where D is the outer diameter [m] of the core and d the inner diameter [m] of the core. The value of A further depends on the height[m] of the core h and the value of l depends on π which is a mathematical constant.

$$A = \frac{(D - d)}{2} \cdot h \tag{4.4}$$

$$l = \frac{(D + d)}{2} \cdot \pi \tag{4.5}$$

Dimensions of the core are usually specified in mm in datasheets.
Some core manufacturers in the United States specify the type of their core together with the material type in inches/100.
As an example a ferrite toroid core with a diameter of two inches of material type 43 will be specified as FT200-43 where F stands for ferrite, T for toroid, 200 for two inches and material type 43.
In some cases the number of windings for the inductance of a coil can be calculated with an induction factor A_L which represents $\frac{\mu_r \mu_0 A}{l}$ from formula 4.3.

$$L = N^2 \cdot A_L \tag{4.6}$$

This A_L value is sometimes given in μH per N^2 turns nH per N^2 depending on the manufacturer. Calculations with these values should be checked against measurements if possible since the $A_L$value is usually specified with a variation between ±5% up to 25%.
In a clear explanation from [**27**] and [**28**]the formula for the complex permeability of core material was given in equation 4.7.

$$\mu = \mu_s' - j u_s'' \tag{4.7}$$

This formula contains the real inductive component μ_s' and the imaginary component u_s''.

The real and imaginary loss component of the core material are also used to describe the loss tangent of the material $tan\delta_m$ in equation 4.8.

$$tan\delta_m = \frac{u_s''}{\mu_s'} \qquad (4.8)$$

The components of the core material also describe the quality factor or Q of a material in equation 4.9 that tells us how good a core performs at a certain frequency.

$$Q = \frac{\mu_s'}{u_s''} \qquad (4.9)$$

Unfortunately not all core manufacturers supply graphs or tables with Q, $tan\delta_m$ or μ_s' and u_s'' over a wide frequency range in their datasheets.
Some manufacturers only show the impedance for 1 or 2 windings versus frequency over a limited frequency range.
The frequency range where a ferrite core can be used as a TLT is the part where the $\mu_s' > \mu_s''$. The part of the complex permeability where $\mu_s' < \mu_s''$ the ferrite is used to block unwanted conducted emissions. For high frequencies however, the induction of the coils in the TLT depend more on the number of windings than solely on the permeability of the core.

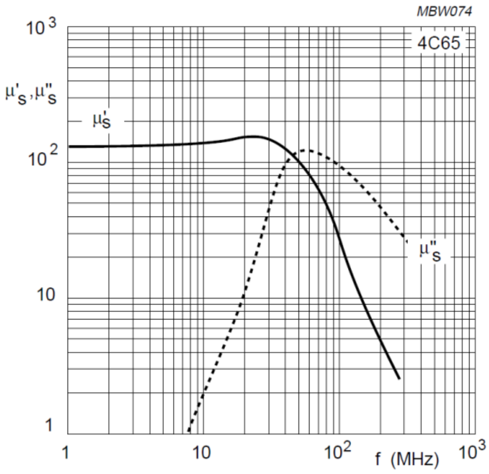

Fig 4.6, Complex permeability, taken from [29]

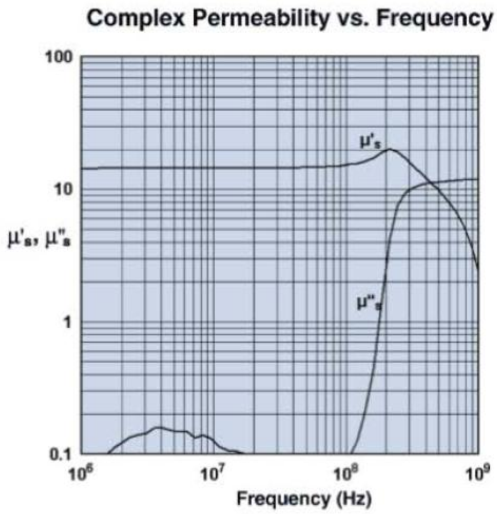

Fig 4.7, Type 68 complex permeability, taken from [30]

In Fig 4.6 and Fig 4.7 the complex permeability depicted from material 4C65 from Ferroxcube and Type 68 material from Fair-rite have been shown from their respective data sheets . These materials have been used for the ununs in chapter 7-9.

4.3 Antenna tuners

To match impedances to transmission lines one can use tunable lumped element such as coils and capacitors which can make a match on different frequencies.
Systems with several switchable or tunable coils and variable capacitors are known as antenna tuners (atu).
Known configurations are Pi, L or T-networks.

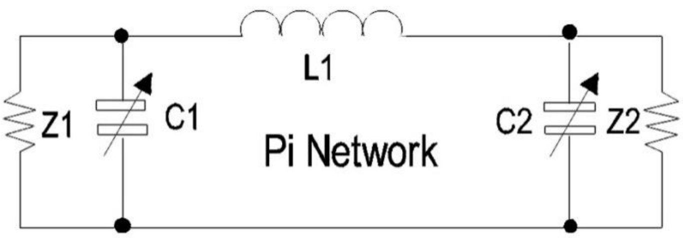

Fig 4.8, A schematic of a Pi-network based antenna tuner

Several high power antenna tuners are available from commercial vendors with power ratings available of 500W, 1kW and 1.5 kW [**31**], [**32**], and [**33**].

Using an antenna tuner for the EMC radiated immunity testing at Thales in Hengelo places certain demands on the antenna tuner.
Preferably the antenna tuner should be controllable using the IEEE-488 standard which is also known as GPIB which is used to control all EMC testing equipment at Thales.

The standard setup that is used at the Thales EMC lab uses the substitution method for radiated immunity testing.

The substitution method requires the electric field to be measured without any equipment in the anechoic chamber or near the antenna.
When then later the antenna is used in EMC testing the electric field strength can change due to the influence of the equipment in the near field.
The substitution method would require the antenna tuner to be matching always in same way regardless of impedance change due to the equipment under the stripline antenna.

Another method that can be used to test for radiated immunity measures the electric field strength on each frequency step near the equipment.
This method is known as the sensor method.

Chapter 5 Computational Electromagnetics, packages and principles

The calculation of the strength of electric and magnetic fields on different surfaces can be done using vector calculus and Maxwell's equations.
For perfect conductors and infinitely long lines and plates this can be done by hand for some special cases.
With help of conformal mapping [**13**], [**34**] calculations on electric and magnetic fields can be extended for some other shapes.
In this manner several formulas for microstrip like problems [**21**], have been obtained and also numerical approached of these formulas are used as a rule of thumb for initial calculations.
For the finer details however only solving the Maxwell equations using full-wave methods for the electric and magnetic fields can provide a clear view of the problem.
In order to solve the Maxwell equations for electric and magnetic fields several methods have been developed. These divide the problem into thousands or millions of smaller meshed or volumes where the fields can be considered static and where Maxwell's equations can be solved using computational electromagnetics (CEM) software [**35**].
These methods which are very suited for computation with a computer which provide a very close approximation of the real electric and magnetic fields when the problem has correctly been modeled.

5.1 The finite element method and the models in HFSS

The finite element method (FEM) requires that all space and surfaces are discretized into small pieces called elements and solves the Maxwell equations in differential form.

A disadvantage from the FEM method in this particular case is that is requires everything to be meshed including the air (free space) around the antenna.
For radiating problems such as the stripline antenna one has to add boundaries to the problem so that a finite volume can be meshed.

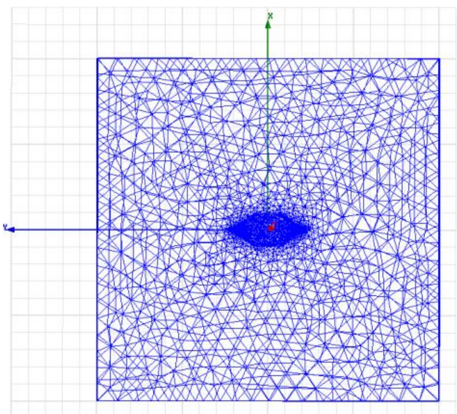

Fig 5.1, Mesh top view from HFSS

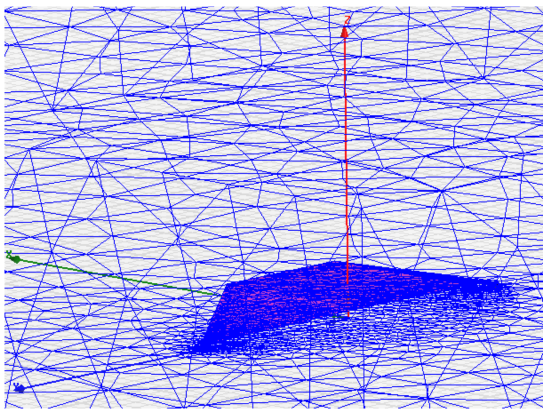

Fig 5.2, Mesh detailed view from HFSS

To achieve results with a relative small error the boundaries need to be relative far away from the stripline antenna which in turn increases the calculation time.
The FEM suite that is used is HFSS from Ansoft this software uses its own discretization algorithm called adaptive meshing.

5.1.1 The solid model in HFSS

A model in HFSS was made out of a small rectangular shaped plate center of the rectangle above the point (0,0,0) in xyz-coordinates.
Two triangles which were created by connecting three wires together.
To give each triangle a finite thickness the triangles were swept upwards.

One problem that remains is that the geometry of the different parts don't connect in a solid manner to each other. When the material is swept up the edges of the tapering triangles that connect with the stripline antenna no longer make perfect contact with the sides rectangle. This results in a broken model and the model can't be meshed and simulated properly in HFSS. To fix this problem small cylinders needed to be inserted to fill this gap.

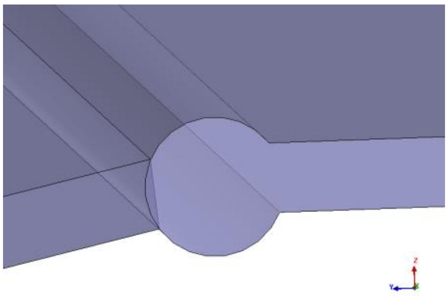

Fig 5.3, Cylinder to fill the gap between the plates in HFSS

The feeding points in HFSS were modeled as the centre connection from a coax cable.
The model for the 50Ω coax cable was designed from cylinders in HFSS.
Information about the coax cable material was obtained from a datasheet about RG219U [**36**].
Excitation for the model was provided by using a waveport on the edge of the model in the groundplane.

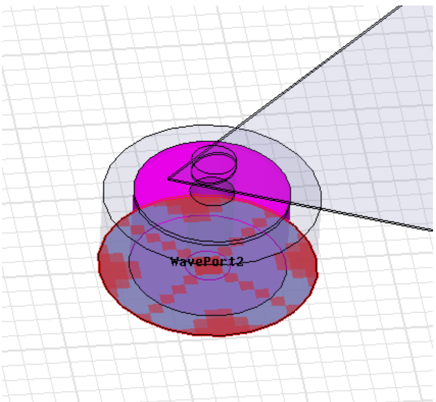

Fig 5.4, Coax cylinders with waveport in HFSS

The model of the stripline antenna was initially enclosed in boundaries 3m, 6m, 1.5m for the x,y and z dimensions.
To smoothen the Delta-S graph in Fig 5.5 from HFSS the size of the box around the SLA were increased to 10m, 10m, by 2m.

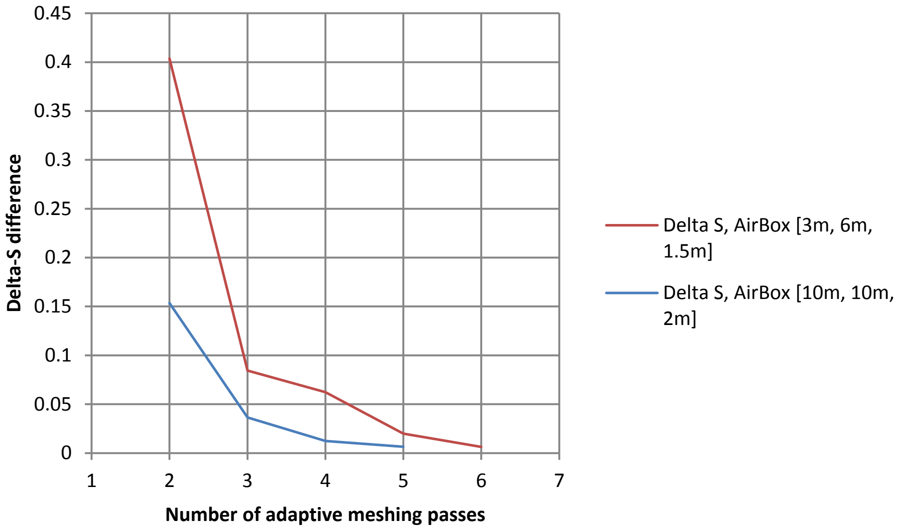

Fig 5.5, Number of adaptive meshing passes versus Delta-S

There is no exact metric for the goodness of the simulated model but if possible the graph with the number of adaptive meshing passes versus Delta-S should be relative smooth and contain no peaks.
If this taken into account in the model; the bigger the air box around the SLA, the more accurate the solution will be compared to free space.

5.2 The method of moments and the SLA models in FEKO

Another method to calculate solutions for the Maxwell equations is the Method of Moments which is in the literature from [**35**] and [**37**]. The MoM discretizes conducting surfaces of a model in triangular patches and wires in small wire segments.

The discretization MoM is dependent on the free space wave length therefore on the maximum frequency used in the stripline antenna.

$$\lambda = \frac{c}{f} \tag{5.1}$$

Where λ is the wave length in meter, c is the speed of light and f the frequency in Hz.

A rule of thumb for discretization for the maximum patch edge length or maximum wire length is $\lambda/10$.
For more accurate and refined results the edge length can be decreased and is generally taken an order of magnitude finer e.g. $\lambda/100$, this mesh edge length is acceptable for surfaces.
The solver calculates the currents which are flowing through the structure and uses these currents to calculate the electric and magnetic fields.

One of the few commercial available packages to use the method of moments is FEKO [**38**] which is also used at Thales.

5.2.1 A solid plate model in FEKO

In FEKO a model was created using the program Editfeko using different so called cards. The cards are described in depth in the FEKO manual [**38**].
By defining points in space using the DP card which were then connected using the BQ card for rectangles and the BT card for triangles to create the surface of the stripline antenna.
In Fig 5.6 the feed end can be seen which is a wire that connects between the endpoint of the SLA and the ground plane. On both the feeding point with a voltage source and the endpoint wire sections have been labeled with the LA card and generated with the BL card. The stripline antenna feeding point using the voltage source A1 card was placed on one wire segment between the ground plane and the stripline antenna.
The load was created using the LZ card and added to the labeled wire segment between the end of the stripline antenna and the ground plane.
The BO card was used to indicate that an infinitely large conducting ground plane was used.

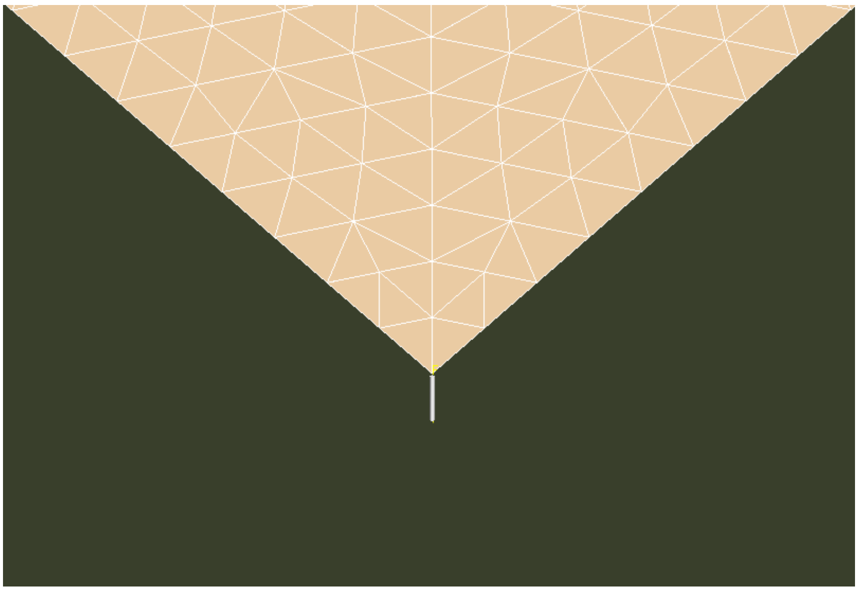

Fig 5.6, Wire segment to feed the SLA

For the evaluation of the comparison of the models two mesh sizes were used.
The first model was calculated with a mesh size where the triangle edge length was $\lambda/10$ for a frequency up to 160 MHz.
Another model was meshed with a mesh size with a triangle edge length of $\lambda/100$ for lower frequencies.

As can be seen in Fig 5.7 and Fig 5.8 the mesh size differs between $\lambda/10$ for 160 MHz and $\lambda/100$ for 70 MHz.

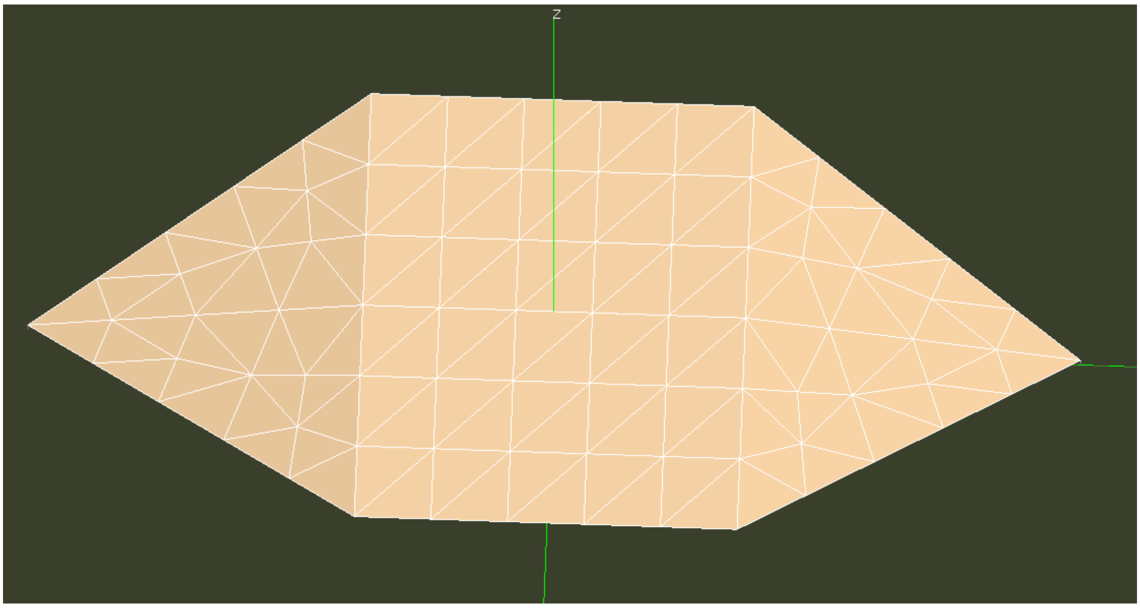

Fig 5.7, FEKO SLA model with triangles lamba/10 for 160 MHz

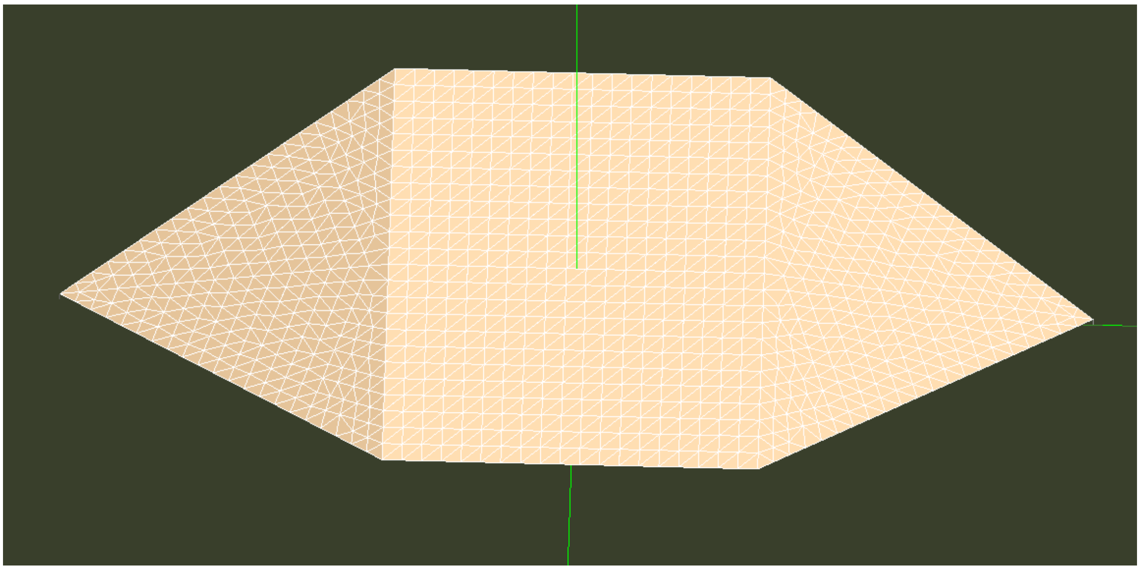

Fig 5.8, FEKO SLA model with triangles lamba/100 for 70 MHz

5.3 Stripline antenna results in Computational Electromagnetics

The experiments using the computational electromagnetics packages were done to see whether the formula 3.6 from paragraph 3.2.2 which was taken from the ISO 11452-5 standard [**20**] would give comparable results to the impedances that can be calculated.

A first model from Fig 5.7, FEKO SLA model with triangles lamba/10 for 160 MHz was to be simulated in CEM software first and then to be created for measurements and experiments.

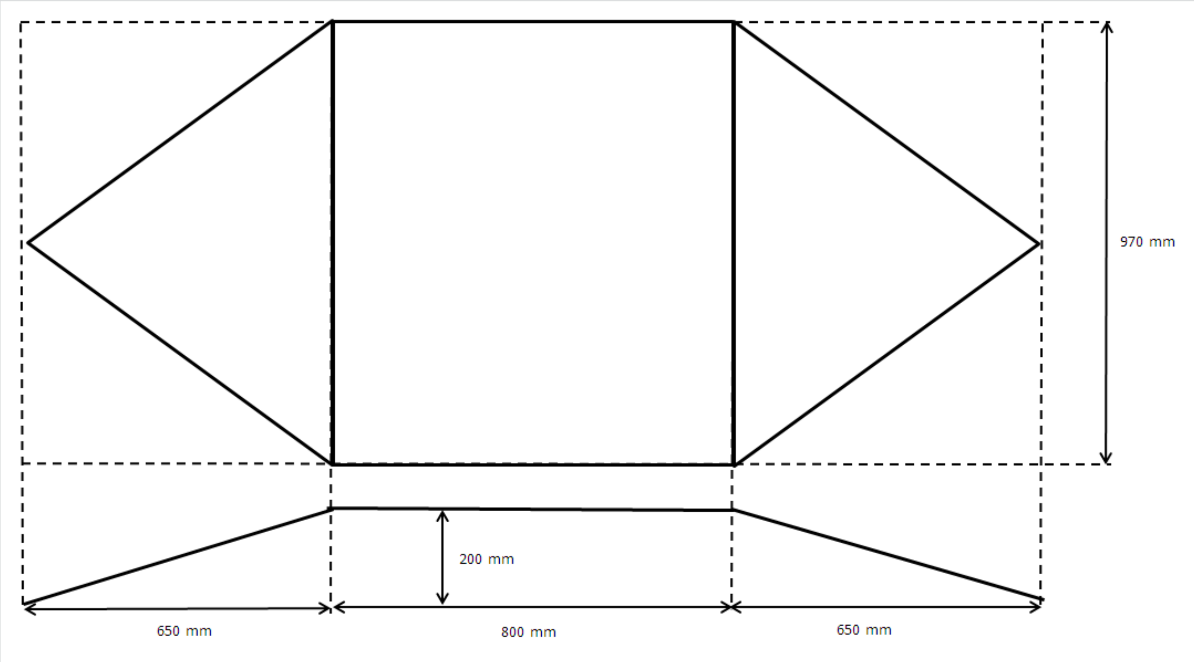

Fig 5.9, Solid SLA table model

To compare the results of the different software packages one of the interesting parts is the time computations take to complete and the memory used.

	FEKO λ/10	FEKO λ/100	FEKO λ/100	HFSS Air Box x,y.z (3m ,6m ,1.5m)	HFSS Air Box x,y,z (10m, 10m, 2m)
Freq range [MHz]	0.5 – 160, .5 MHz step	0.5 – 50, .5 MHz step	0.5 – 70, .5 MHz step	1 – 160, 1 MHz step	1 – 160, 1 MHz step
Computation Time	4 min, 4 sec	16 min, 14 sec	1h, 23 min, 9 sec	47 min, 02 sec	8h, 28 min, 58 sec ?
Memory used	632 kB	37.8 Mb	124.6 Mb	264 Mb	1.57 Gb

Table 5.1, Time and memory use of FEKO and HFSS

From the results as calculated in the different CEM packages the S11 parameter could be extracted and plotted so a measure for the impedance match could be compared.

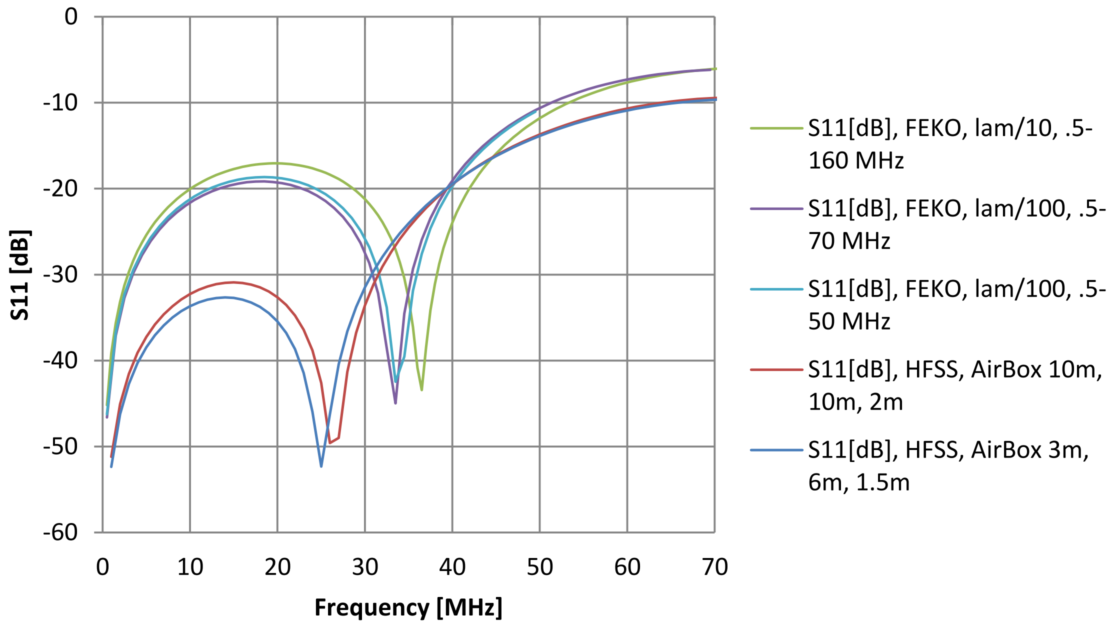

Fig 5.10, Computational Electromagnetics results for the table model

The simulation results in Fig 5.10 make it presumable that a 50Ω table model SLA from the formula and Fig 5.7 provides a decent S11 match of -10 dB over a wide range of frequencies from 1 MHz to roughly 50 or 65 MHz.

5.3.1 The equipment under the stripline antenna

When a large piece of equipment with large amount of conductive material is placed under the stripline antenna in such a way that it is also grounded (as required by certain tests) this has quite some consequences for the impedance and therefor the S11 parameter of the stripline antenna .

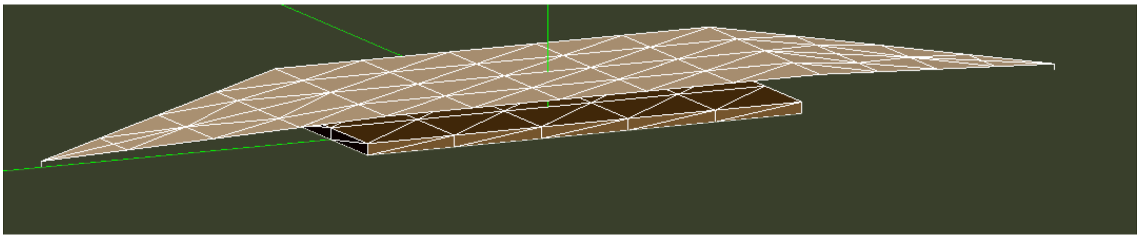

Fig 5.11, Rectangular box under the SLA

From Fig 5.12 it is clear that as soon as the equipment gets bigger than 20 or 30 percent of the height of the stripline antenna the S11 parameter is bigger than -10 dB for frequencies above 30 MHz.

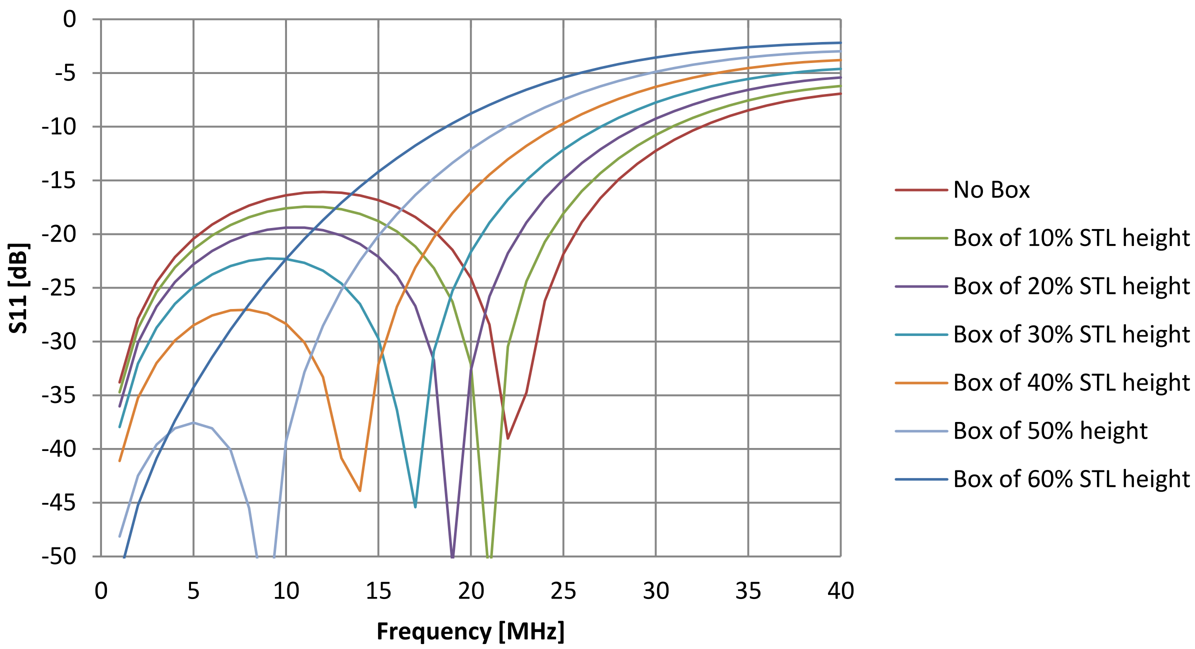

Fig 5.12, Influence of the height of an object under the SLA

The influence of the height of an object under the SLA does not have to be as much of a problem as stated here. The normal measurement procedure for radiated immunity measurements first measures the field strength with no EUT in place and later assumes the field strength is the same with the EUT in place.

5.3.2 Angles of the feeding part of the SLA

The feeding part of the SLA with the sloped edge has to increase and decrease from the point where power is fed to the SLA to the height and width of the SLA for use as a stripline antenna.

The influence of the slope of the feed point has been computed with FEKO using a model with a length of where the horizontal plane is 0.8m, with a height of 0.2m and a width of 0.97m.

The angle α has been defined as the angle between the vertical normal and the feeding taper in Fig 5.13.

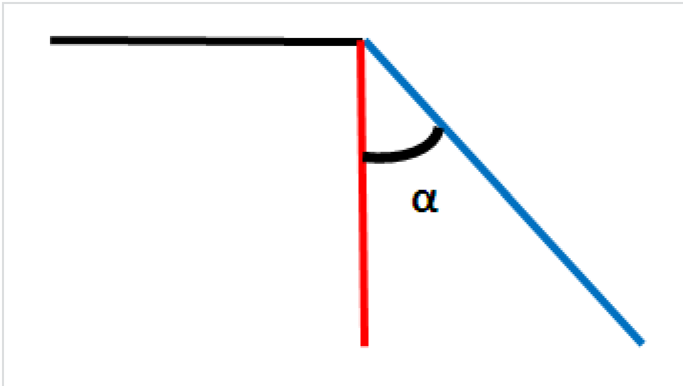

Fig 5.13, The angle alpha between vertical normal and feeding taper

The angle α as defined in Fig 5.13 does not really influence the S11 in Fig 5.14 as long as the angle stays under 60 degrees.

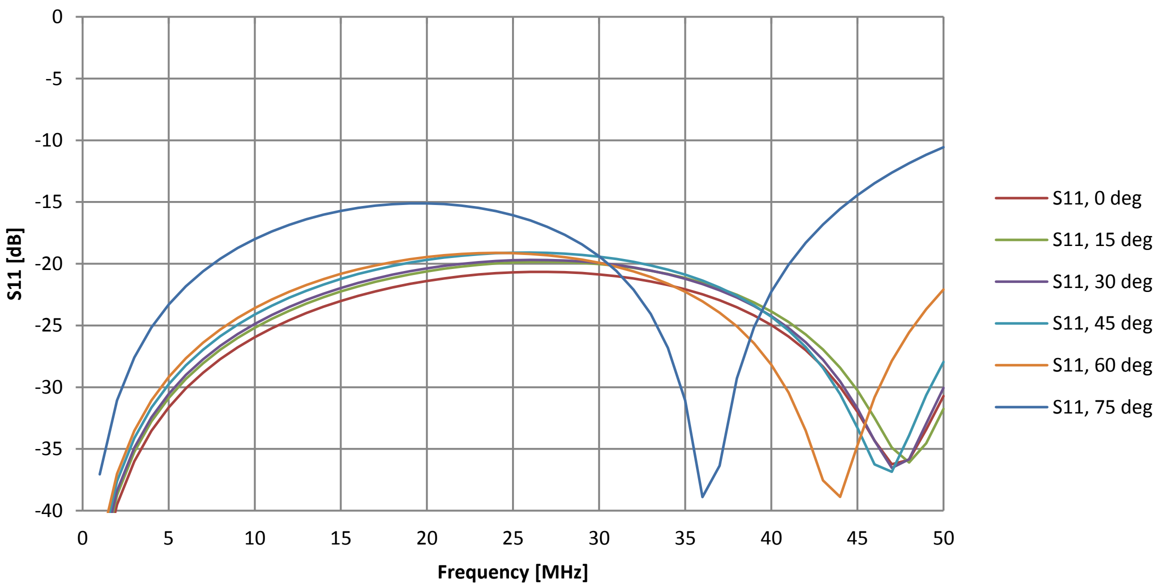

Fig 5.14, FEKO results for the S11 for different angles of the feeding edge

Another reason for using a relative large angle for feed for the SLA is that we only want a vertical field from the horizontal plane to the ground plane.
The electric field under the tapering could radiate onto the EUT from the tapering when small angles would be used.

Chapter 6 A 50Ω SLA realization and measurements

Information from the literature and papers together with simulations does probably not provide all the necessary information needed to design and build an SLA for the lab at Thales Hengelo. In order to be able to test an SLA a small model that will simply fit on a table has been built somewhat based on the model from the ISO 11452-5 Standard [**20**].

6.1 An aluminium foil 50Ω SLA

A stripline antenna made out of plate material as seen in [**16**], [**39**] has been simulated using computational electromagnetics software in chapter 5.

A first model of the stripline antenna was based on a modified model from the stripline antenna from the ISO Standard 11452-5, Annex A [**20**] which is show in Fig 6.1.
The original model from the ISO standard is about 4.3m long, 0.15m high and 0.74m wide.

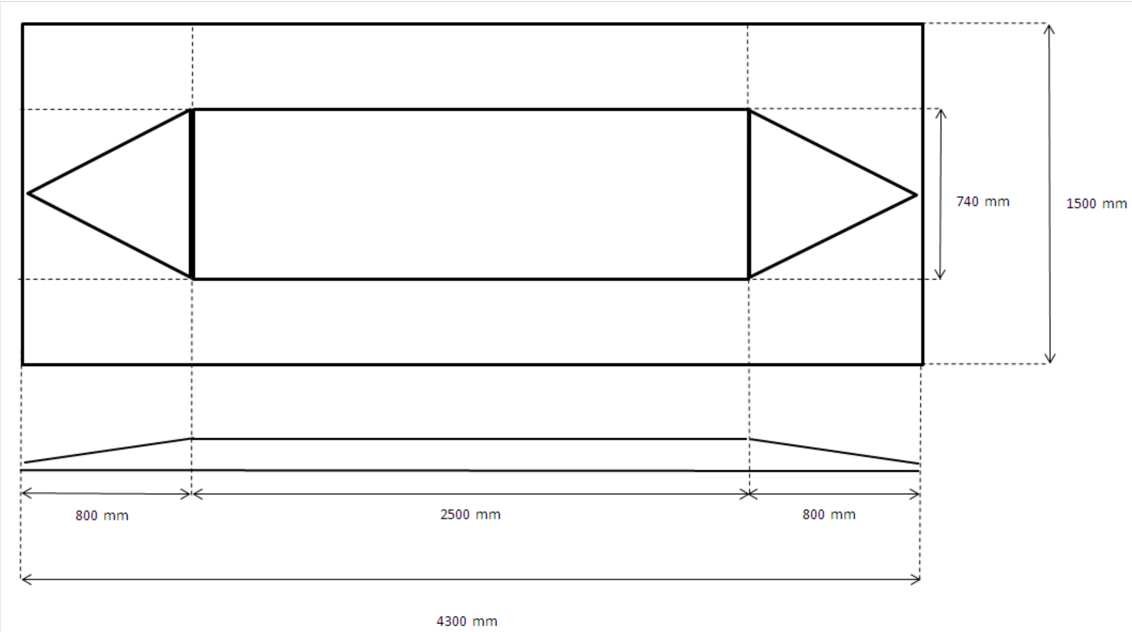

Fig 6.1, ISO-11452-5 Stripline antenna model

Since the tables which are used in the lab are only 2.1m long and the stripline antenna formula does not mention any limitation influence of length the length of the stripline antenna was reduced to 2.1m. A picture of the reduced table model can be seen in Fig 6.2.

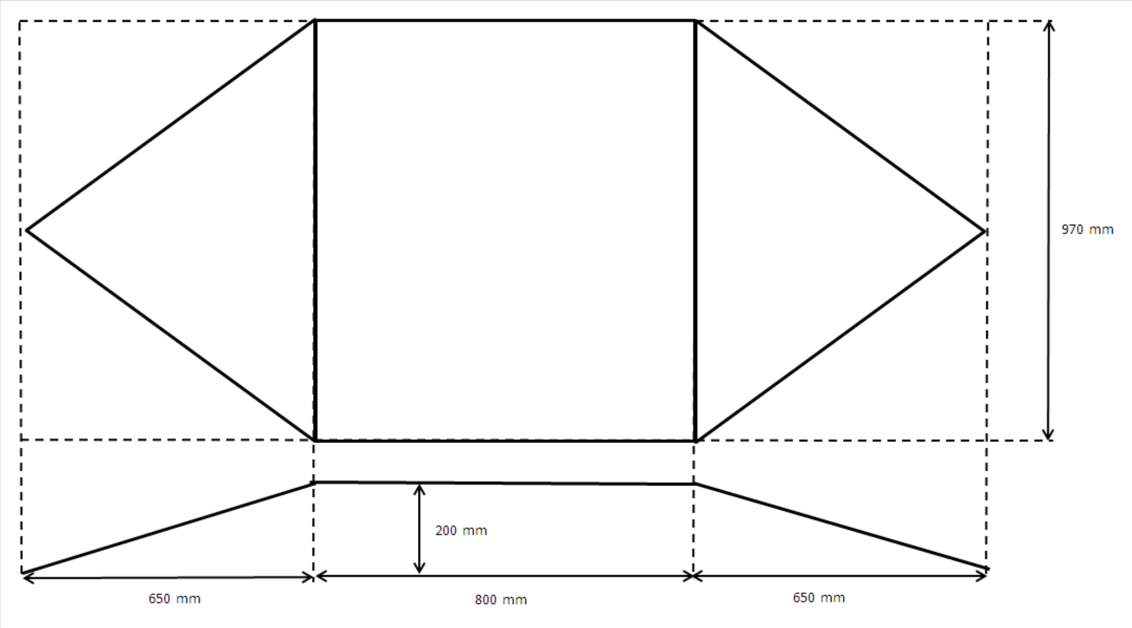

Fig 6.2, Table SLA with 50Ω impedance

The first model to perform measurements on was made out of aluminium foil which was 0.97m wide and 6.25 µm thick. The foil was cut to stripline antenna dimensions of 0.97m wide and 2.10m long which was spanned over foam supports of 20cm high which can be seen in Fig 6.3.

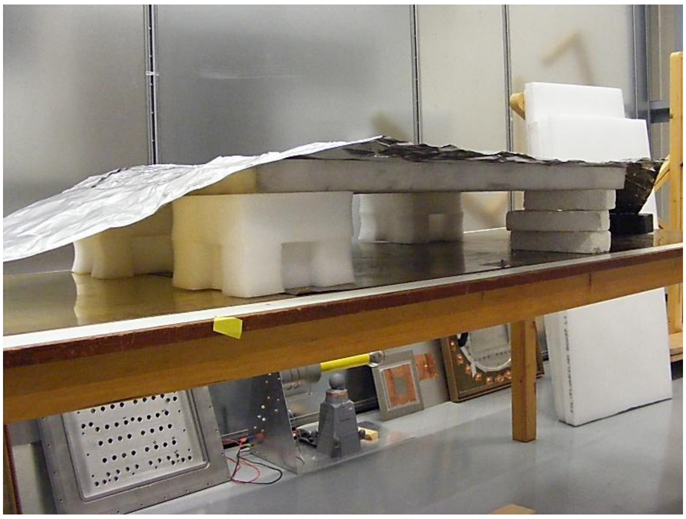

Fig 6.3, The aluminium foil stripline antenna

The height of 20cm under the foam supports enabled the use of the field strength probe from Fig 6.4.

Fig 6.4, Close up of the HL-4422 fieldstrength probe

The fieldstrenght probe in Fig 6.4 is the Holaday HL-4422 which has a usable frequency range from 10 kHz to 1 GHz. The probe is attached to a Holaday HL-4416 readout unit in Fig 6.5 by means of a fiber optic cable.

Fig 6.5, HL-4416 field strength readout unit

Feeding of the SLA is done as can be seen in Fig 6.6.
The center pin of the N-connector is soldered to adhesive copper tape which has been wrapped around the edge of the SLA.

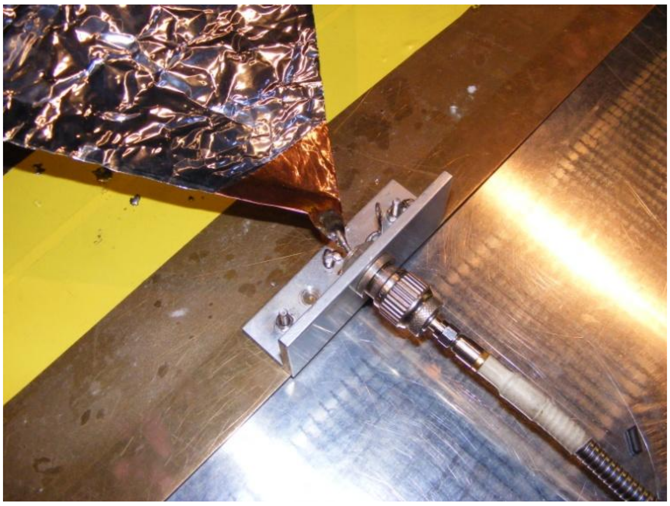

Fig 6.6, Connector Attached to the foil stripline antenna

According to formula 3.6 from paragraph 3.2.2 the impedance from this stripline antenna should be 50.7Ω which is very close to the required impedance of 50Ω.

The S11 and S21 were measured with a Rohde and Schwarz (R&S) ZVL Vector Network Analyzer (VNA) in Fig 6.7. which has a usable frequency range from 9 kHz to 13.6 GHz.

Fig 6.7, Rohde & Schwarz ZVL Vector Network Analyzer

Both N-connectors from the SLA were attached to coaxial cables which were each connected to port 1 and 2 on the VNA which can be seen in a schematic manner in Fig 6.8.

Fig 6.8, The connection schematic of the VNA to the 50Ω SLA

Measurements were done by placing the whole SLA with the table with ground plane as shown in in the semi anechoic chamber (SEC1) so that no reflections from the nearby walls, other objects, or signals would disturb the measurements.

Fig 6.9, SLA measurement in SEC1

In Fig 6.10 the S11 from the measurement in SEC1 are shown for different lengths of the 50Ω SLA with the same height, width and feeding taper.

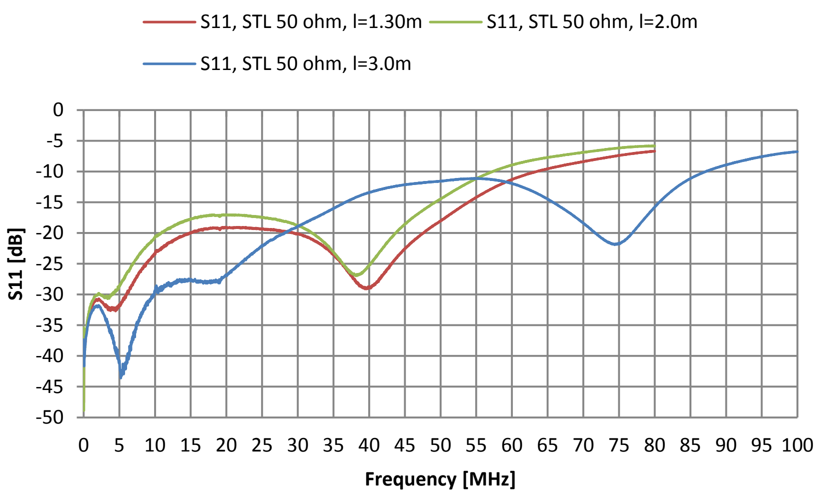

Fig 6.10, S11 for 50Ω SLA with different lengths

The results from the S11 in Fig 6.10 and S21 in Fig 6.11 show that the length of the SLA does make a difference in the goodness of the impedance match.

If a limiting S11 of -10 dB as described in 2.3.1 is taken as the upper limit for the use of the SLA it can be seen that the 2.0 m long SLA has a maximum frequency of 56 MHz, the 1.3m long SLA has a maximum frequency of 62 MHz and the 3.0m long SLA has a maximum frequency of 85 MHz.

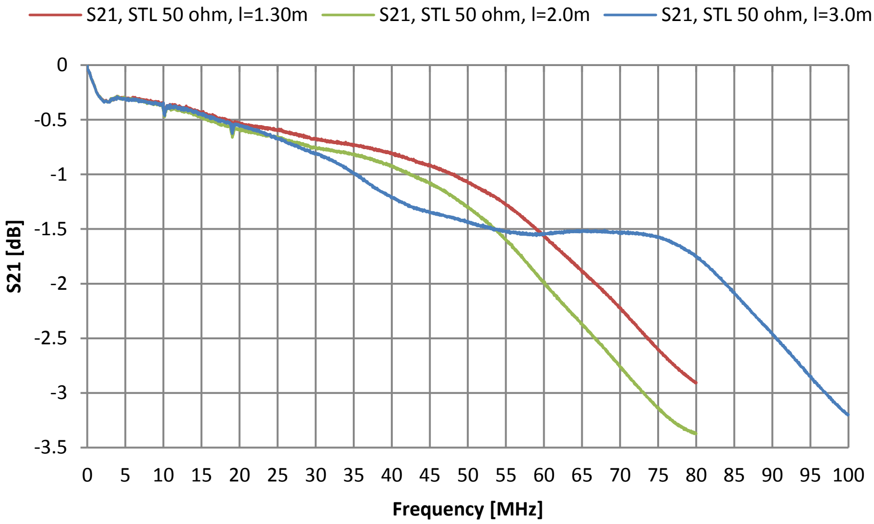

Fig 6.11, S21 for different 50Ω SLA's

For the S21 the maximum use frequency depends on the accepted transmission loss which was also discussed in paragraph 2.3.1, The maximum acceptable loss is here taken as -1.5 dB. In case of -1.5 dB loss the maximum usable frequency lies a 55 MHz for the SLA with a length of 2.0 and 3.0m and a maximum usable frequency of 57 MHz for the 1.3m long SLA. In practice the use of the SLA is not meant to transmit energy as efficient as possible from port 1 to port 2 but to radiate onto EUT's under the SLA.

One set of field strength measurements was done with the field strength meter under the center of the SLA in Fig 6.13. A R&S SM 100A signal generator which is visible in Fig 6.12 between to the HL-4416 and ZVL provides a signal 30 dBm which is equal to 1W.

Fig 6.12, Measurement overview for the 50Ω SLA

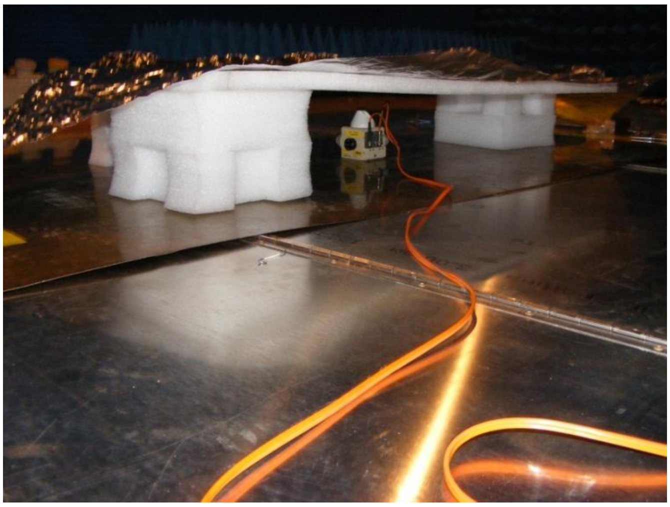

Fig 6.13, HL-4422 field strength sensor under the SLA

The results from the field strength measurement have been plotted in Fig 6.14.
The average field strength from the measurements with the 2.0m long SLA is 27.3 V/m over a frequency range from 2 MHz to 80 MHz.

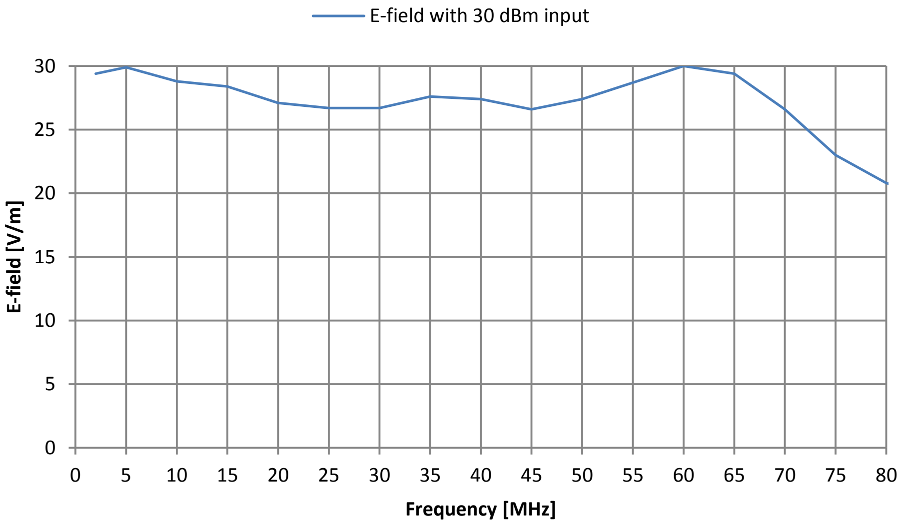

Fig 6.14, Field strength measurement result from the 2.0m SLA

The expected field strength under the SLA from the formula 3.4 in paragraph 3.2.1would be:

$$E = \frac{\sqrt{1 \cdot 50}}{0.20} \tag{6.1}$$

$$E \sim 35\, V/m \tag{6.2}$$

The power that was used to create electric field has been calculated using the average field strength value over the frequency range from 2 to 80 MHz as follows using equation 3.4:

$$P = \frac{(E \cdot h)^2}{Z} \quad (6.3)$$

$$P = \frac{(27 \cdot 0.2)^2}{50} \quad (6.4)$$

$$P = 28\ dBm \quad (6.5)$$

The loss from the signal generator output to the electric field of 27.3 V/m is:

$$P_{loss} = 30\ dBm - 28\ dBm \quad (6.6)$$

$$Loss = 2\ dB \quad (6.7)$$

This means that about 40% percent of the energy from the signal generator is lost. The efficiency of the 50Ω SLA including cable loss which was not measured can therefore be considered roughly 60%. A graph with the loss plotted between 2 and 80 MHz as plotted in Fig 6.15 shows that the loss between 2 and 70 MHz in the 50Ω SLA is at maximum 2.5 dB.

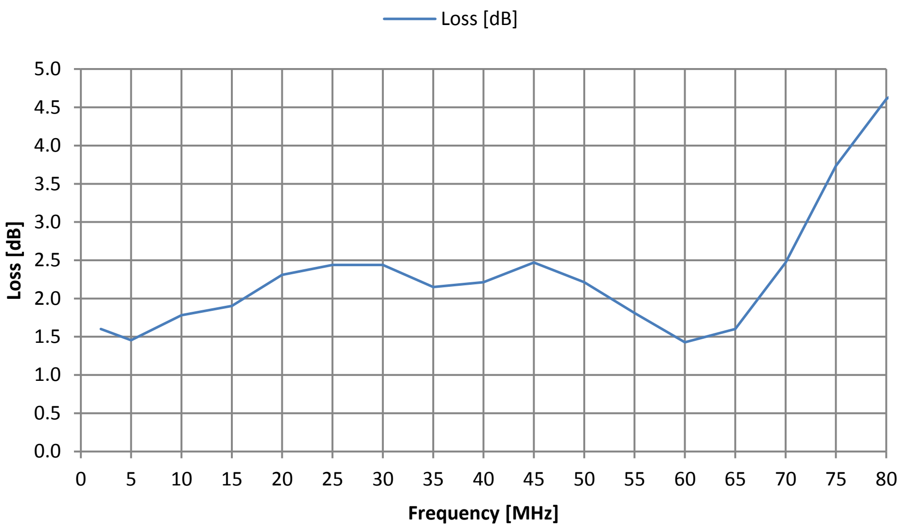

Fig 6.15, Transmission loss in the SLA

As practical results have shown in this chapter, building a scale model SLA yield usable results for a frequency range from 2 MHz to 50MHz or 70 MHz depending on the length of the SLA with respect to a S11 limit of -10dB.

Chapter 7 A 200Ω SLA with two 1:4 ununs, 50:200Ω

As can be found in chapter four the impedance matching over a broad frequency range is done best either with an unun type transmission line transformer or an antenna tuner. The unun in paragraph 4.2.2 which has the simplest schematic is the 1:4 unun from Fig 4.3. This chapter describes the implementation of an impedance matching 1:4 unun which matches 50Ω to 200Ω. First the initial attempts to select cores using an Gunella1:1 unun on will be described in 7.1. Second the calculations for the unun are described in paragraph 7.2, and last the measurements from the 1:4 ununs and ununs with a 200Ω SLA are shown in paragraph 7.3.

7.1 A Guanella 1:1 Balun to select cores

In order to build a successful unun first a suitable core material had to be selected.
The process of finding a selecting these materials was not so easy.
Most documentation about ferrite or iron powder cores is either about functionality as common mode chokes or about power transformers in switching power supplies.

The first influence that needs to be taken into account is the frequency response for each of the materials that are available.
One of the first tests to see how core materials react over a broad frequency range was to wind a few windings on the core materials that were already available at Thales.
The simplest test that at that moment could be devised with a signal generator and an RF power meter at hand was to wind a Guanella 1:1 unun with inspiration from the schematic from Fig 4.2. These 1:1 ununs consisted of a pair or wires wound on a core where one wire was attached to ground and one wire was attached to the signal end of the N-connector on each side as can be seen in Fig 7.1.

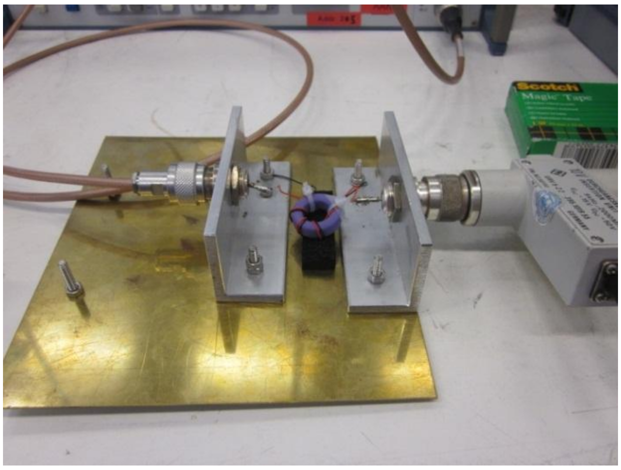

Fig 7.1, Measurement of a Guanella 1:1 unun

This unun with N-connectors would then be attached to a signal generator on one side and a measurement head and an RF power meter on the other side which can be seen in Fig 7.2.

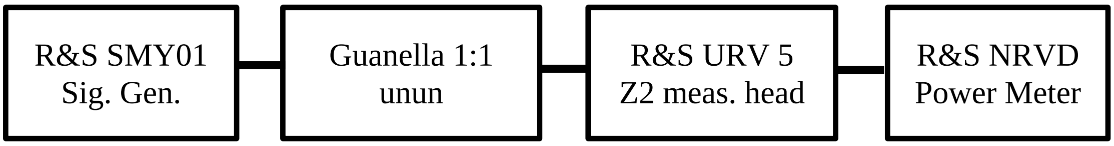

Fig 7.2, Schematic of the Guanella 1:1 measurements

The measurements from different cores show in that the Würth-Elektronik (W.E.) 7427015 core has the lowest transmission loss of -1.5 dB at 30 MHz in this case.

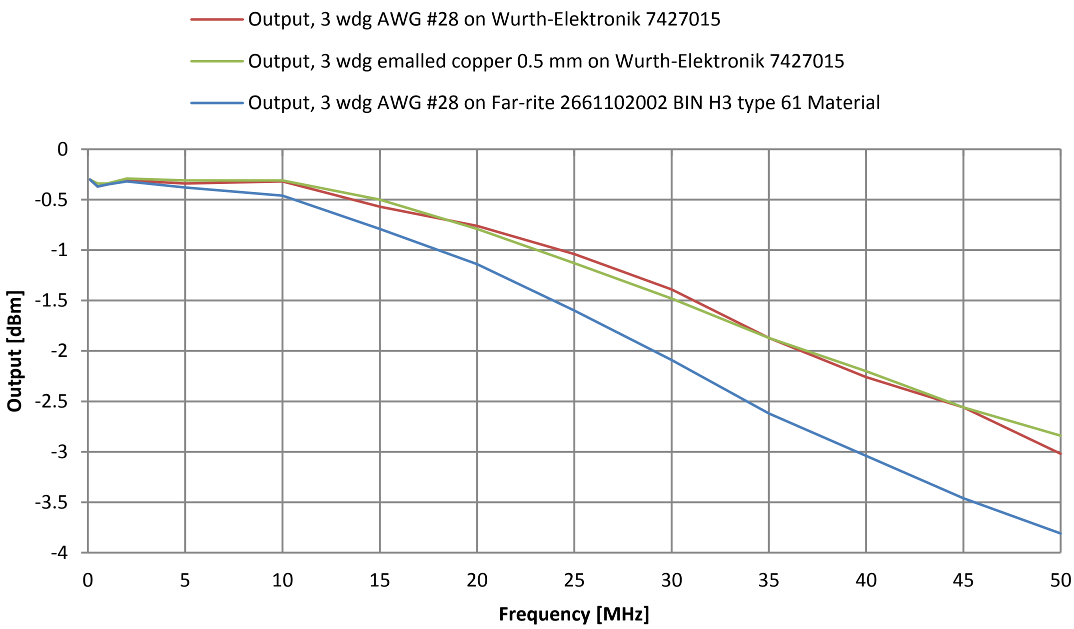

Fig 7.3, First Balun experiments

From these experiments the W.E. 7427015 cores were selected for the first experiments with Ruthroff 1:4 ununs to transform the impedance from 50Ω to 200Ω and vice versa.

7.2 A 1:4 Ruthroff unun

As can be seen in paragraph 7.1 the W.E. 7427015 cores from Würth Elektronik were selected to do the first experiments to build a 1:4 Ruthroff unun.
The Ruthroff unun for 50Ω to 200Ω from [**24**] is one of the simplest ununs to build.
For a 1:4 unun it is necessary to wind two windings in parallel on a core.
The schematic details about a 1:4 unun can be found in paragraph 4.2.2 in Fig 4.3 and in Fig 7.4.

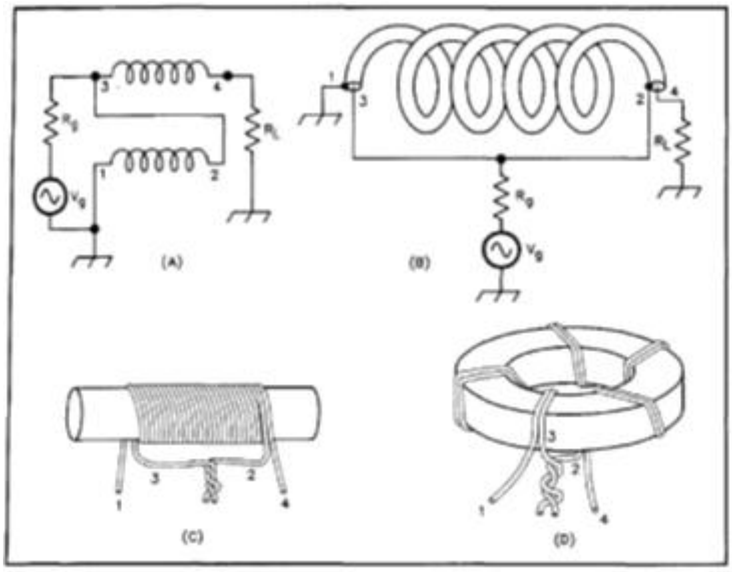

The Ruthroff 1:4 unun: (A) wire schematic, (B) coaxial cable schematic, (C) rod pictorial and (D) toroid pictorial.

Fig 7.4, Ruthroff 1:4 unun details from Sec 6.2 [24] by J. Sevick

Calculations for the unun were done as follows:

$$X_L = j\omega L \tag{7.1}$$

Here X_L is the reactance of a coil with a self-inductance of L Henry when driven with a frequency of $\omega = 2\pi f$.
The impedance of a coil Z_L is represented by the reactance X_L and the resistance in a coil R.

$$Z_L = X_L + R \tag{7.2}$$

Since the resistance R of the wire is negligible small compared to the reactance X_L of the wire the R component has been ignored.

A rule of thumb [**40**] that the coil inductance for the lowest frequency used should at least be 5 five times higher than the lowest impedance that needs to be matched. For the maximum usable frequency no formula or rule of thumb has been found. For the 50Ω to 200Ω unun with a minimum working frequency of 2 MHz calculations were done as follows.

$$Z_L = 5 \cdot 50\Omega \tag{7.3}$$

$$Z_L = \ 250\ \Omega \tag{7.4}$$

$$Z_L^2 = j\omega L\ \cdot -j\omega L \tag{7.5}$$

$$Z_L^2 = (2\pi f)^2 L^2 \tag{7.6}$$

$$L = \sqrt{\frac{Z_L^2}{(2\pi f)^2}} \tag{7.7}$$

$$L = \sqrt{\frac{250^2}{(2\pi \cdot 2 \cdot 10^6)^2}} \tag{7.8}$$

$$L = 1.99 \cdot 10^{-5} H \tag{7.9}$$

$$L \sim 20\mu H \tag{7.10}$$

To calculate the required amount of windings needed the formula for the self-induction on a toroid is as follows.

$$L = N^2 \cdot A_L \tag{7.11}$$

Here N is the amount of windings needed, and A_L is given in nH/ N^2 or µH/N^2 usually given by the toroid manufacturer.

The toroid used here is a core from Würth Elektronik type nr 7427015 which was already available in the lab and seemed to give the best performance in the HF frequency range with the first Guanella 1:1 balun.
The datasheet specified no A_L value, nor a complex permeability.
In this case the A_L was determined by measuring a coil on a toroid with a given amount of windings.

$$A_L = 1.44 \cdot 10^{-7} \tag{7.12}$$

$$N = \sqrt{\frac{L}{A_L}} \tag{7.13}$$

$$N = \sqrt{\frac{20 \cdot 10^{-6}}{1.44 \cdot 10^{-7}}} \tag{7.14}$$

$$N = 11.78 \tag{7.15}$$

$$N = 12 \tag{7.16}$$

These windings were laid using Teflon isolated AWG #16 wire with Teflon isolation.
In this case the wire diameter has been specified in American Wire Gauge which a American standard for the diameter and cross section of wires. Each wire diameter is specified with a corresponding number and usually denoted with a '#' where the higher the number the denotes low the cross section of the wire.
After winding the ununs these were measured first individually and later together connected with the 200Ω sides. The measurement on the single unun was done by replacing in Fig 4.3 the voltage source V_g and the 50Ω resistor Rg with a Rohde & Schwarz ZVL VNA and the load end resistor R_L with a simple 200Ω metal film resistor which is made out of two 100Ω resistors in series that make together 200Ω.

Fig 7.5, Measurement setup for a single unun

The unun with the resistor were simply soldered onto the L-shaped frame which has a 50Ω N-connector as shown in Fig 7.6. The N-connector is then used to connect the unun to the VNA using a coax cable.

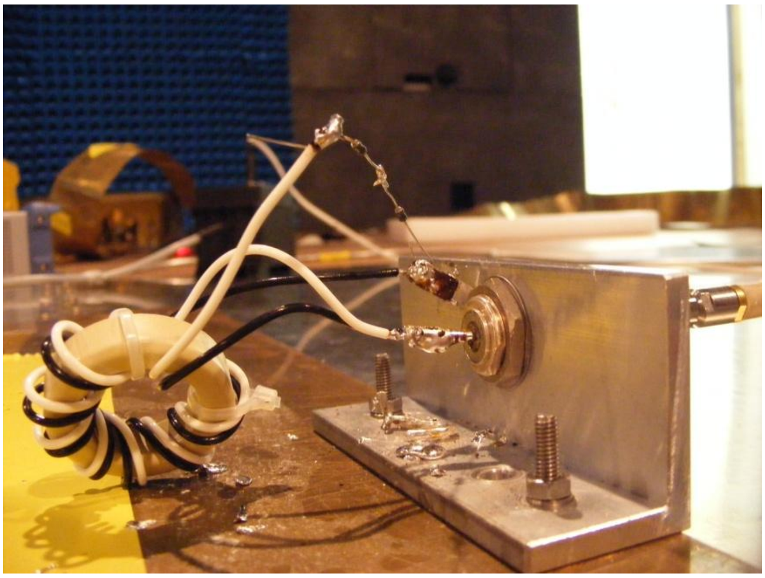

Fig 7.6, Single 1:4 unun with a 200Ω combined resistor as a load

The first measurement in Fig 7.7 indicates that the unun seems to perform well within a frequency range from less than 1 MHz up to 70 MHz if we take the S11 of -10 dB as limit.

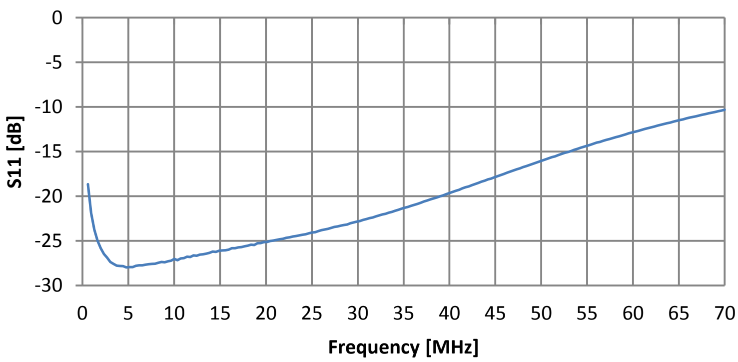

Fig 7.7, S11 from the 1:4 unun

A closer look at the frequency range from 0 to 5 MHz in Fig 7.8 show that the initial calculation for the unun to work from 2 MHz in formulas 7.3 to 7.16 is a bit off the mark.

The unun already seems to work from a frequency of around 500 kHz with a lowest point of more than -27.5 dB at 5 MHz.

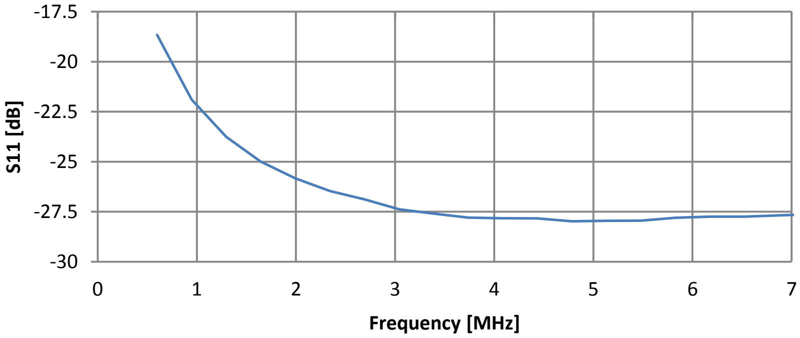

Fig 7.8, Low frequency detail from the S11 measurement of a 1:4 unun

After the testing of a single unun a second unun was build and tested in series with the first unun. The first unun was connected with the S1 port of the VNA on the side of V_g and R_g. The second unun was connected to the first unun with both 200 oh sides connected to each other.The last connection of the second unun was connected to the S2 connection on the VNA.

After this interconnection the S21 parameter of the both connected ununs were measured using the R&S ZVL VNA. The schematic of these measurements can be seen in Fig 7.9 with a close-up of the ununs in Fig 7.10.

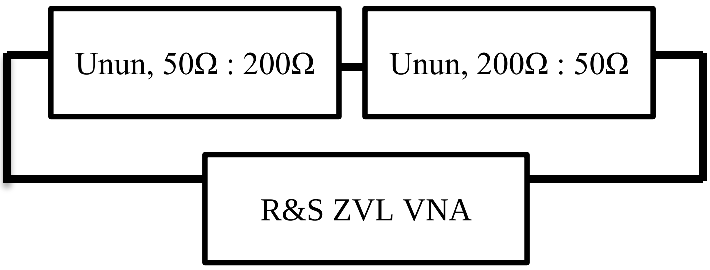

Fig 7.9, Schematic of the S21 measurement

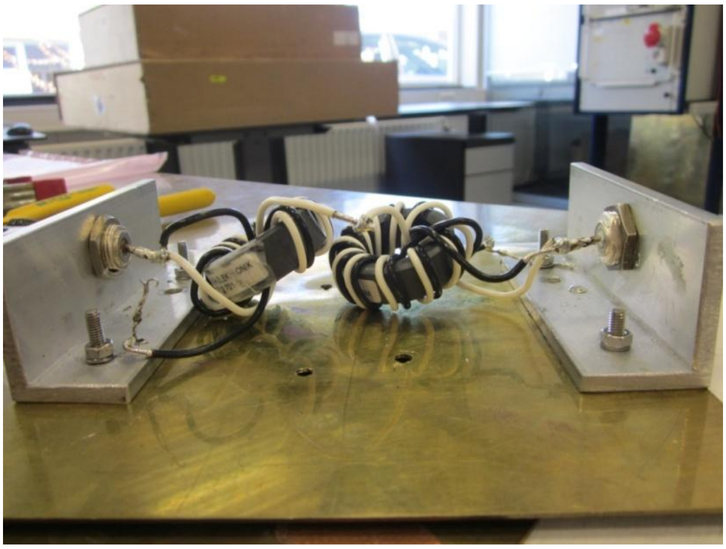

Fig 7.10, Two ununs with the 200Ω sides connected to each other

The results from the S21 measurement can be seen in Fig 7.11 and Fig 7.12
In Fig 7.11 it is visible that the ununs perform well between a frequency lower than 5 MHz up to 60 MHz with a loss of less than -1 dB.
When a loss of -3 dB would be acceptable the ununs seem to work well up to a frequency of 75 MHz.

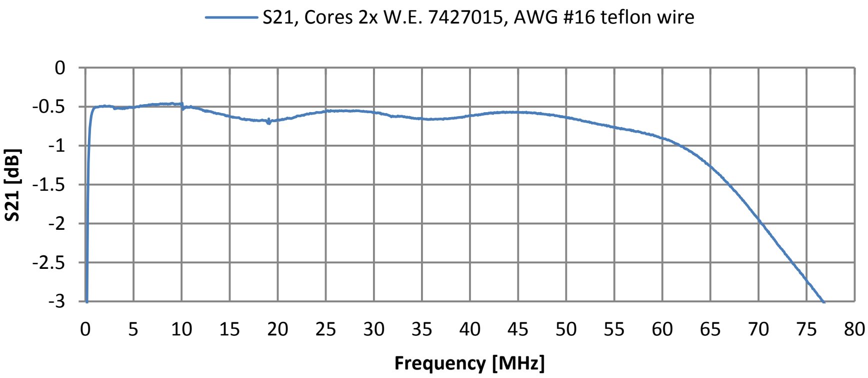

Fig 7.11, S21 measurement of two ununs

In Fig 7.12 it can be seen that the loss of the coupled ununs lies around -1 dB at 375 kHz and lowers to -0.5 dB from 1 MHz upwards.

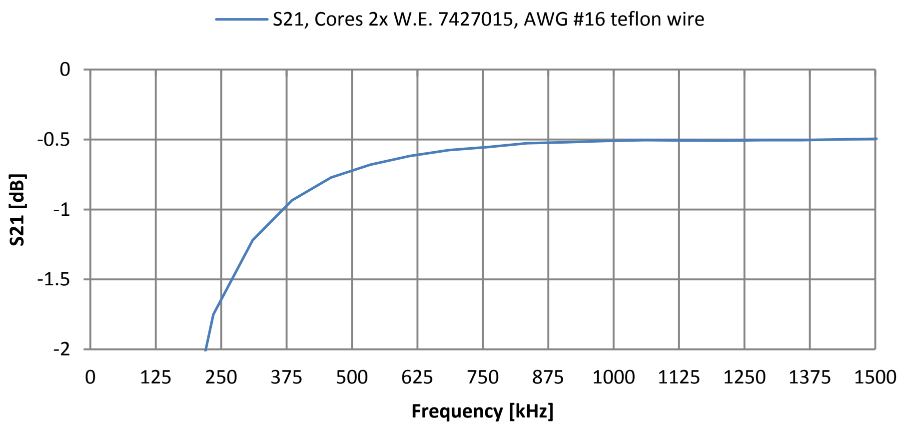

Fig 7.12, Low frequency detail from two ununs connected together

In sources among ham radio operators [**41**] iron powder cores are in some cases used as a core material for baluns and ununs.

From Micrometals Inc. samples from their type 7 and type 6 material were obtained with a size of two inch in outer diameter to see if these core could be used in ununs.
In their documentation [**42**] these materials are listed as high Q material for use between 1-25 MHz for the white coated type 7 material and 3-40 MHz for the yellow coated type 6 material.

Fig 7.13, Iron powder cores, type 6 (left) and type 7 (right)

The cores as seen in Fig 7.13 were wound with AWG #14 and AWG#22 wire because the iron powder cores have a much lower permeability than ferrite cores.
As a result these iron powder cores require more windings than ferrite core for the same impedance.

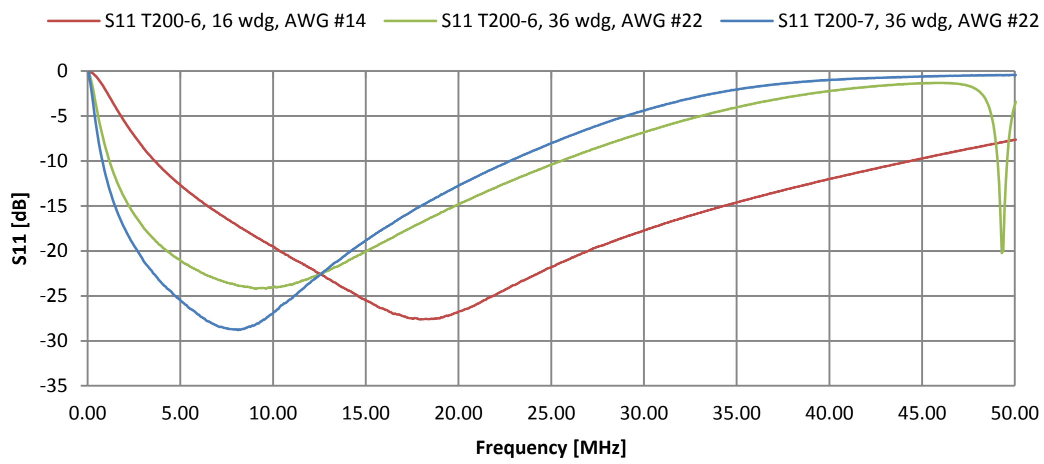

Fig 7.14, Low frequency range for Micrometals Inc. type 6 and type 7 cores

As can be seen in Fig 7.13 the iron powder cores can be used with S11 of -10dB over a frequency range from 700 KHz to 22 MHz for the 36 windings on type 7 or type 6 materials.

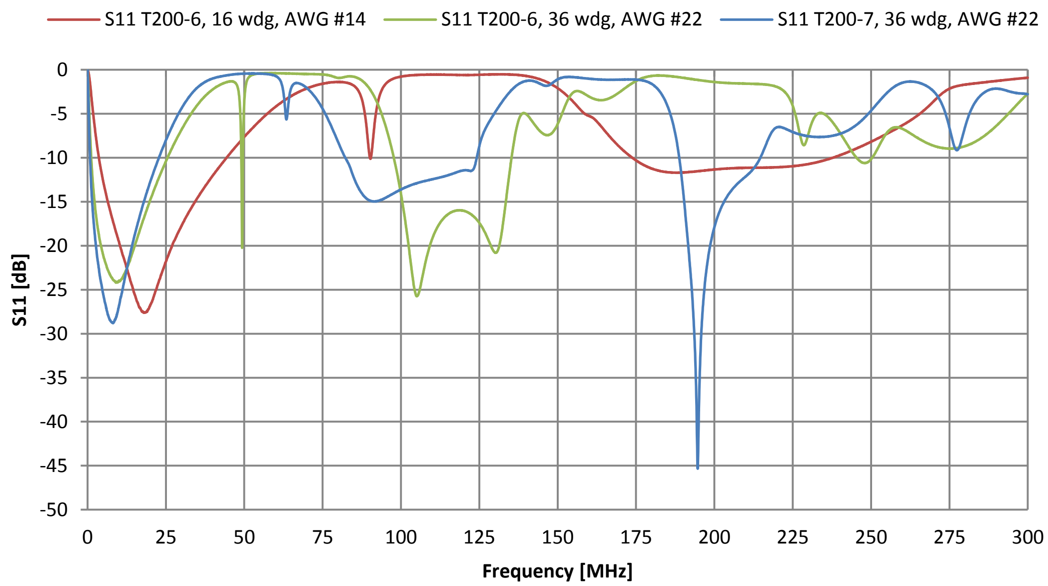

Fig 7.15, Broad S11 on iron powder cores of different wire types

When a broad frequency range between 9 kHz and 300 MHz is taken into consideration such as in Fig 7.14 might be possible to use the iron powder cores also in a high frequency range above 30 MHz with a S11 smaller than -10 dB.

7.3 A 200Ω SLA with ununs

After testing the cores for a 200Ω unun a small 200Ω testing SLA was built to see if the principle of two ununs with in between the ununs a 200 Ω SLA would work.

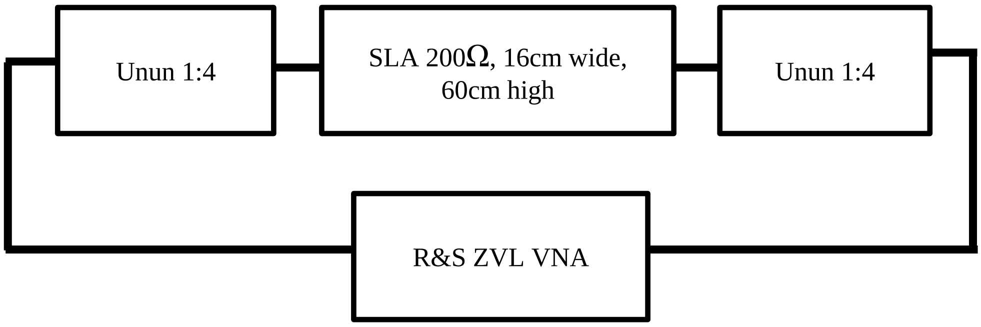

Fig 7.16, Schematic with two 200Ω ununs with a 200Ω SLA

The SLA was made out of aluminium foil and the size of the SLA was 16cm wide and 60cm high and 2.1m long.

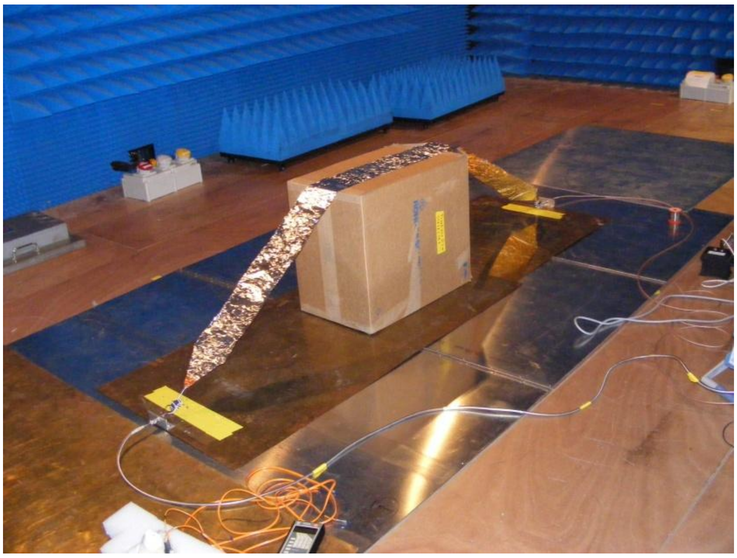

Fig 7.17, The small 200Ω SLA with two ununs

Besides the Würth Elektronik (W.E.) 7427015 core also cores made out of the 4C65 material from Ferroxcube were constructed.

As can be seen in in Fig 4.6 the 4C65 material has a useful complex permeability up to at least 30 MHz, this can be seen from the high Q as given in formula 4.5 in paragraph 4.2.3. Both the 4C65 and W.E. 7427015 cores that were used as 1:4 ununs.

The S11 in Fig 7.18 from the measurement shows that when an S11 of -10 dB is accepted the 4C65 cores have a useful range between 2 MHz and 63 MHz and the Würth Elektronik 7427015 core have a usefull frequency range between 1.4 MHz and 55 MHz.

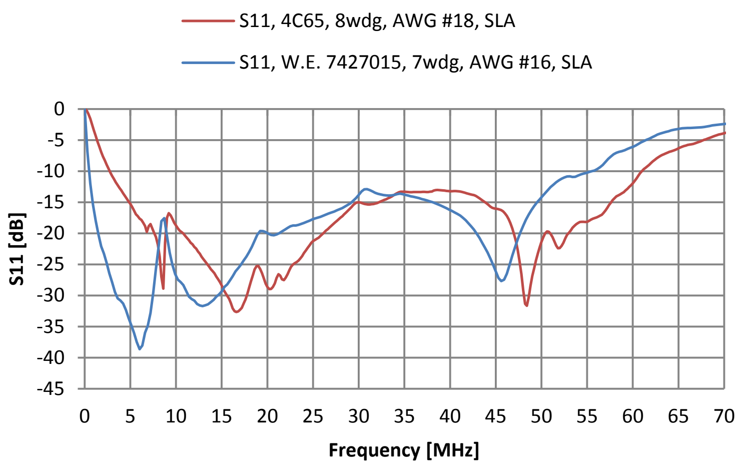

Fig 7.18, S11 for 200Ω SLA with 2x 1:4 unun with 4C65 and W.E. 7427015 cores

7.4 Electric field strength measurements with a 200Ω SLA

In order to measure the electric field strength the under the SLA with an impedance of 200Ω the following setup was devised and shown in Fig 7.19 to feed and measure the SLA with the two 1:4 ununs. An R&S SML03 signal generator provides a stable signal for the 150W Bonn amplifier which will increase the signal strength. The strong signal is sent through the coupler which transmits almost the whole signal to the 3 dB attenuator.

From the first 1:4 unun the impedance is transformed from 50Ω to 200Ω and fed into the 200Ω SLA .

After the SLA the remainder of the signal is transformed to 50Ω with another unun.

The signal with a 50Ω impedance from the last unun is then attenuated twice before being finally absorbed into the 50Ω load.

The power meter at the AR 3400 coupler has two functions, first to measure the amount of power being fed into the, second to measure the amount of signal that is reflected from the ununs and SLA in the direction of the amplifier. If the signal that is send to the unun and SLA would get reflected back to the amplifier this might cause the final stage of the amplifier to be damaged. That is why the signal in backward direction is measured and is also the reason why the first -3 dB attenuator is in place. If the signal then is reflected, the signal is first attenuated before being send back into the amplifier.

The Holaday equipment is used to measure the electric field strength; both units are connected using a fiber optic.

The thermo couple is attached to the unun to see if the unun would heat up during the usage and is to be measured using the thermocouple readout unit.

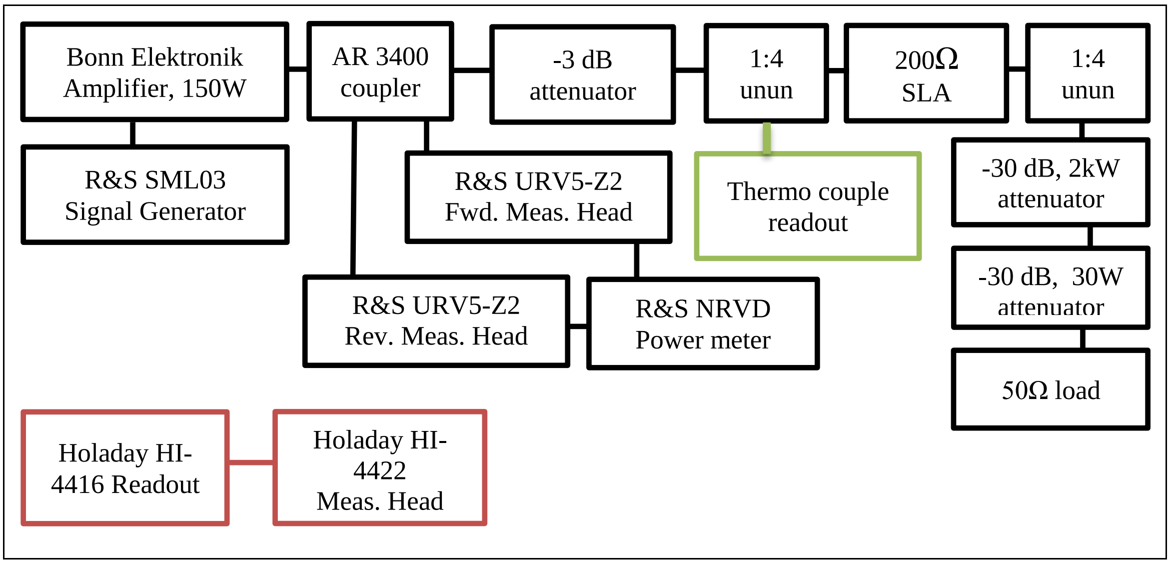

Fig 7.19, Schematic setup of the field strength measurement

In Fig 7.20 from top to bottom the R&S SML03 signal generator, R&S NVRD power meter and Bonn Amplifier are visible.


Fig 7.20, Signal generator, power meter and amplifier

In Fig 7.20 the car with the signal generator is placed on the right, the 200Ω SLA with ununs is visible at the center on a table and the 2kW attenuator visible on the left side.

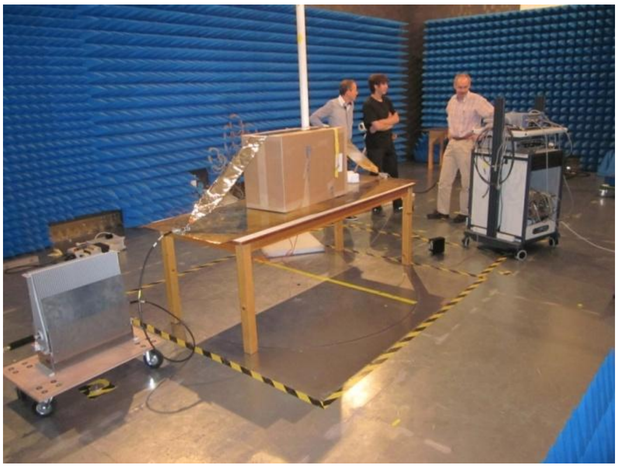
Fig 7.21, Equipment car and SLA, with attenuator

In Fig 7.22 the on the inside of the SLA the white plastic supports the Holaday field sensor which is located barely visible behind the 200Ω SLA.

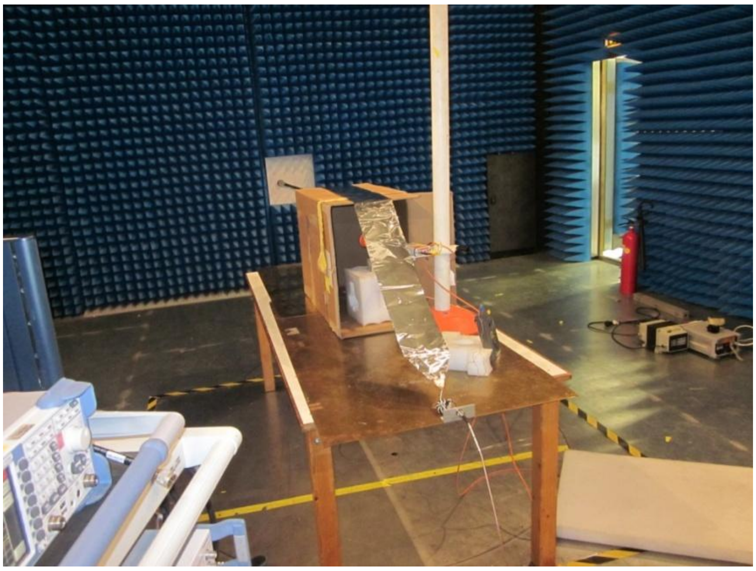
Fig 7.22, SLA with ununs and field strength meter

Some first experiments with a amplifier in the anechoic chamber revealed that it is possible to generate an electric field of ~ 125V/m with an input of 48.75 dBm (75W) power in a 200Ω SLA of 60cm high.

Fig 7.23, Electric field strength readout

In order to see if the temperature would rise during experiments the a lead of a thermocouple from a temperature meter was attached just between the windings of the core and the core itself an fixed it with special tape that is used for thermocouples.
Unfortunately the thermocouple seems to be coupling electromagnetic fields into the temperature reading unit which makes the temperature reading unreliable in this manner.

The R&S NVRD power meter was used measure to the amount of power that was sent into the ununs and the stripline antenna.
For the whole frequency range was stepped manually through a range from 1 MHz to 50 MHz using the signal generator in steps of 1 MHz.
With the Holaday field strength meter the strength of the electric field was measured at the center of the stripline antenna at half the height of the stripline antenna.

The efficiency from the SLA has been calculated in a similar manner as for the 50Ω SLA, thereby ignoring cable losses.
The expected field strength under the SLA from the formula 3.4 in chapter 3 would be:

$$E = \frac{\sqrt{75 \cdot 200}}{6.0 \cdot 10^{-1}} \tag{7.1}$$

$$E \sim 204\ V/m \tag{7.2}$$

The power that was used to get the effective electric field has been calculated as follows using formula 3.4:

$$P = \frac{(125 \cdot 0.60)^2}{200} \tag{7.3}$$

$$P \sim 44.5\ dBm \tag{7.4}$$

The efficiency can thus be seen as the ratio of the input power over the power send to the SLA with ununs.

$$48.75\ dBm - 44.5\ dBm\ = 4.25\ dB \tag{7.5}$$

$$Loss = 4.25\ dB \tag{7.6}$$

$$Efficiency = 1 - 10^{\frac{-4.25}{10}} \tag{7.7}$$

$$Efficency \sim 62.4\% \tag{7.8}$$

The efficiency can thus be seen as being roughly 62.4%.
These results might be partially explained due to the fact that the SLA was only 16cm wide and the Holaday measurement head is 10cm wide.

In this chapter different 1:4 ununs and a scale model 200Ω SLA have been tested.
The S11 limit of -10 dB showed promising results, the efficiency was no more than 62.4% in terms of the generated electric field strength. This could be due to a small stripline antenna with a width of 16cm in combination with a measurement head with a size of 10cm.

Chapter 8 A 100Ω SLA with 2 ununs 50:100Ω

In an the impedance of the is determined by SLA the width over height ratio as was explained in chapter 3. One of the more compact options to build an SLA is to change the impedance of the SLA as can be seen in Table 3.2. As previously tested in 7.3 and 7.4with a 200Ω SLA, in this chapter an attempt is made to build a 100Ω stripline antenna with 1:2 or 1:2.25 ununs. First the 1:2 and 1:2.25 ununs are devised in paragraph 8.1, second the maximum amount of power that can be transmitted through the ununs is treated in paragraph 8.2 and 8.3.

8.1 Ununs for 50:100Ω

In order to be able to match a 100Ω stripline antenna to a 50Ω input impedance a Ruthroof type unun which matches in a 1:2 or 1:2.25 is needed.
These ununs are described in chapter 4 of this thesis and in chapter 7 from [**24**].
The schematic of the 1:2.25 and 1:2 unun in Fig 8.1 looks familiar like the 1:4 unun from Fig 7.4. In Fig 8.1 a third parallel winding has as to be wound.

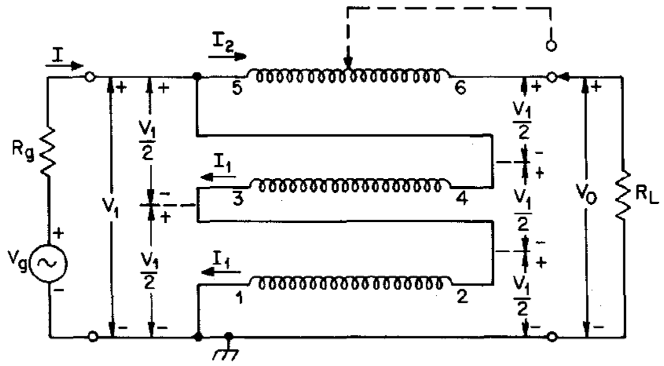

Fig 8.1, Schematic of a 1:2.25 or a 1:2 unun, taken from [24**]**

One of the first attempts to match 50 to a 100 stripline antenna was done using a 1:2.25 impedance transformer.
The reason was that the description in [**24**] about the unun was not clear about whether the tap as indicated by the dashed line in Fig 8.1 on top of the windings between point 5 and 6 should be grounded or not. A measurements have shown both the tap and the end from nr 6 should be attached to R_L.
The 1:2.25 match compared to 1:2 obviously creates a mismatch but has the advantage of being simpler to wire and wind and since no additional tap on one of the windings is needed.
The unun was wound on a 36mm wide core of 4C65 ferrite material which had proven to have favorable frequency characteristics in testing the 1:4 unun configuration.
The S11 parameters were measured using a Rohde and Schwarz ZVL VNA
over a frequency range from 9 kHz tot 50 MHz with a 100Ω resistor as a load.

The results from the S11 measurement can be seen here in Fig 8.2.

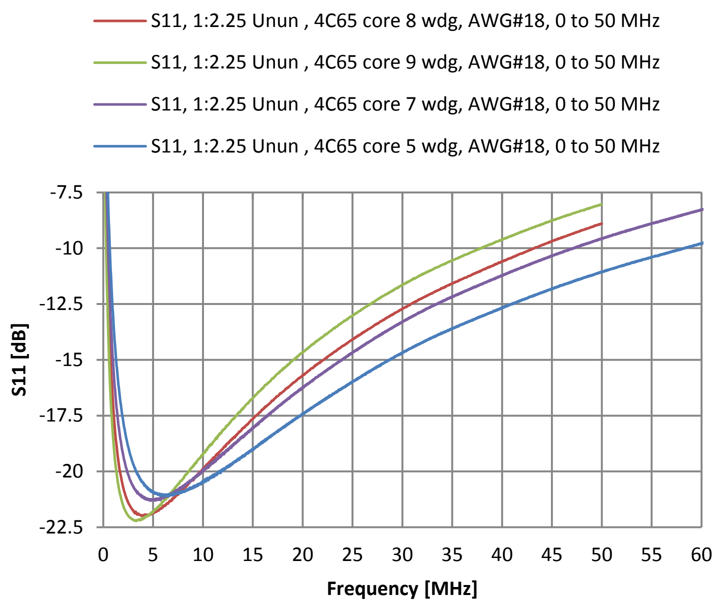

Fig 8.2, The S11 measurement from a single 1:2.25 unun wound on a 4C65 core

In a more detailed graph in Fig 8.3 the lowest usable frequency varies between 300 kHz for a single 1:2.25 unun with 8 windings to 640 kHz for a single 1:2.25 ununs with 5 windings. This makes it clear that the minimum usage frequency shifts up when windings are taken off.

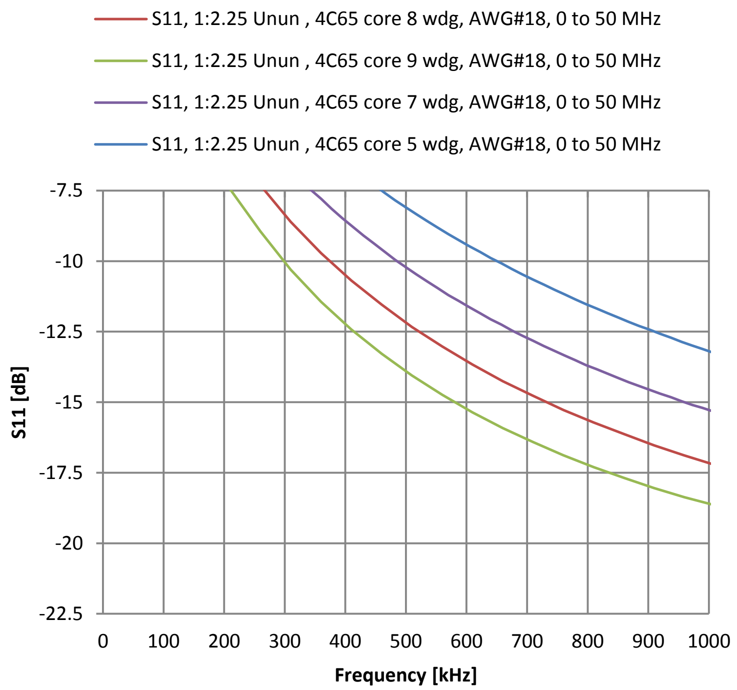

Fig 8.3, The S11 for the 1:2.25 unun with the lowest usable frequency in detail.

The lowest usable frequency shifts from 300 kHz to 660 kHz and the highest usable frequency shifts from 38 MHz to 58 MHz.

After the experiments with the 1:2.25 unun a 1:2 unun was wound.
Here the winding on which the tap was laid was changed instead of the number of windings that was used. Results from these experiments can be seen in Fig 8.4 which show that for a single unun with 9 windings and a tap at 8 windings the maximum usage frequency lies around 48 MHz.

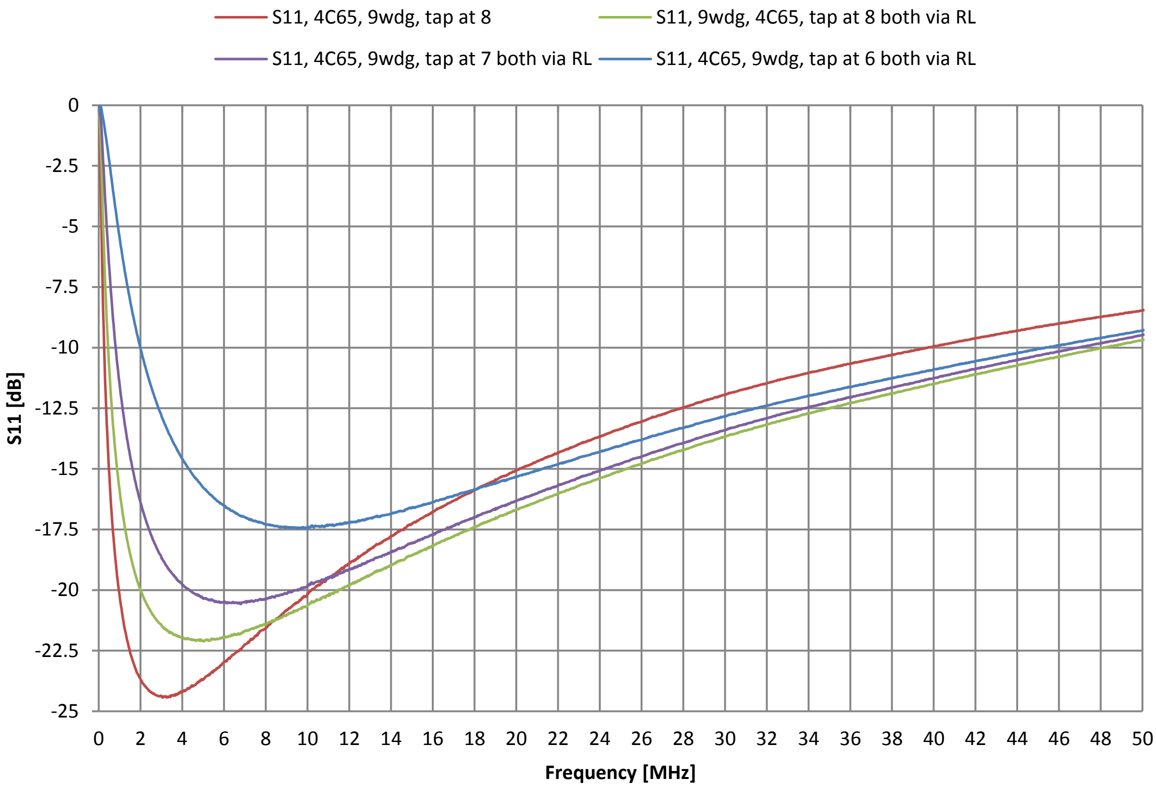

Fig 8.4, The S11 for different taps for a 1:2 unun

Since these experiments seemed to work well the S21 parameters were measured in the same setup as in Fig 7.9 and Fig 7.10 which was used to test the 1:4 ununs.

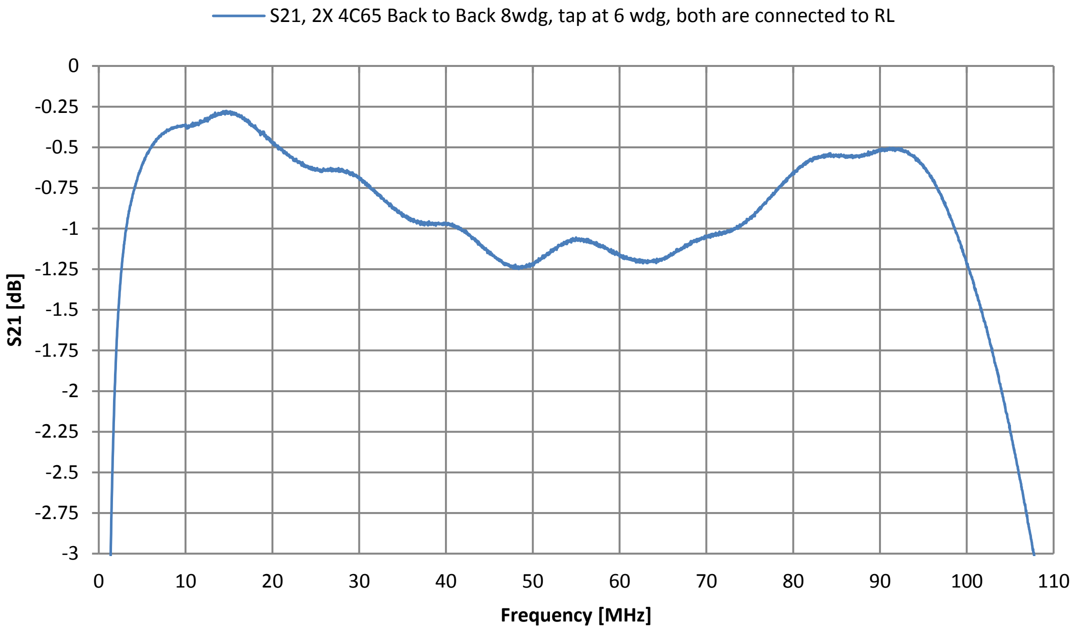

Fig 8.5, The S21 for a 1:2 unun

An unexpected consequence of the back to back coupling is that the lowest usable frequency with the S21 -1 dB margin shifted to 5 MHz instead of at least 2 MHz.
The highest possible usage frequency for an S21 of -1 dB stops around 40 MHz instead of the expected 45 or even 50 MHz. A positive point seems to be however that the 4C65 ferrite core looks usable up to a frequency of around 95 MHz. If the unfortunate dip around 50 MHz in the S21 can be brought back from -1.25 dB to -1 dB or if possible -0.5 dB this would be a very welcome result.

8.2 Power ratings for different core materials

The amount power that is needed to create an electric field of at least 200 V/m rises very fast as can be seen in Fig 3.2 and Table 3.1
For the SLA itself the amount of power fed into it does not matter to much in free space or in a (semi) anechoic chamber because the energy is directly transmitted to the EUT of the groundplane.
However, care should be taken however not to destroy the impedance transmission line transformers. The literature about the amount of power that the unun cores can handle is very scarce. In [**24**] the power that can be send through a TLT has been gathered together in a small table which is reproduced here in **Error! Reference source not found.**. In **Error! Reference source not found.** the core size, wire size and power rating are listed. These data are said to be valid for Nickel Zinc ferrite core with a permeability < 300.

Core size	**Transmission Line wire**	**Power Rating**
1.0 inch (T100) = 25,4mm	AWG #16 - #18	200 W
1.5 inch (T150) = 38.1mm	AWG #14	1000 W
1.5 inch (T150) = 38.1mm	AWG #10-12 or coax	2000 W

Table 8.1, Powerratings for TLT's from [24**]**

Another good reason to stick with Nickel Zinc Ferrite cores comes from Transmission Line Transformers [**24**], Chapter 3 pag 3-15: "Only nickel zinc ferrites with permeabilities below 300 produce efficiencies in excess of 98 percent. High-permeability material like manganese-zinc ferrite, do not, and are not recommended for power applications" Precautions should be taken however that the ferrite or iron powder core is not driven into saturation with the magnetic field and that the temperature increase while operating is kept within the limits of the core. The Curie temperature is the temperature where the core is damaged irreversibly and the ferrite loses it's useful properties Curie temperatures for different ferrite types are usually listed in in respective datasheets. For 4C65 material a Curie temperature of 350°C has been listed and for Type 68 this temperature is 475°C.

8.2.1 Wire for ununs

The maximum voltages and currents that can possibly be found in ununs from 100Ω to 50Ω and from 200Ω to 50Ω for our application were estimated as follows:
With the R in this case to be taken as the impedance of our SLA and P the maximum power of 2.5 kW from the amplifier taken as the input.

$$P = U \cdot R \tag{8.1}$$

$$U = I \cdot R \tag{8.2}$$

$$U = \sqrt{P \cdot R} \tag{8.3}$$

$$U_{z=100} = \sqrt{2500 \cdot 100} \tag{8.4}$$

$$U_{z=100} \sim 500\,V \tag{8.5}$$

$$U_{z=200} = \sqrt{2500 \cdot 200} \tag{8.6}$$

$$U_{z=200} \sim 708\,V \tag{8.7}$$

$$I = \sqrt{\frac{P}{R}} \tag{8.8}$$

$$I = \sqrt{\frac{2500}{50}} \tag{8.9}$$

$$I = 7.1\,A \tag{8.10}$$

Here R is one of the impedances of either 50Ω, 100Ω or 200Ω, P is the power in Watt, I is the current in Ampères and U is the voltage in Volts.
.
The equations above have been filled in with either 100Ω or 200Ω to achieve the maximum values that could be found in a TLT.
If a maximum voltage of 708V and current of 7.1A are taken it is clear that wire of ordinary thickness can't be used.
The high voltage wire that was available in Thales stock according to the NEMA HP3 standard was 1000V dc.

For the maximum current there were two ratings, one for single wires and one for a bundle of wires.
The high voltage wire was specified with a maximum of 6.5A/mm^2 for a bundle of wire. The thinnest wire available with a usable thickness was AWG #16, isolated flexible wire with a diameter of $1.23mm^2$ with silver coated copper strands.

$$\frac{6.5\,A}{mm^2} \cdot 1.23mm^2 = 7.95A \tag{8.11}$$

8.2.2 Maximum core flux

The maximum flux density for both iron powder and ferrite cores was given in [**43**] and here shown in Table 8.2

Frequency	100 kHz	1 MHz	7 MHz	14 MHz	21 MHz	28 MHz
Flux Density in Gauss	500	150	57	42	36	30

Table 8.2, Maximum flux density in Gauss for different frequencies

The formula to prevent saturation in ferrite cores was found in [**44**].

$$B_{max} = \frac{E \cdot 10^2}{4.44 \cdot A_e \cdot N \cdot F} \tag{8.12}$$

Where B_{max} is the maximum flux in Gauss, E is the applied RMS voltage in volts, A_e is the cross section of the core area in cm^2, N is the number of wire turns and F is the frequency in MHz.

For the largest core that is available, the 4C65 core TX102 with a diameter of 102mm the A_e is 2.83 cm^2 and for a frequency of 2 MHz the result is as follows.

$$B_{max} = \frac{\frac{1}{2} \cdot \sqrt{2} \cdot 500 \cdot 10^2}{4.44 \cdot 2.83 \cdot 4 \cdot 3 \cdot 2} \tag{8.13}$$

$$B_{max} \sim 118\ G \tag{8.14}$$

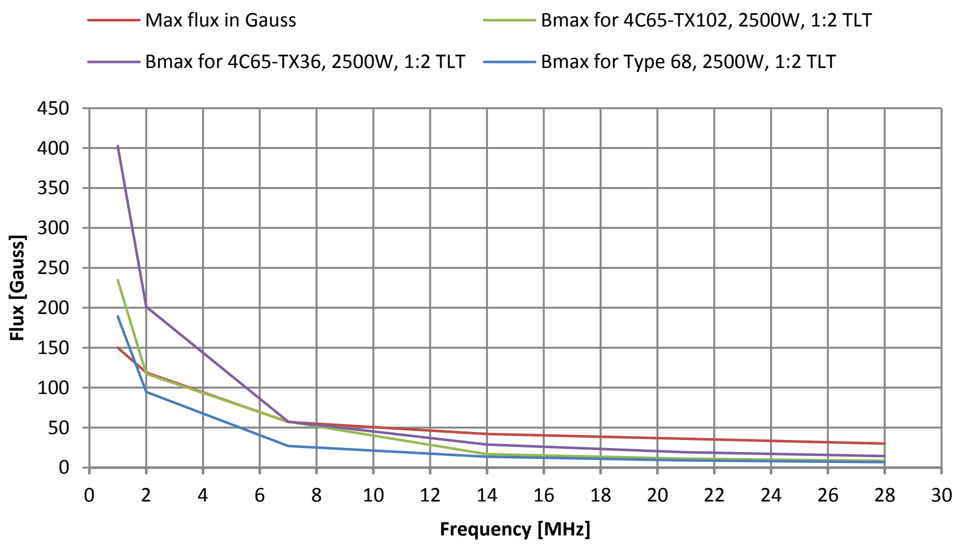

Fig 8.6, Maximum core flux for cores 4C65-TX102, 4C65-TX36 and Type 68

The graph in Fig 8.6 shows that the 4C65-TX102 and Type 68 cores stay below the limit line of Max flux in Gauss for use in a 1:2 unun in terms of maximum flux allowable from Table 8.2.

8.2.3 Temperature increase in ferrite transmission line transformers

In order to see if the selected ferrite cores might be able to provide the required impedance transformation an experiment was done.
A small 100Ω SLA of 60cm high and 97cm wide was built on a table with a pair of TLT's, one TLT on each end.
Power was fed to the TLT and SLA with a IFI 400W amplifier.
With a coupler rated at a maximum power of 200W and a R&S NRP power meter the power send to the TLT and SLA was limited to 200W.

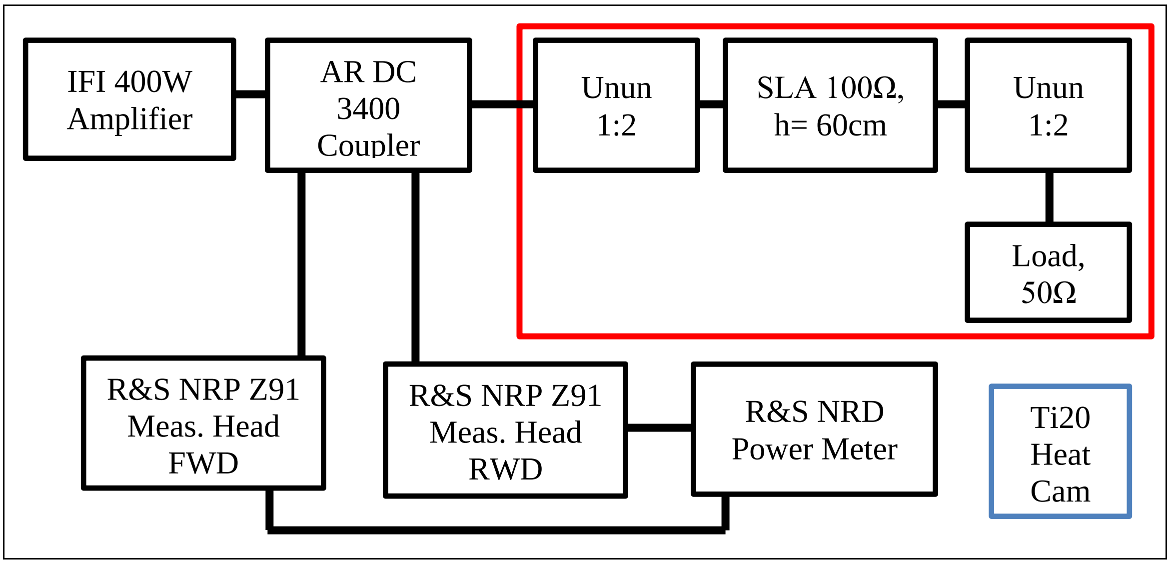

Fig 8.7, Schematic of the unun temperature measurements

In the test two different ununs were used with cores of 4C65 material with a diameter of 36mm and material type 68 with a diameter of 60mm. Both cores have previously been selected for a good Q factor between 2 and 30 MHz and have been wound with a trifilair 1:2 unun. The initial expectation was that both the 4C65 and Type 68 cores would increase in temperature with the increase the power that is sent through the TLT's from the power ratings in Table 8.3.
In order to do temperature measurements within limited time constraints the temperature was measured from a limited number of frequencies where the cores were used for 10 minutes at the same frequency with either 100 or 200W send to the ununs and SLA. In the light of the limited amount of time available and the unfamiliarity of how fast the temperature will be increasing a limited set of frequencies between 2 and 40 MHz has been taken. At each frequency a 10 minute waiting period is kept while sending 100 or 200W to the SLA with TLT's. After 10 minutes waiting the transmitter is powered down and the temperature of the cores is measured using a Ti-20 thermal imager from Fluke Instruments. The transmitter not only for has to be switched off for safety reasons but also because the thermal imager is very sensitive to electromagnetic fields.
Two images in Fig 8.8 and Fig 8.9 show that the 4C65 cores heat up to almost 60°C for the feed end temperature at 25 MHz or almost 50°C at the load end when 200W is send through the ununs.

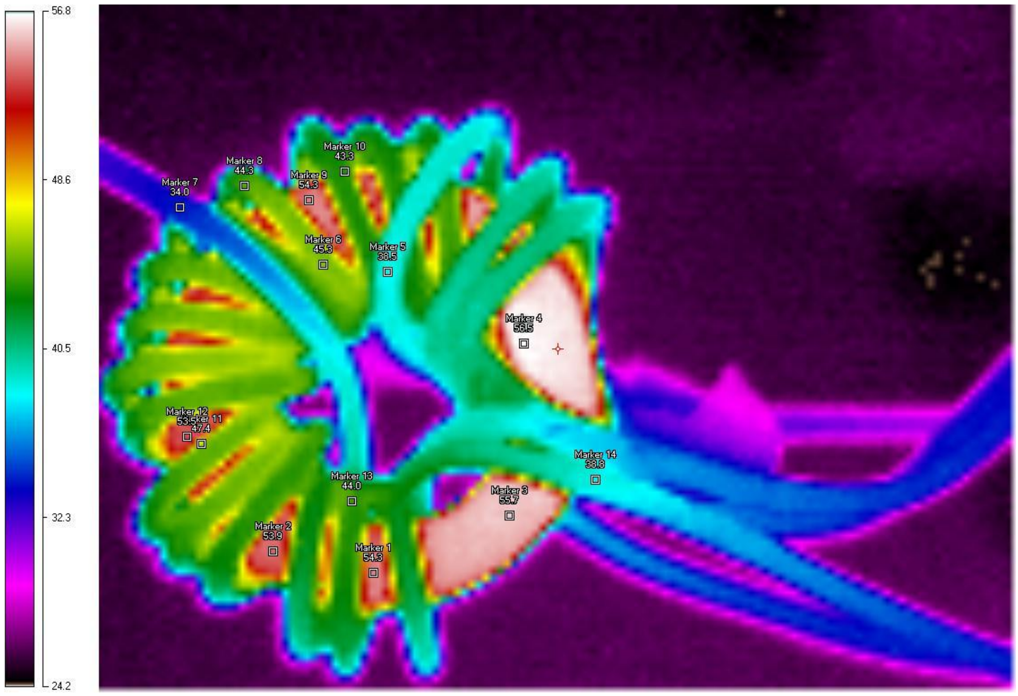

Fig 8.8, Feed-end temperatures in °C at 25 MHz and 200W input

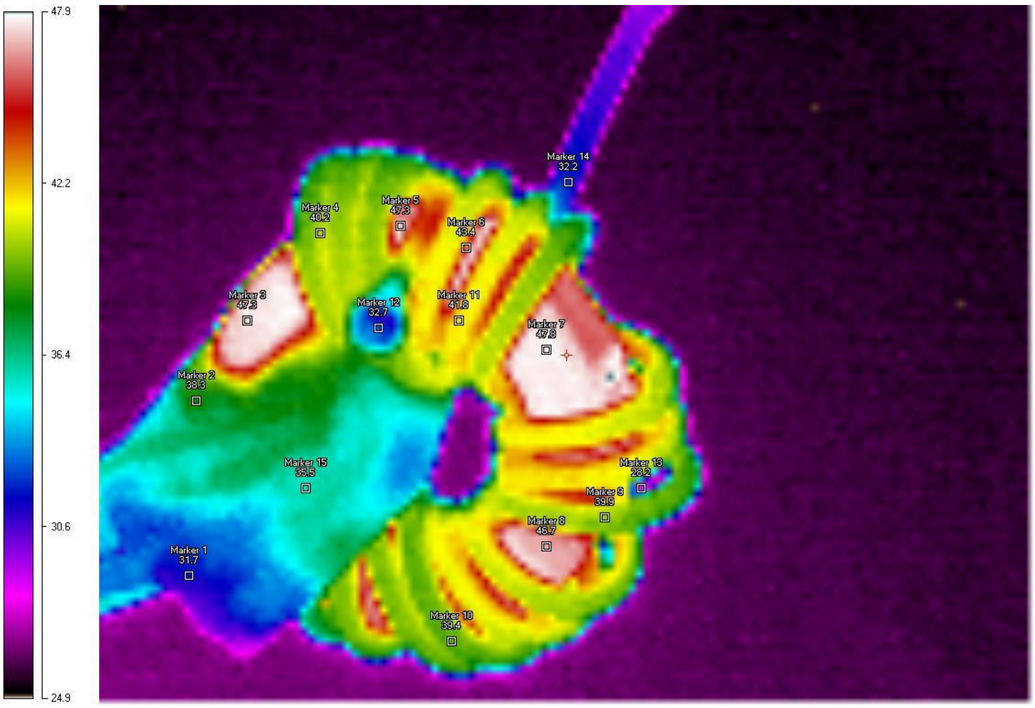

Fig 8.9, Load-end temperature in °C at 25 MHz and 200W input

During the measurements in the anechoic chamber the temperature was roughly 25°C when measuring the temperature of TLT's.

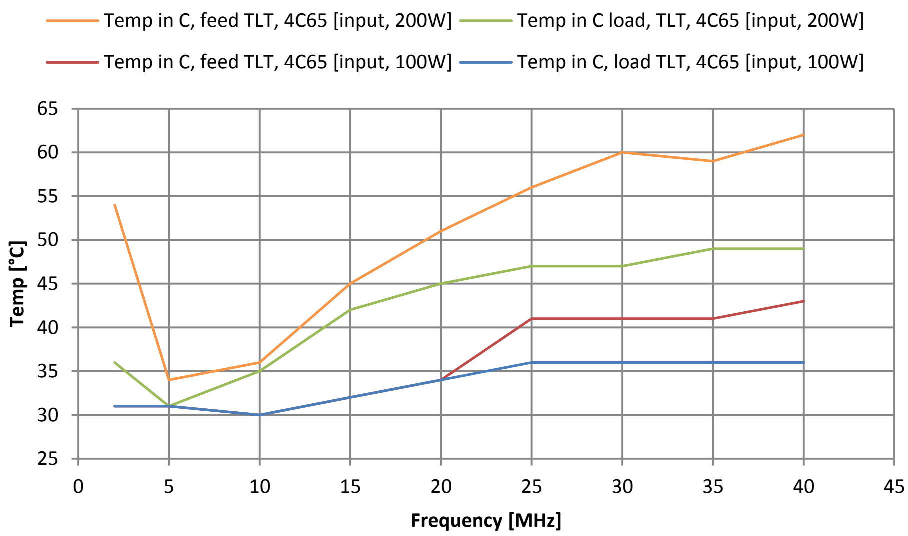

Fig 8.10, Temperature of 4C65, 36mm ununs

As can be seen from the temperature graphs in Fig 8.10 the temperature of the TLT core on the end of the transmitter is warming up to a higher temperature than the temperature of the TLT core on the low end. The temperature would increase to 36°C to 40°C when using 100W but significantly increase to almost 60°C when using 200W. Measurements on the type 68 TLT's with SLA showed that these bigger TLT core can handle more power than the smaller 4C65 core without heating up fast.

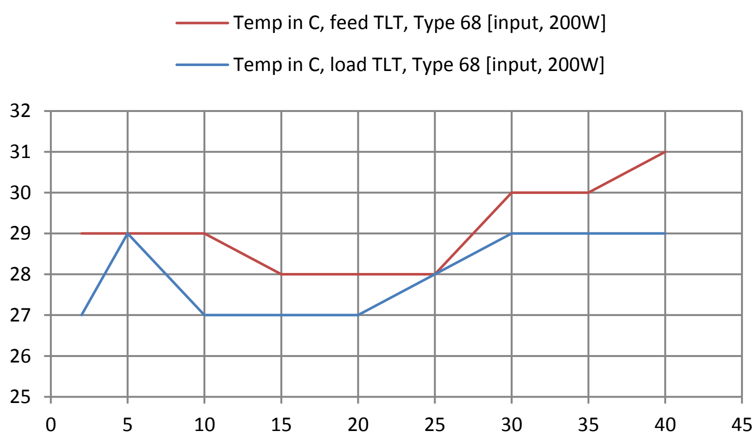

Fig 8.11, Temperature of Type 68, 60mm ununs

By measuring the returned power using the R&S NRP Power meter it was also possible to determine the reflection coefficient which is also known as S11 which is shown in Fig 8.12.

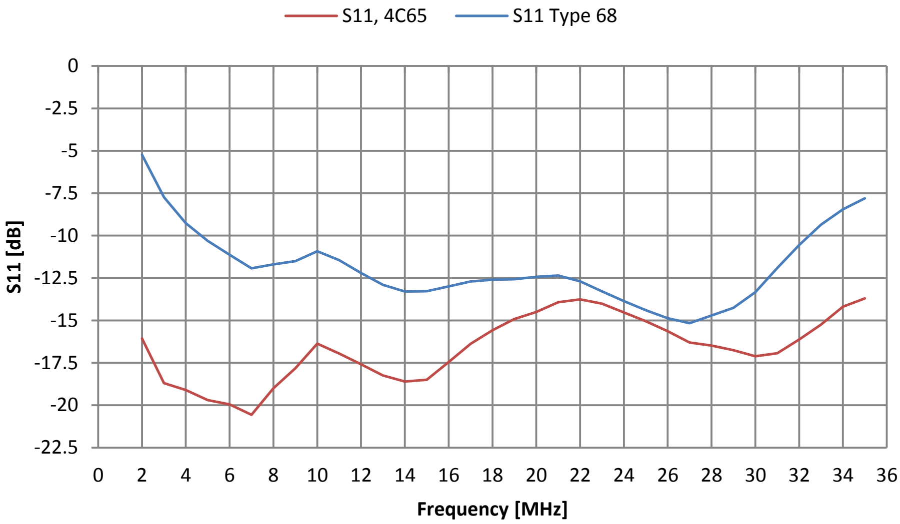

Fig 8.12, S11 from the reflected power

Despite warming up to quite high temperatures the S11 in Fig 8.12 from TLT's made of the 36mm 4C65 cores is better than the S11 from the 61mm type 68 TLT's.
The 200W power that is fed into the ununs and the SLA is the limit for the 4C65 cores with a diameter of 36 mm, the Type 68 ununs with a diameter of 61mm should be able to handle more power.

8.3 Power measurement of stacked cores

The power measurements in paragraph 8.2.3 have shown that the small 4C65 cores suffer from temperature increase at an input power of 200W.
One of the ways this might be mitigated is by using a small stack of multiple cores this increases the volume where the heat is generated and changes the path length over the ferrite core.
Another option is the use of bigger cores of the same 4C65 material with a bigger larger inner- and outer diameter and a larger core cross section.
This paragraph both options have been tested for 2 and 4 stacked 4C65 36mm cores and with a much bigger 4C65 core with a diameter of 102mm.

8.3.1 Construction of TLT's with stacked cores

For the design of a TLT with stacked cores the inductance of the stacked cores with 10 windings were measured using a Hameg 8118 LCR bridge.

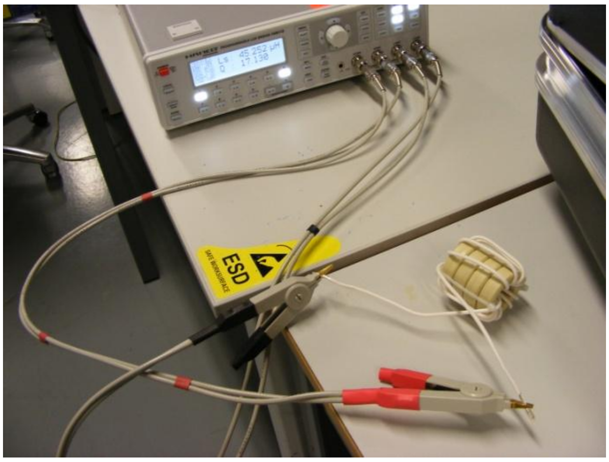

Fig 8.13, Measuring coil inductance using a Hameg 8118

The first reason to do this was because the inductances for windings on stacked cores are not mentioned in the core data sheets.
Another reason to do these measurements was that while constructing a TLT with four cores, two cores fell to pieces on the floor which can be seen in Fig 8.14 and Fig 8.15.
Ferrite cores are very brittle and should not be exposed to shocks.

Fig 8.14, Ferrite core in two pieces

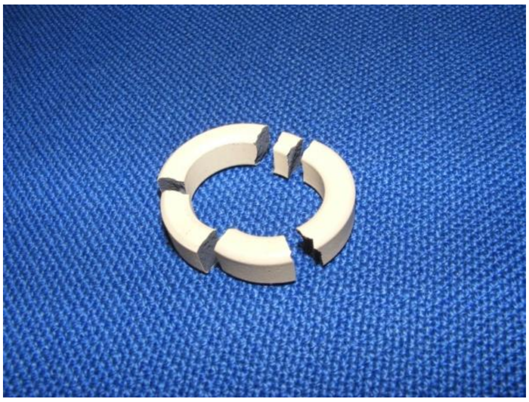

Fig 8.15, Ferrite core in five pieces

Repairing these cores could be done with glue from a list obtained from [**45**] which recommend several types of glue and specific pressure using a spring.
These specific glues were unavailable and the quick option was to glue all pieces together with Loctite 460.

In order to keep the ferrite cores together for the experiments, sets of two cores were taped together and sets of 4 cores were held together using tie-wraps such as can be seen in Fig 8.16.
The windings of the TLT's with the small 4C65 cores were laid using AWG #16 which is the same as for the TLT's in 0.

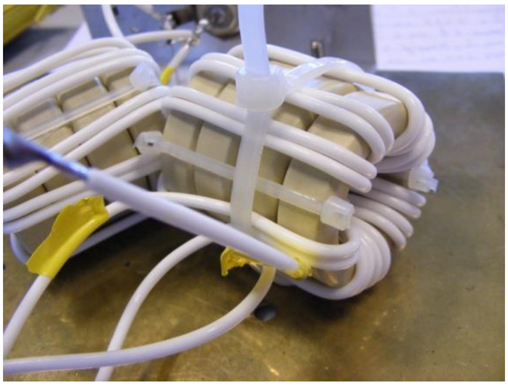

Fig 8.16, Details of 1:4 TLT's with four cores

As can be seen from Table 8.3Table 8.3, Inductance for 1, 2 and 4 cores stacked the impedances with 10 windings differ somewhat for whole or broken cores.

Number cores	L in uH for 10 windings
1 core (glued)	11-13 µH
1 core (normal)	12 - 15µH
2 cores (glued)	22 - 25 µH
2 cores (normal)	24 - 30 µH
4 cores, (2 glued)	45µH
4 cores (normal)	60µH

Table 8.3, Inductance for 1, 2 and 4 cores stacked

The S11 was measured with single TLT's in the same manner as seen in Fig 7.5 and Fig 7.6 with a resistor of 100 or 200Ω for the 1:2.25 and 1:4 TLT.

The windings of the TLT determine using a similar design procedure as in paragraph 8.1 except for the tap on the windings of the 1:2.25 TLT's.
In this the choice was made not to try to build the best possible TLT but to create TLT's that have some properties in common, in sacrifice for performance at the high end of the frequency range. This was done to see if the temperature increase more would be when the S11 would get worse.

TLT	**Windings**
1:4, two cores	2x 9wdg
1:4, four cores	2x 9wdg
1:2.25, two cores	3x 5wdg, no tap
1:2.25, four cores	3x 5wdg, no tap

Table 8.4, Winding details for different TLT's

Gluing the cores did have some impact in the high frequency range of the TLT usage.
For the S11 of the 1:2.25 TLT the maximum usable frequency decreased from 32 to 30 MHz as seen in Fig 8.17.

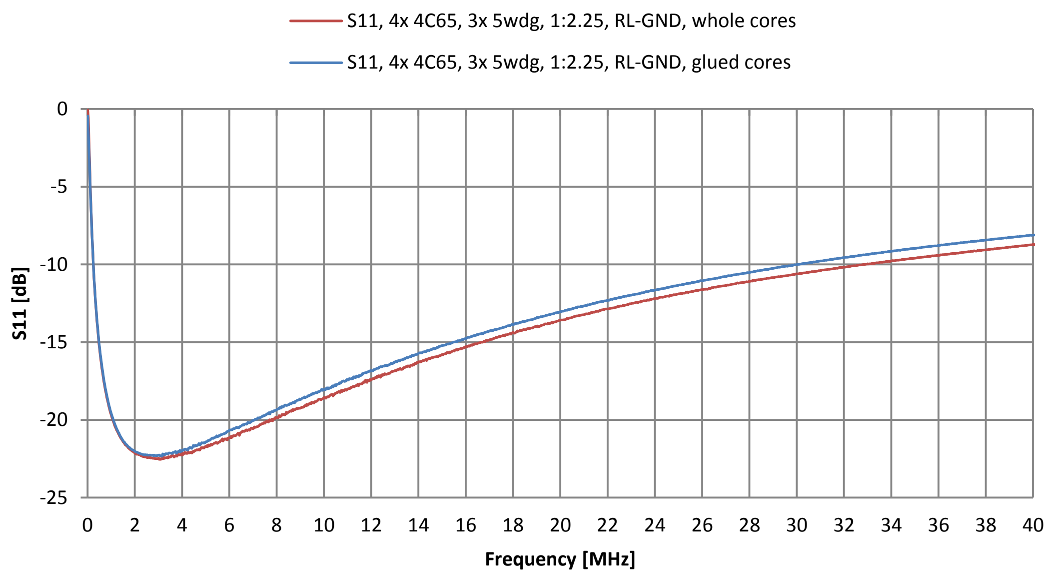

Fig 8.17, S11 for glued and normal cores with a 1:2.25 unun

The S11 for the 1:4 TLT decreased roughly 2-3 dB in the frequency range between 4 and 26 MHz for the glued cores, the maximum usage frequency increased from 40 to 42 MHz which can be seen in Fig 8.18.

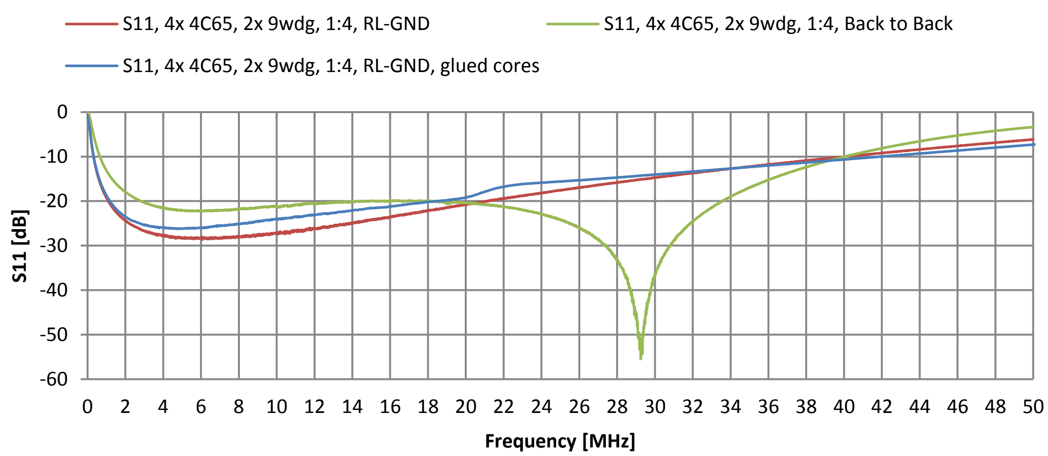

Fig 8.18, S11 TLT's 1:4 with glued, whole cores and back to back measurement

The glued cores have a slightly decreased performance for the 1:2.25 TLT's in the high end of the frequency range.

8.3.2 Temperature increase in stacked and large core TLT's

The temperature increase was measured a similar manner as in paragraph 8.2.3, the temperature of the semi anechoic chamber where the experiments were performed stayed almost constant around 23°C.
The test setup was almost the same as in Fig 8.7. Changes to the setup were that the thermal imager was replaced by the Fluke 65 infrared temperature meter as can be seen in Fig 8.19 and the setup was modified for testing 1:4 TLT's. For testing the 1:4 TLT's

the 100Ω SLA was replaced with the 200Ω SLA from Fig 7.5 and the 1:2 TLT's were replaced by the 1:4 TLT's.

Fig 8.19, Temperature measurement with the Fluke 65

The temperature increase for the 1:4 TLT's with two cores has been plotted in Fig 8.20 for the TLT at the feeding end of the SLA. With an input of 50 dBm (100W) the temperature increases gradually up to 37 °C at a frequency of 50 MHz. When an input of 53 dBm (200W) is send to the TLT's with ununs the temperature increases also gradually from 31 °C at 5 MHz up to 47 °C at 50 MHz with a fast rising temperature to 60 °C at 55 MHz and peak temperature of 64 °C at 60 MHz.

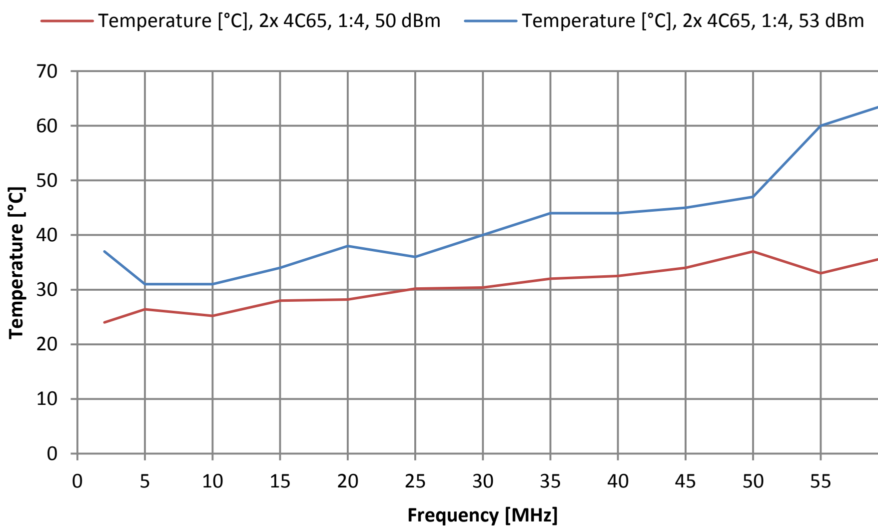

Fig 8.20, Temperature increase for two cores as a 1:4 TLT

The temperature increase for the 1:4 TLT with two cores differs between 5°C and 10°C when the power is increased from 50 dBm to 53 dBm for the frequency range between 2 and 50 MHz.
Temperature increase for input of 50 dBm (100W) is a little lower when using four cores instead of two cores.
In Fig 8.21 it can be seen that for all frequencies the temperature of the 1:2.25 TLT's is between 1°C and 2°C lower for the TLT with four cores compared to the TLT with two cores.

The temperature increase for the 1:4 TLT's in Fig 8.21 with two cores varies in such a wild manner between 2 and 15 MHz that there is not much of an advantage to be seen for the use of four cores.

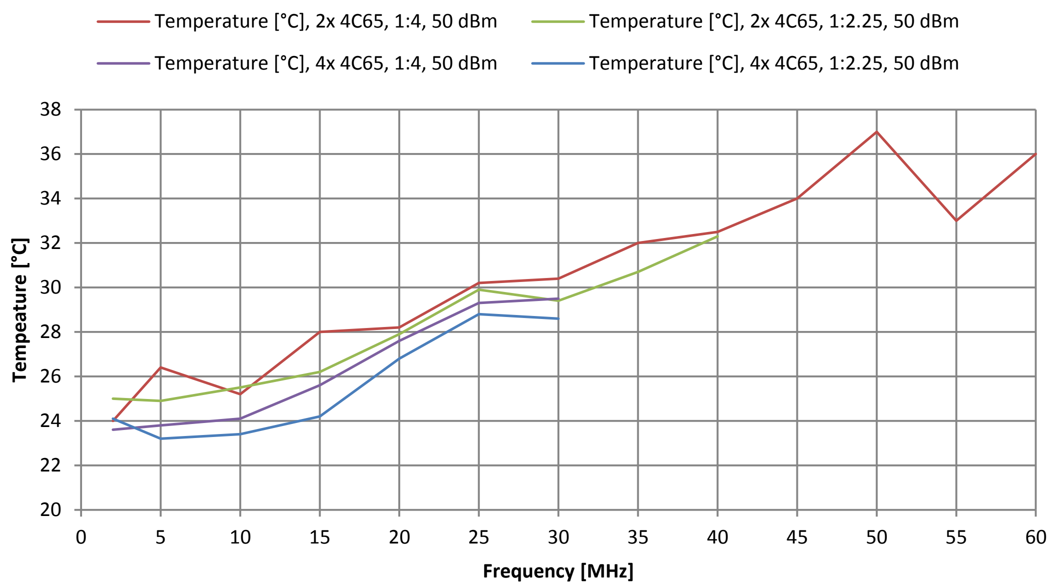

Fig 8.21, Temperature increase for 50 dBm input

For the input power of 53 dBm (200W) the temperature graph is given in Fig 8.22. The core temperatures for TLT's with 2 cores vary between 30°C and 40°C, and vary between 25°C and 39°C for TLT's with four cores. In almost all cases the temperature of the TLT's with four cores is lower than the temperature of the TLT's with two cores.

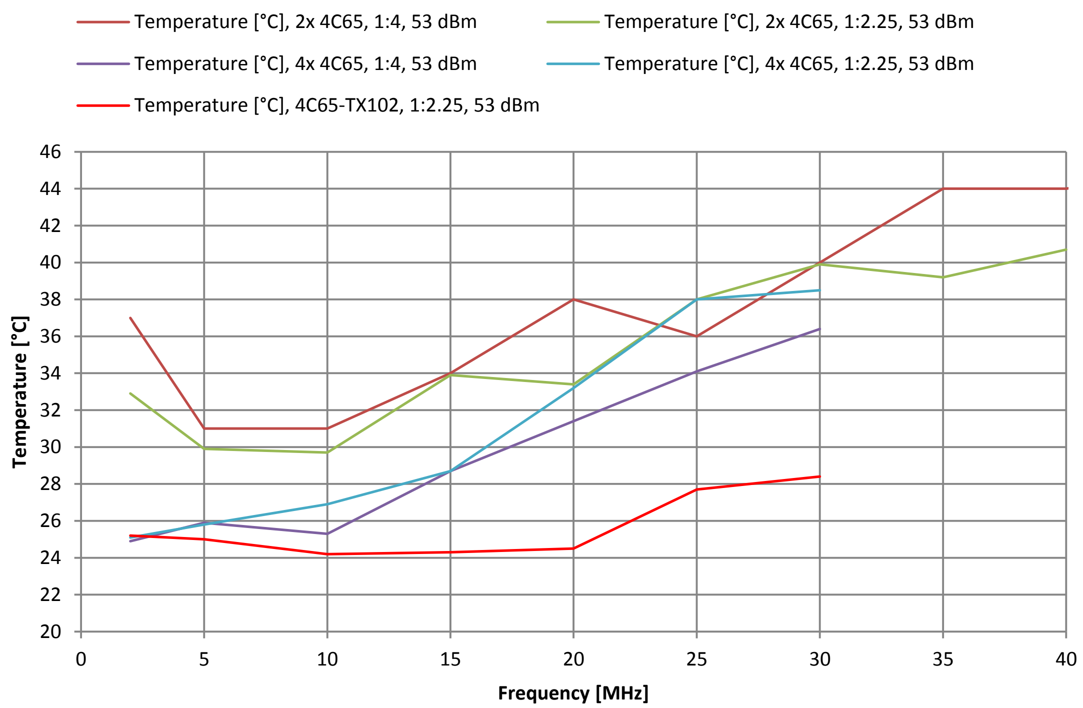

Fig 8.22, Core temperatures with 53 dBm input

One TLT with a noticeable lower temperature in Fig 8.22 is the TLT which has been constructed using a 102mm wide 4C65 core. The temperature for the large TLT's varied between 24°C and 29°C. These large TLT's were wound with 3x 4 windings of AWG #10 wire as shown in Fig 8.23.

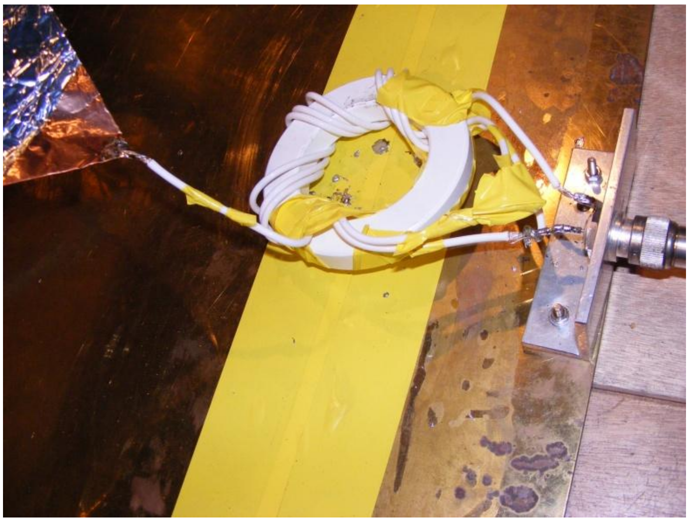

Fig 8.23, 4C65 core with 102mm diameter

Despite the fact that several cores were glued together their temperature in when used as a TLT did not vary significant between the normal or the glued cores this can be seen in Fig 8.24. The image was taken with the Ti-20 thermal imager just after the 10min waiting time at 50 MHz with 50 dBm input. Both glued cores were positioned at the center of the set of stacked cores. The temperature of the stack is the same at 37°C.

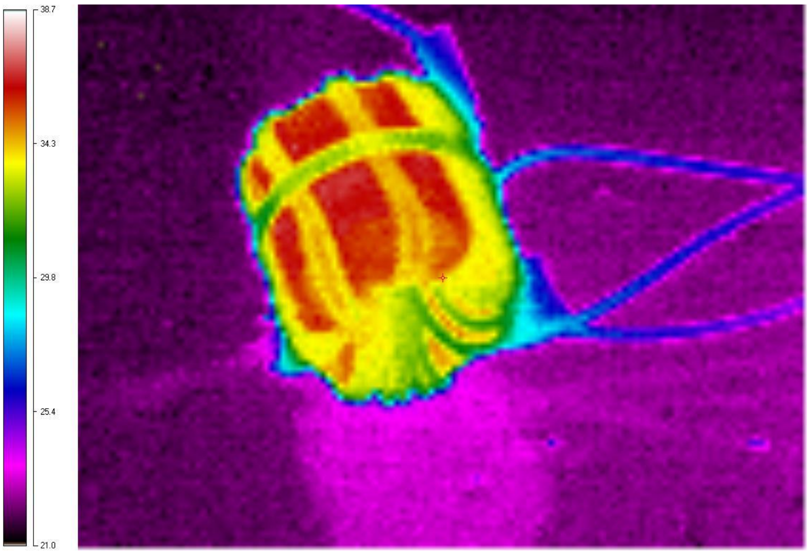

Fig 8.24, Thermal image of the 4x 4C65, 2x 9wdg, 1:4 TLT

The S11 for TLT's with increased temperature in Fig 8.25 showed not in all cases a direct overlap between the S11 getting better or worse with the increase of frequency and the temperature increases in Fig 8.21 and Fig 8.22.
For the frequencies of 2 and 5 MHz the S11 gets better for every TLT. This can be seen in Fig 8.25 and Fig 8.26 which only leads to a temperature decrease for the TLT's with a big core or two cores in Fig 8.22.
The temperature increases for each TLT at 50 dBm in Fig 8.21 or at 53 dBm in Fig 8.22 between 10 and 15 MHz but the S11 actually gets better for three out the five tested TLT's in Fig 8.25 and Fig 8.26.
Only between 15 and 30 MHz the temperature increases for all TLT's in Fig 8.21 and Fig 8.22 and the S11 gets worse in Fig 8.25 and Fig 8.26.

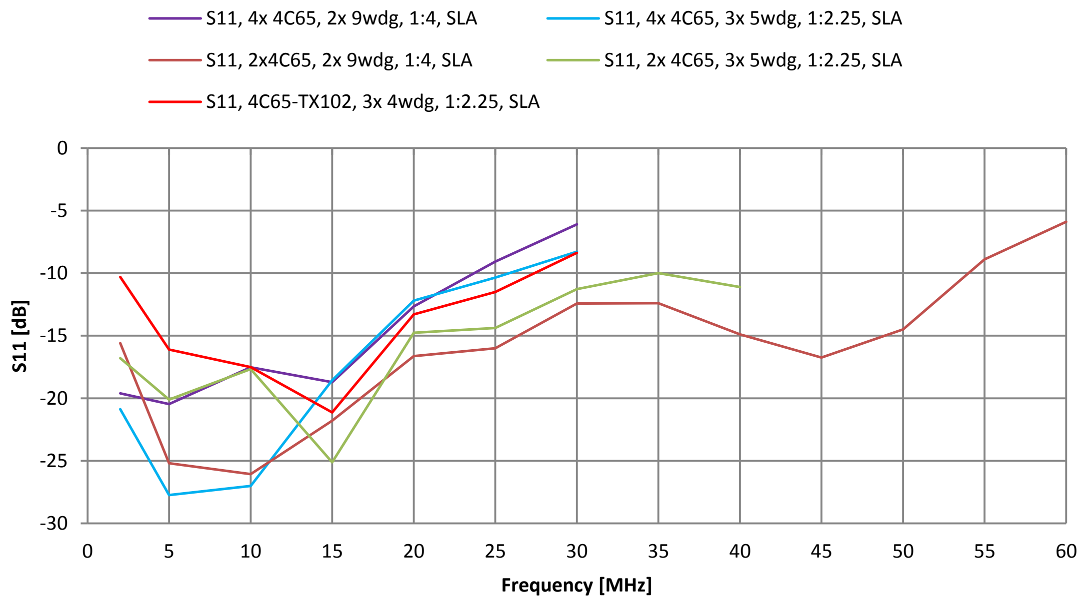

Fig 8.25, S11 calculated from 53 dBm input

When comparing the S11 from Fig 8.25 which was calculated from the reflected power during the temperature measurements and S11 which was measured with the R&S ZVL 13 in Fig 8.26 it is easy to see that the S11 does not significantly while being fed with 53 dBm.

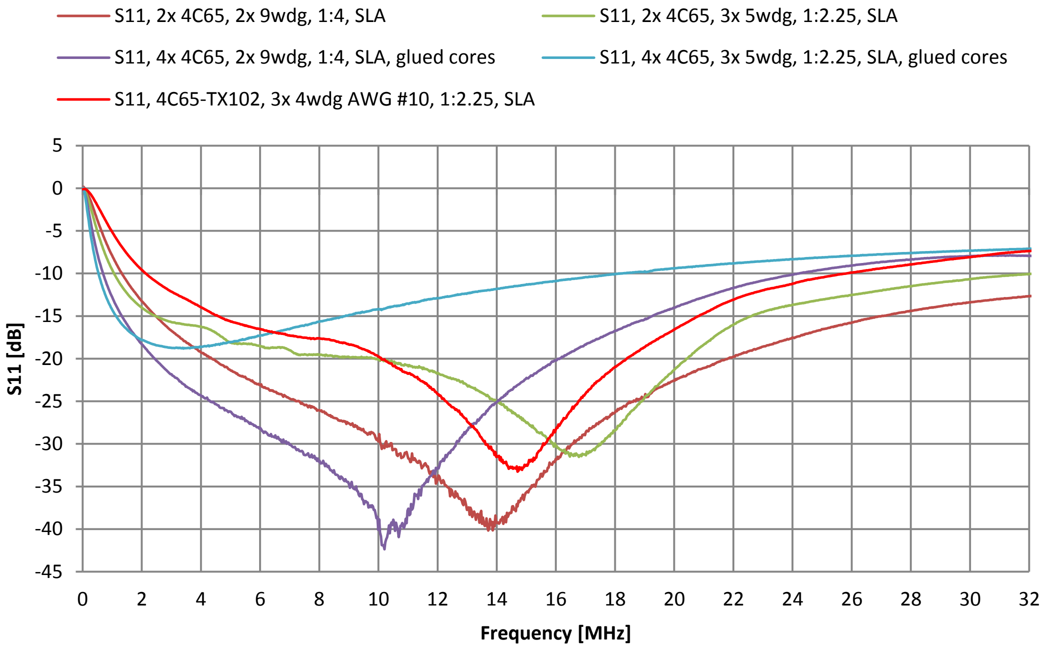

Fig 8.26, S11 measured with R&S ZVL 13 VNA

As can be seen from Fig 8.20, Fig 8.21 and Fig 8.22 the stacking of multiple small cores doesn’t offer a solution for the temperature increase in TLT’s that offers the perspective of using the >2 kW required to generate an electric field of 200 V/m for testing equipment of 2.0m high.

In this chapter the 1:2 and 1:2.25 ununs have been tried tested with different results.
The small 4C65 with a diameter of 36mm have a better S11 than other cores. Unfortunately single or multiple of these small cores or heat up to temperatures of over 60°C with only 200W of input power.
The large 4C65 core with a diameter of 102mm with a maximum temperature of 28°C and the Type 68 ferrite with a diameter of 61mm with a maximum temperature of 31°C can probably withstand testing with more transmission power before heating up to higher temperatures.

Chapter 9 Wire based striplines

The creation of a 100Ω SLA with a large volume that can be used to test equipment with a height of 2m might be done in foil or using large plates.
The large size and weight make is very hard to handle a very large SLA made out of metal plates or foil.

For the creation of an SLA different approaches can be taken as can be read in [**46**].
The SLA can built using solid plate material or one can be constructed out of parallel wires.

9.1 Spacing between the wires and stripline antenna height

When the plate at the top is replaced by a number of parallel wires the e-field changes and the effective height changes.

The equation for the added change in height as taken from is:

$$\Delta y = \frac{d}{\pi}\ln\left({}^{d}\!/_{\pi c}\right) \tag{9.1}$$

Where Δy is change in effective height, $2d$ is distance between the wires, c is the core diameter of the wire.

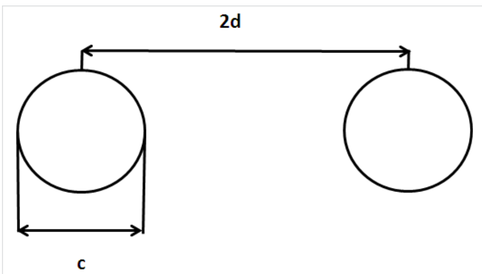

Fig 9.1, Core diameter and distance between wires

The width of the SLA and the width between the wires are two variables that can be played with while designing a wire based SLA.
The total amount of possibilities in building different wire SLA's is nearly infinite.
The closer the wires are and the more wires there are the more the SLA resembles an SLA made out of plate material.
Since no further specifications are known, the replacement of the plate model with a wire construction is a thankful CEM exercise.

9.2 Wire models in FEKO

For the SLA simulation in FEKO two models were created. One model with 9 wires in Fig 9.2 and one model with 17 wires in Fig 9.3. The reason for creating these model with an odd number of wires was that the middle wire could be center wire could be exact at the center of the wire SLA with 4 or 8 wires on each side. The initial height was assumed to be 60cm with a width of 1m and a length of 2.1m. Just as in the SLA FEKO models with plates from paragraph 5.2.1 the ground plane in computational model is assumed to be a perfect electrical conductor.
The exact description of these SLA models as they were used in FEKO can be found in Appendix E.

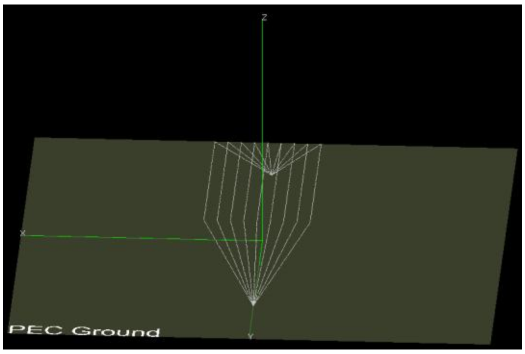

Fig 9.2, FEKO 9 wire model

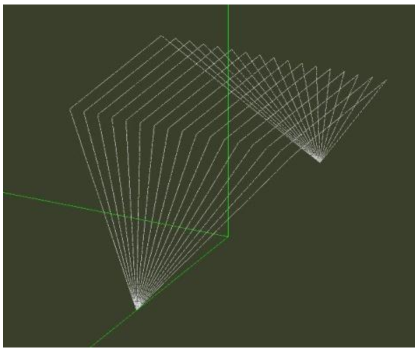

Fig 9.3, FEKO 17 wire model

The results of the S11 parameter of the FEKO models with 9 and 17 wires can be seen in Fig 9.4. As is clear from the S11 graph the models with 9 and 17 wires perform well with a minimum S11 of -20 dB at a frequencies between 2 and 30 MHz.

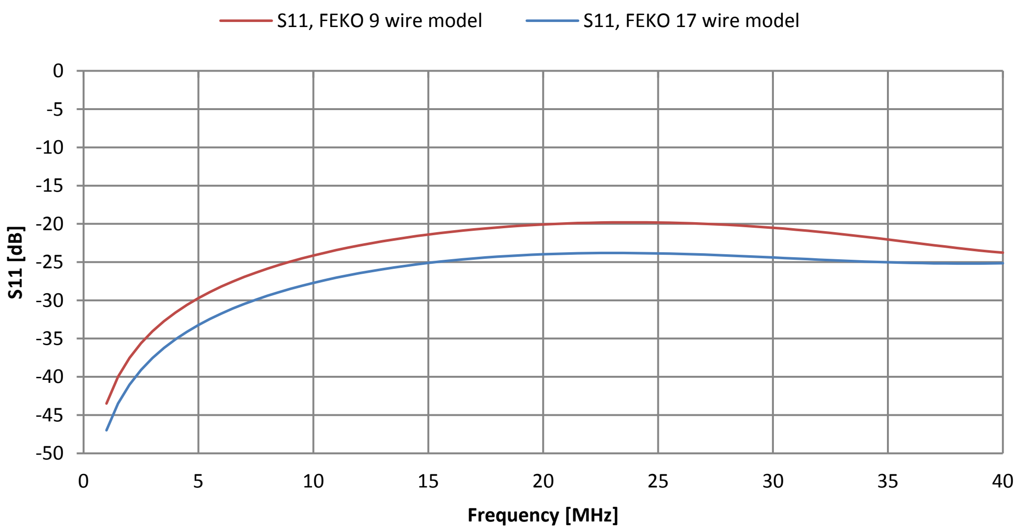

Fig 9.4, S11 for FEKO models with 9 and 17 wires

Since the ground plane of the SEC1 nor an small laid ground plane in SEC2 extend to infinity the FEKO model had to change accordingly.
Another question was also how many wires would at least be needed to create an SLA which would work with the least amount of wires. In Fig 9.5 picture a model of a wire SLA with 7 wires and a limited ground plane made of small triangles can be seen. The

points in M1 and M2 are for the center wire, the numbered points A, B, C and D are for the SLA wires. Not clearly visible in the picture but used in the model are the points E and F for the load and feeding wire.
The ground plane with the points named G was simulated as a copper plate. This ground plane was extended to 1.5 times the SLA width and l.1 time the SLA length to resemble a situation in with a limited ground plane that might be encountered in SEC1 or SEC2.

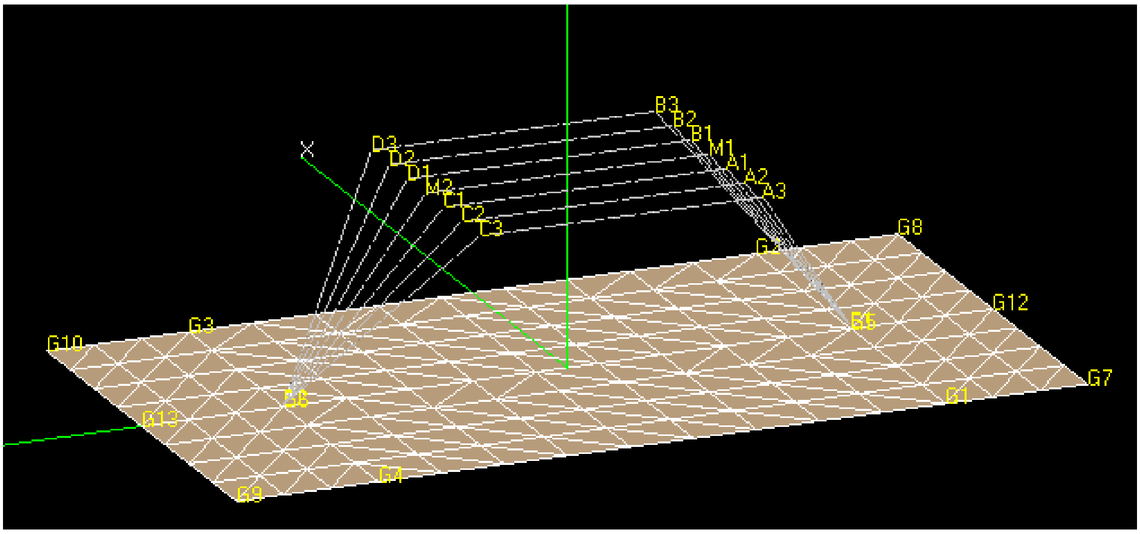

Fig 9.5, The FEKO wire model with surface triagles

The BO graph in Fig 9.6 stands for the model with an infinite ground plane and the GP graph stands for the limited ground plane made out of surface triangles.
A limited and meshed ground plane means that the Greens function is no longer used by FEKO. This not only makes that the computation takes longer but also increases the S11 to -8 dB as can be seen Fig 9.6.

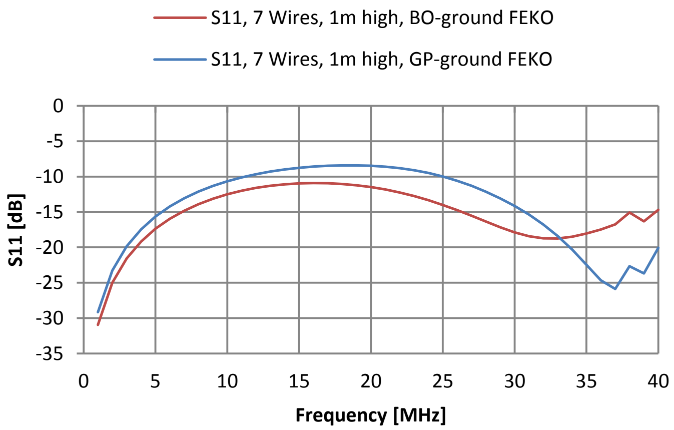

Fig 9.6, S11 for 100Ω FEKO wire models with 7 wires

9.2.1 Large wire models in FEKO

Before realizing a large SLA in the SEC1 a study of the computational models was done. The earlier created models were in this case simply increased in the number of wires and in the physical size of 4.85m wide 3.00m high and 7.0m long. To keep the computational time low, the refinement of the wires was limited to $\lambda/10$ instead of the finer meshed $\lambda/100$.
As can be seen in graph Fig 7.9, the S11 is bigger than -10 dB form models with 9 wires with frequencies between 5 and 8 MHz and a strange peak around 26 MHz which is appears in all models.

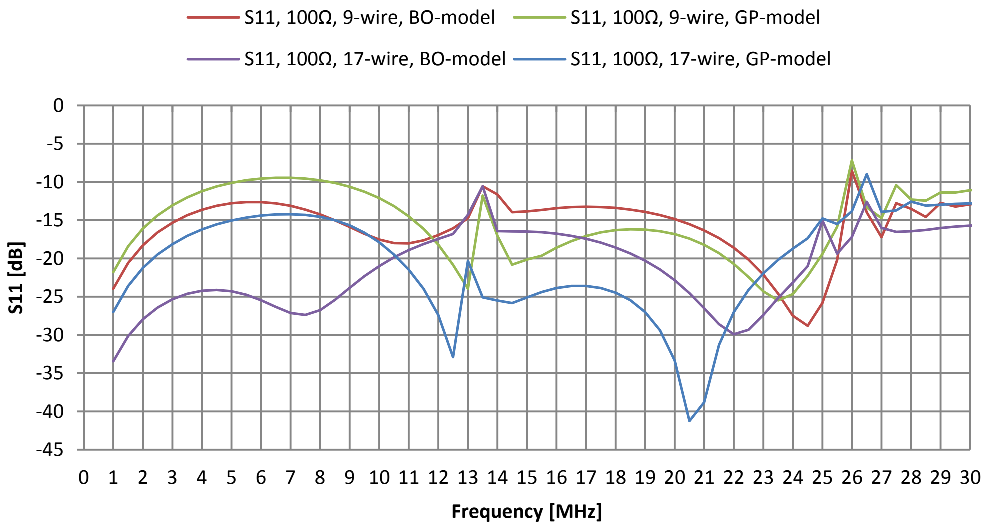

Fig 9.7, S11 from FEKO 100Ω wire models

One of the attempts to make a better working SLA model in FEKO was to add horizontal wires at the transition points between the sloped wires and the horizontal wires.

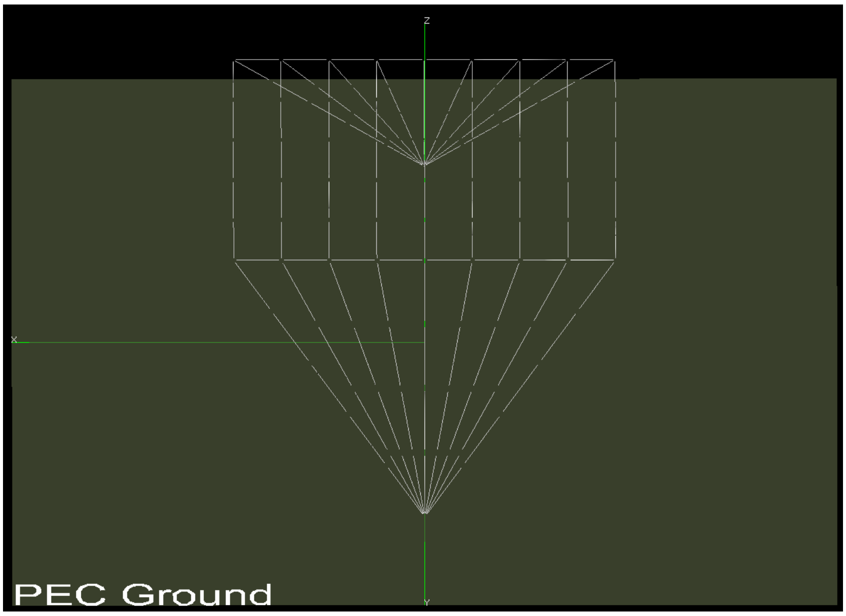

Fig 9.8, FEKO 9-wire 100Ω model with horizontal wires

As the results in Fig 9.9 show is that the disturbances between 13 and 15 MHz in the Fig 9.7 graph are not visible. The peak around 26 MHz from Fig 9.7 is no longer visible in Fig 9.9 the smaller disturbances 22 to 25 in graph XY are below -10 dB which means that the antenna fulfills our -10 dB requirement.

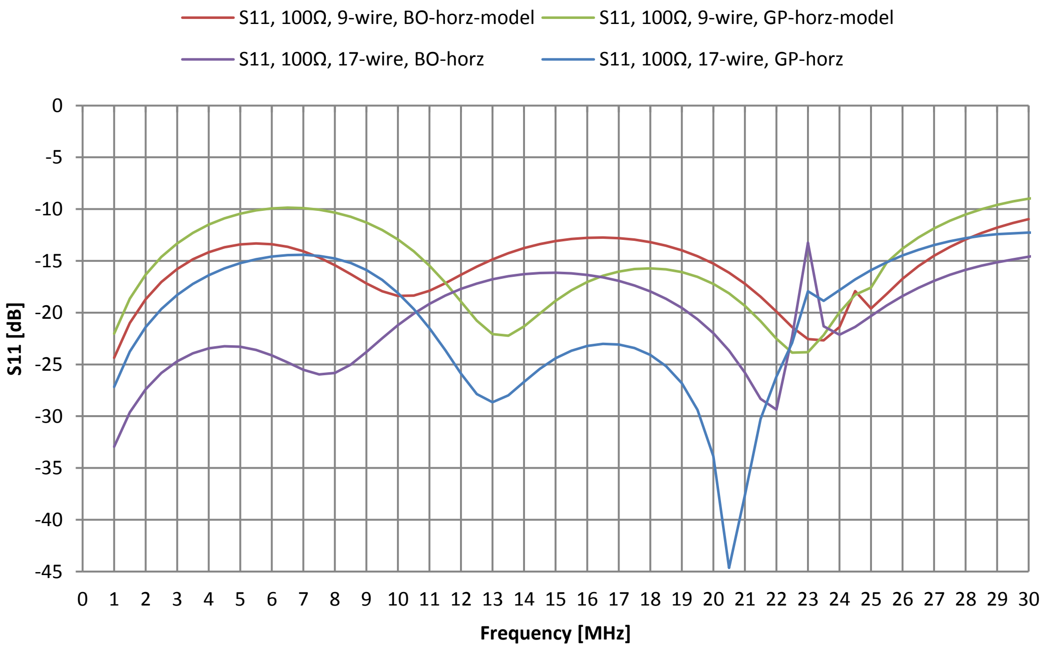

Fig 9.9, S11 for the FEKO 100Ω wire models with horizontal connection

In another simulation the 200Ω wire SLA with a width of 0.85m and a height of 3.0m and a length of 7.0m has also been tried. This 200Ω wire SLA model can be seen in Fig 9.10

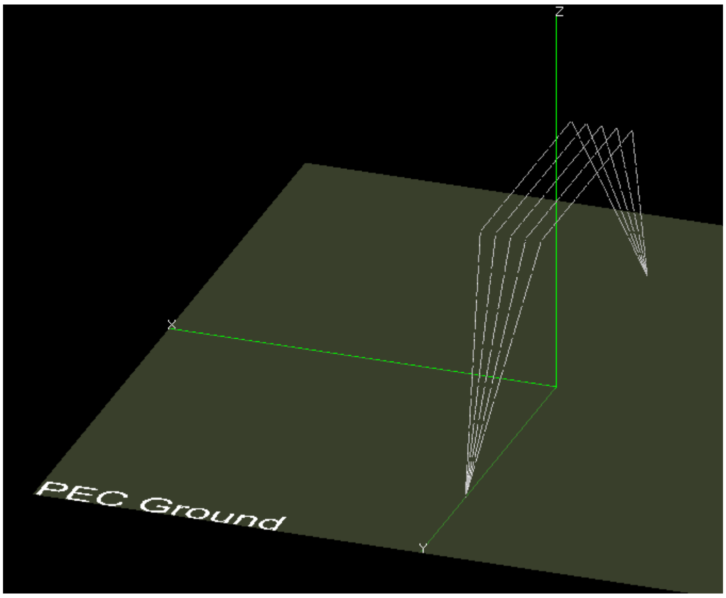

Fig 9.10, FEKO 200Ω, 5-wire SLA model

The S11 graph in Fig 9.11 shows that this model has an S11 which is better than -20 dB over a frequency range from 2 to 30 MHz..

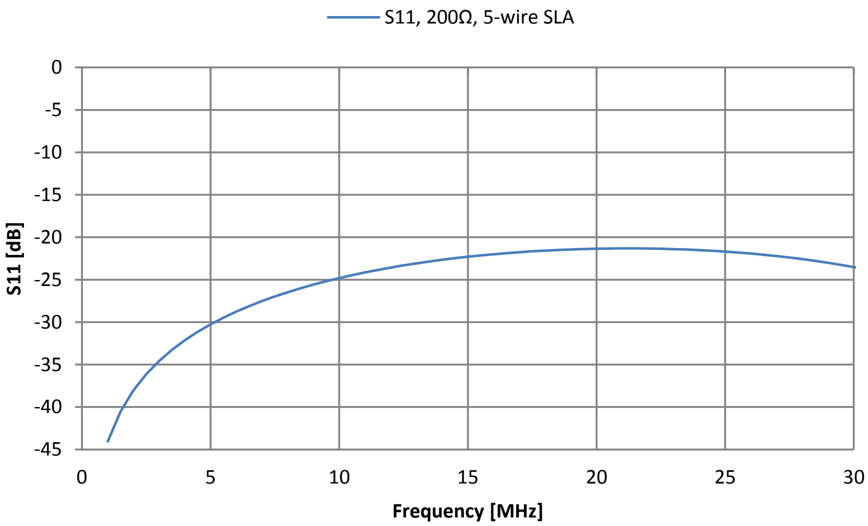

Fig 9.11, S11 for the FEKO 200ohm, 5-wire SLA

9.3 Practical stripline antennas in anechoic chambers and open air testing

To test wire SLA’s two small realizations each with different amounts of wire were built to see whether the wire SLA would work in practice. The construction of wire SLA’s was undertaken with three different models.

I. One SLA with 9 parallel wires, 60cm high, 1m wide, visible in Fig 9.12
II. One SLA with 16 parallel wires, 60 cm high, 1m wide, visible in Fig 9.13
III. One SLA with 7 parallel wires 1m high, 1.60m wide, visible in Fig 9.15

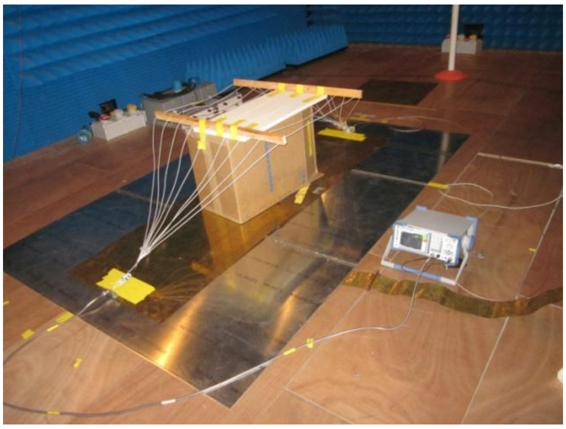

Fig 9.12, Wire SLA with 9 wires measured in SEC2

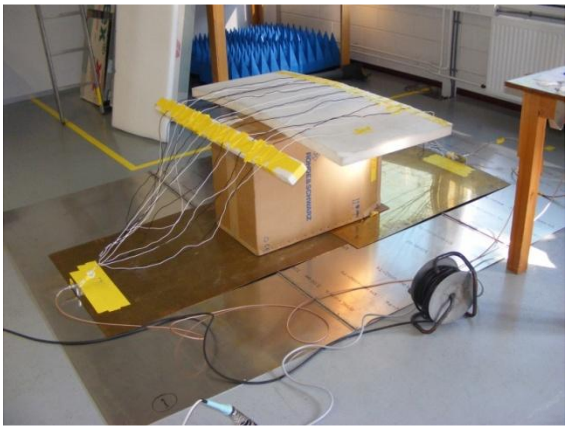

Fig 9.13, Wire SLA with 16 wires measured outside SEC2

The S11 graph of 60cm the high wire SLA’s can be seen in Fig 9.14 with a -10 dB bandwidth between 2 and 30 MHz when used in combination with the TLT’s on 4C65 cores from paragraph Ununs for 50:100Ω from paragraph 8.1 with 7 windings.

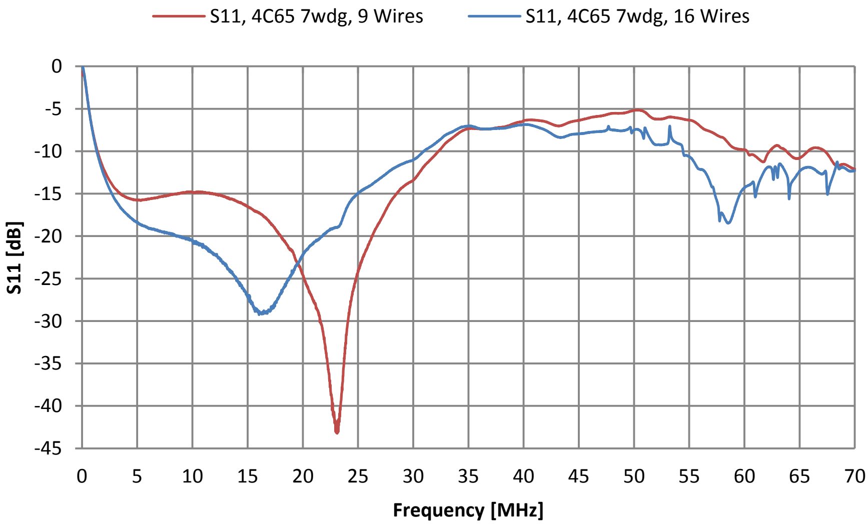

Fig 9.14, S11 measurement of two 60cm high wire SLA’s with 9 and 16 wires

Since the S11 in Fig 9.14 is equal or better than -10 dB the wire SLA seem to have the potential to replace the plate SLA.

The final wire SLA model that has been scaled up from the small models with a height of 60cm changed to 1m and a width of 1.0 m changed to 1.60m is a 7 wire SLA in Fig 9.15.

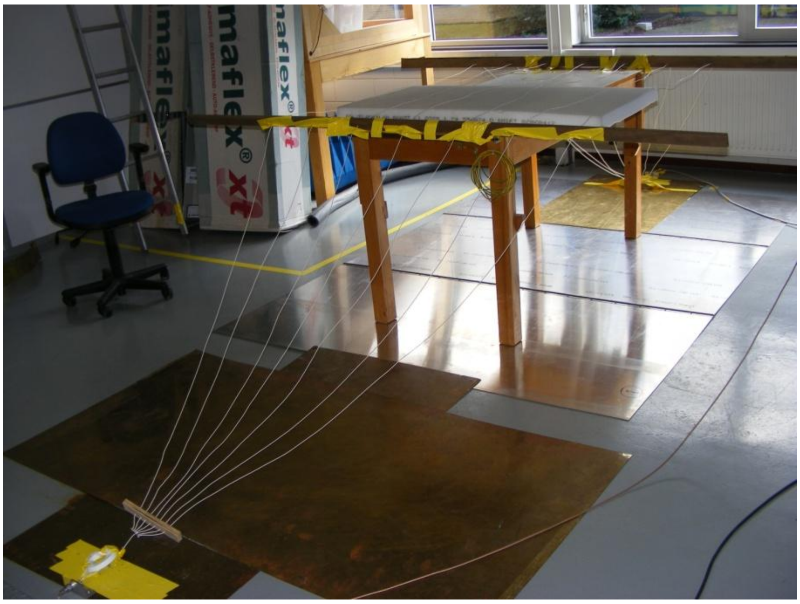

Fig 9.15, The 7 wire SLA outside SEC2

Measurements with the 7 wire SLA were done in three locations:

I. Outside the anechoic chamber, with a ground plane denoted as OAT-GND
II. Inside a fully anechoic chamber with a ground plane placed on the floor denoted as SEC2-GND
III. Inside a semi-anechoic chamber with a full conducting ground plane, denoted as SEC1.

The TLT's used in the measurements from Fig 9.16 are wound on a large 4C65 core with an outer diameter of 102mm with 5 windings of AWG #16 wire.
The S11 measurement results from the 7 wire SLA can be seen in Fig 9.16 and Fig 9.17. Clearly visible in Fig 9.16 is that the used TLT and wire SLA provide a sufficient S11 bandwidth of -10 dB between 2 and 38 MHz.

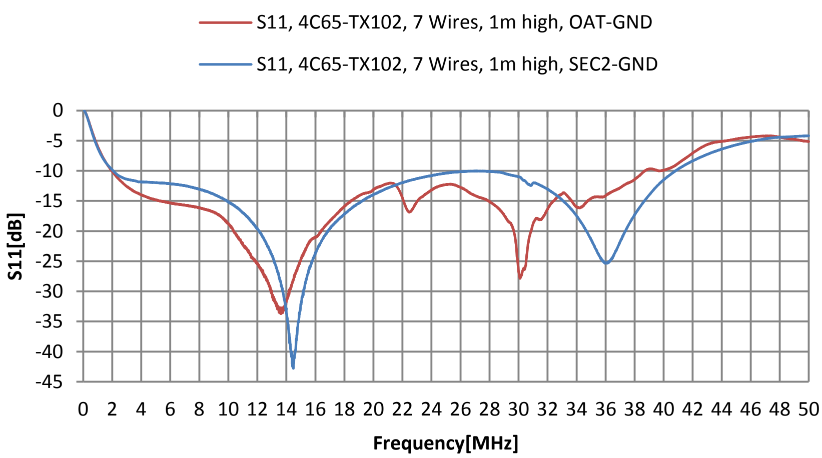

Fig 9.16, Measurements of the 7 wire SLA with a 4C65 core of 102mm diameter

The usage of TLT's on Type 68 cores in combination with the SLA in the configuration as measured and plotted in Fig 9.17 provides a usable S11 -10 dB bandwidth between 6 and 17 MHz and between 34 and 40 MHz.

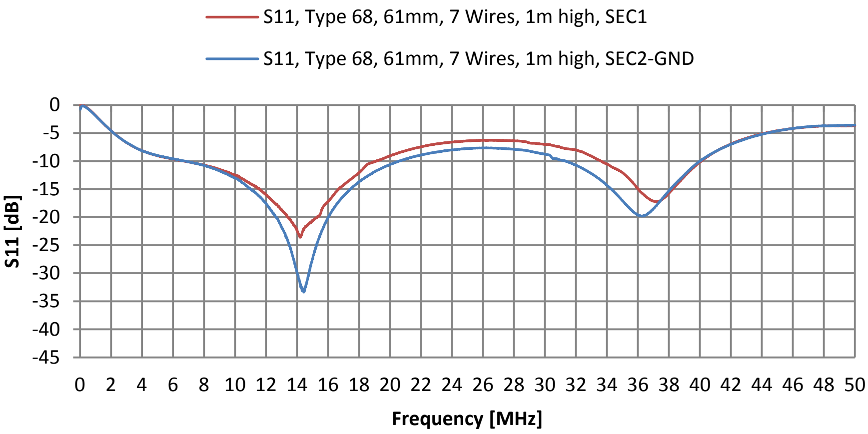

Fig 9.17, Measurements of the 7 wire SLA with a Type 68 TLT

9.3.1 Field strength testing

Measuring the strength of the electric field was done in two different ways.
The first measurements were done by feeding 30 dBm (1W) to the SLA at different frequencies with an R&S SMB 100 signal generator. Measurements were done at 7 different positions at a height of 55cm and 5cm. These positions are shown in Fig 9.20 were the height of 55 cm is shown in Fig 9.18 and 5cm high in Fig 9.19. The reason for these measurements was to see if the field strength was uniform at different frequencies under the wire SLA.

Fig 9.18, Measurement at 55cm high

Fig 9.19, Measurment at 5 cm high

The measurement points for the first measurement with heights of 55cm and 5cm were defined as can be seen in Fig 9.20.

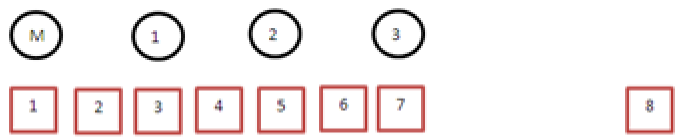

Fig 9.20, Measurement positions under the SLA and at 60 cm from the SLA

The positions were chosen such that the M is the center wire of the 7 wire SLA and the wires 1, 2 and 3 are the companioning wires on one side of the SLA.
Position nr 8 was chosen at 60 cm from the SLA to see what the field strength there would be.

The field strength as a function of the positions 1-7 under the SLA at a height of 55 cm is shown in Fig 9.21. It is clearly visible in Fig 9.21 that the field strength for each position almost the same and that the field strength only changes by using different frequencies.

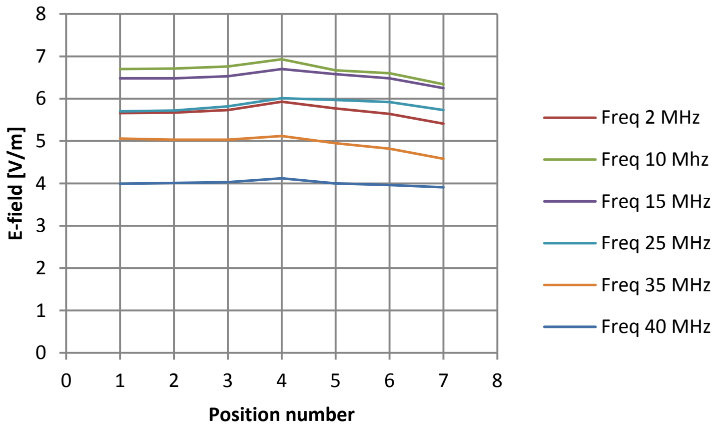

Fig 9.21, E-field strength at a height of 55cm

The field strength measurements at a height of 5cm as a function of the positions 1-7 have been plotted in Fig 9.22. The result from Fig 9.22 shows that the field strength decreases slightly with the change of position to the edge of the SLA.

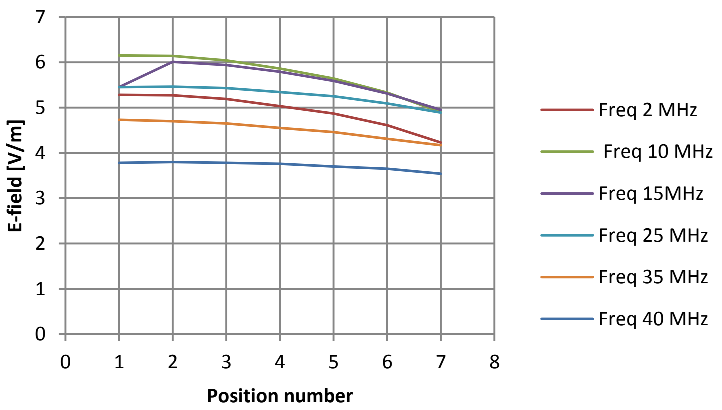

Fig 9.22, E-field strength at a height of 5cm

The second measurement was done by feeding the SLA with 200W and measuring the field strength at one location under the center of the SLA which is the same position as shown in Fig 9.19.

The field strength at a height of 5cm above the ground was measured when powered with 100W and 200W from an amplifier.

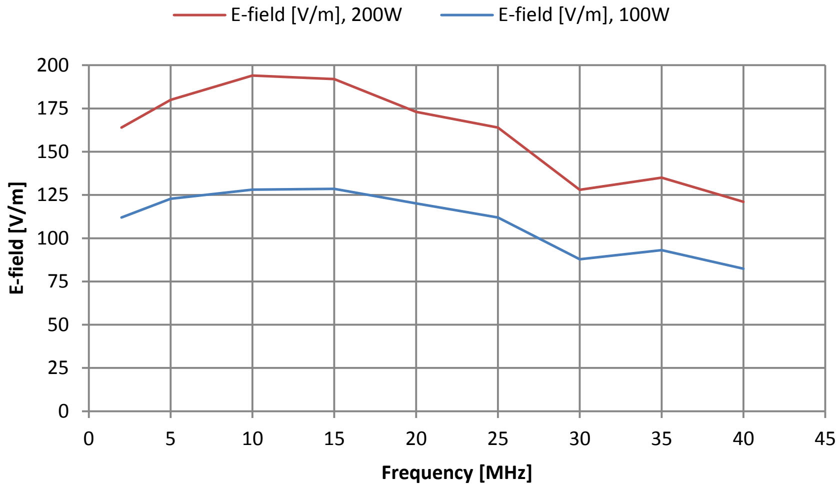

Fig 9.23, The field strength for a 1m high, 1m60 wide wire SLA

The average strength of the electric field is 109 V/m for the 100W input and 161 V/m for the 200W input.

As can be seen from fig 9.10, 9.11 and 9.13 the electric field strength does change with frequency but for each frequency the strength of the electric field remains relative stable under the whole SLA.

One strange effect of these wire SLA is that the electric field strength is exceeding the electric field strength which was expected based on formula 3.4 for all frequencies between 2 and 25 MHz.
The expected electric field strength is 141V/m as can be seen in equations 9.2 and 9.3, where the electric field strength between 2 and 25 MHz exceeds 150 V/m in Fig 9.23.

$$E = \frac{\sqrt{100 \cdot 200}}{1} \tag{9.2}$$

$$E = 141\, V/m \tag{9.3}$$

9.3.2 Wire SLA defects

When measuring one of the first constructed 60cm high SLA's with 15 wires, a disturbing defect was noticed when measuring the SLA with a VNA.
The SLA with a loose wire gave a clearly visble resonance peak at a frequency around 27 MHz regarless of location on a table or in SEC2 with a groundplane.

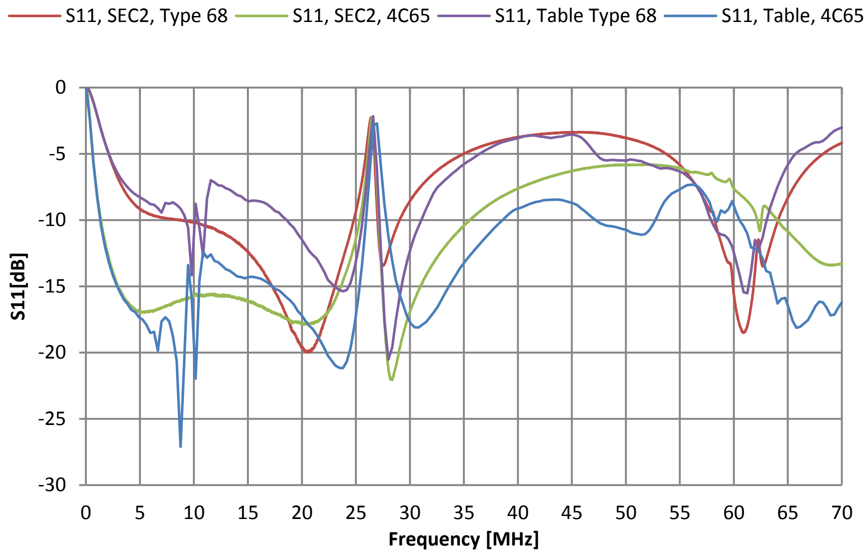

Fig 9.24, First wire SLA measurements, one wire was loose

In order to investigate the problem the S11 graphs from the unun with a 100Ω resistor and the FEKO simulation were plotted to see if there was any overlap with the defect.

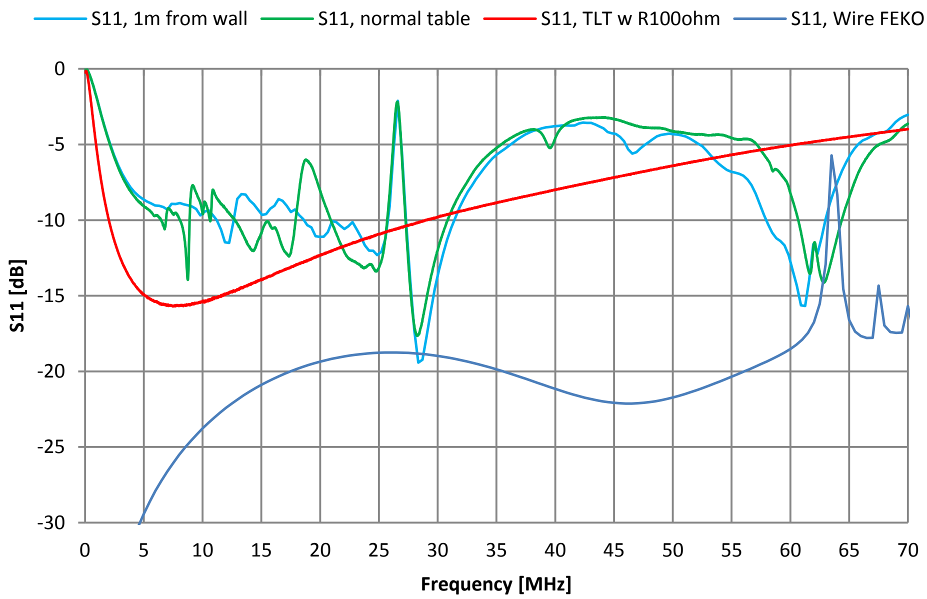

Fig 9.25, Multiple plots concerning S11 for the wire SLA

As can be seen in fig 9.15 neither the TLT nor the FEKO model of the wire SLA give rise to the strange peak at a frequency of 28 MHz.
Later was found out that there was one wire loose from the feeding side of the SLA.
When this result was found also the option of one wire making contact with the ground plane was tested.
The results from this measurement have been plotted here below and could potentially be useful to find defects in the SLA using a VNA.

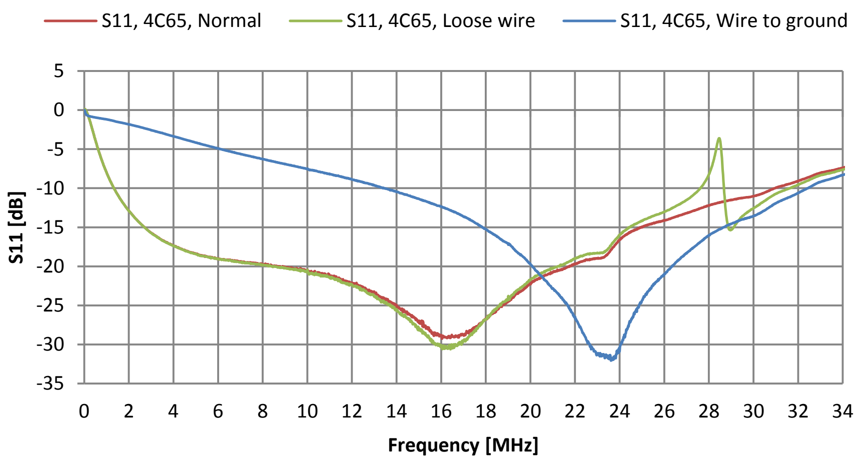

Fig 9.26, S11 for normal, loose wire and grounded SLA measurements

In this chapter the replacement of plates of foil in SLA's has been tested. Computational models in FEKO with infinite and limited ground planes have been tested. These results show that it might be possible to build an SLA of 3.0m high with an impedance of either 100Ω with a width of 4.85m using17 wires or an impedance of 200Ω with a width of 0.86m using 5 wires. The replacement of plates with wires yield a usable S11which is lower than or equal to -10 dB for a frequency range up to 40 MHz when a unun with 4C65 core material is used in combination with a 7 wire SLA at a height of 1.0m. Defects such as wire being loose or making contact with the ground plane have been documented as such.

Conclusions and recommendations

Conclusions

A stripline antenna (SLA) which can test equipment of 2.0m high has not been tested. The question if equipment of 2.0m high can be tested with and electric field of 200 V/m with a 2.5 kW amplifier cannot be answered at this moment.

From the equations in chapter 3 and Table 3.2 it is clear that the impedance of the SLA must be changed from the standard impedance of 50Ω to 100 Ω or 200 Ω to create an SLA that is able to generate an electric field strength of 200 V/m, that that fits in the semi anechoic chamber (SEC1) which is used at Thales in Hengelo, and can generate this 200 V/m field using a 2.5 kW amplifier.

By using computational electromagnetics (CEM) software packages SLA's have been simulated to test the equations from chapter 3. The software package FEKO which uses the Method of Moments is faster and less memory intensive than HFSS which uses the finite element method. By building SLA models using aluminium foil for an impedance of 50Ω the equations from chapter 3 and the CEM simulations were tested and have shown that it is possible to build a small 50Ω SLA. A model with a height of 20cm and a width of 97cm made of aluminium foil has a maximum usable frequency around 50 MHz.

The construction of ununs for impedance transformation from 50Ω to 200Ω and from 50Ω to 100Ω have shown that it is possible to change the input impedance within the required frequency range of 2 MHz to 30 MHz. The the electric field strength for the 200Ω SLA was only 125 V/m,which is only 62.4% of what was expected. This might be due to the fact that the 200Ω SLA was only 16cm wide and that the measurements were done with a measurement head with a width of 10cm.

Tests for the power handling capabilities have also shown that the ununs with small ferrite cores are the bottleneck in terms of power handling by warming up to more than 60°C from a room temperature of 24°C with the use of only 200W input power.

Tests with 53 dBm (200W) of power have shown an uniform electric field strength of more than 150V/m for use with a 1.0m high and 1.60m wide wire based SLA.

Recommendations

If possible testing the 4C65 cores with an outer diameter of 102mm from Ferroxcube and the ferrite Type 68 cores from Fair Rite with a diameter of 61mm is recommended to see how much power these cores can handle when being used as ununs before heating up to temperatures of that approach the Curie temperature which could disable the ferrites.

Construction of wire SLA's with a height of 3.0m and impedances both 100Ω with 17 wires and 200Ω with 5 wires can be undertaken when the ununs can handle ≥2.0 kW.
The 100Ω wire SLA might give a field strength up to 160V/m.

References

[1] US DoD, "RS103," in *DEPARTMENT OF DEFENSE INTERFACE STANDARD REQUIREMENTS FOR THE CONTROL OF ELECTROMAGNETIC INTERFERENCE CHARACTERISTICS OF SUBSYSTEMS AND EQUIPMENT*, MIL-STD-461F, Ed. U.S.A, 2007, ch. 5.20, pp. 127-142.

[2] IEC technical committee 77, Electromagnetic compatibility (EMC) – Part 4-3: Testing and measurement techniques – Radiated, radio-frequency, electromagnetic field immunity test, 2010, IEC 61000-4-3.

[3] D.M. Pozar, "Microwave Engineering second editon," in *Microwave Engineering second editon*, Charity Robey, Ed. New York, United States of America: John Wiley & Sons, 1998, ch. 3.8, p. 716.

[4] M.L. Crawford, "Generation of Standard EM Fields Using TEM Transmission Cells," *IEEE Trans. Electromagn. Compat.*, vol. EMC-16, no. 4, pp. 189-195, November 1974.

[5] R. De Leo, T. Rozzi, C. Svara, and L. Zappelli, "Rigorous Analysis of the GTEM Cell," *IEEE Trans. Electromagn. Compat.*, vol. 39, no. 3, pp. 488-500, March 1991.

[6] Angela Nothofer, Didier Bozec, Andy Marvin, Martin Alexander, and Les McCormack. (2003, January) Measurement Good Practice Guide No. 65, The Use of GTEM Cells for EMC Measurements. [Online]. http://www.yorkemc.co.uk/info/technical/papers/YorkEMC-NPL_gtem-good-practice.pdf

[7] A.J. Walters and C. Leat, "Control of the TE111 Resonance in an Asymmetric TEM Cell," *IEEE Trans. Electromagn. Compat.*, vol. 50, no. 2, pp. 431-434, May 2008.

[8] A.J. Walters and C. Leat, "Assessment of TEM cells for whole aircraft EMV testing," Defense Science and Technology Organisation, Research Report DSTO-RR-0149, 2007.

[9] J.J. Polonis, W.E. Cory, I. Jr. Martinez, D.A. Smith, and H.H. Walker, "Tri-plate test fixture," in *IEEE International Symposium on Electromagnetic Compatibility*, an Antonio TX, 1998, pp. 153-158.

[10] A. Gunsaya, T. Golds, P.J. Page, M.J. Bosley, and J.F. Dawson, "Analysis of Tri-Plate Line, SAE J1113-25, using CAE tools," in *IEEE International Symposium on Electromagnetic Compatibility*, Montreal Que., 2001, pp. 626-631.

[11] Huadong Li, "The field distribution of a tri-plate and its influence on immunity test," in *InternationalSymposium on Electromagnetic Compatibility*, Springboro OH, 2004, pp. 85-88.

[12] S. Satav and V. Agarwal, "Do it Yourself Fabrication of an Open TEM Cell For EMC Pre-compliance," *IEEE EMC Society Newsletter*, no. 218, pp. 66-71, Summer 2008.

[13] R. Schinzinger and P.A.A. Laura, *Conformal mapping: methods and applications*. Amsterdam, The Netherlands: Elsevier, 1991.

[14] Sourceforge.net. (2011, June) Microstrip Line Calculator. [Online]. http://mcalc.sourceforge.net/mstrip.gif

[15] B. E. Roseberry and R. B. Schulz, "A Parallel-Strip Line for Testing RF Susceptibility," *IEEE Trans. Electromagn. Compat.*, vol. 7, no. 2, pp. 142-150, June 1965.

[16] W. Bittinger, "Properties of open strip lines for EMC measurements," in *IEEE International Symposium on Electromagnetic Compatibility*, Dallas TX, 1993, pp. 120-125.

[17] Yeon-Choon Chung, Tae-Won Kang, and Dong-Chul Park, "Design and construction of stripline for measuring electromagnetic immunity of vehicular electrical cables," in *1997 International Symposium on Electromagnetic Compatibility Proceedings*, Beijing, 1997, pp. 9-12.

[18] Yang Zhengguang, Su Donglin, and Lv Shanwei, "Analysis of characteristic impedance of strip double line," in *IEEE International Symposium on Microwave, Antenna, Propagation and EMC Technologies for Wireless Communications*, Beijing, 2005, pp. 95-98.

[19] Wen Lie Liang, Chen Mao-Yuan, and Z. Tseng, "Research into the use of Strip-Line Cell for EMI test for automobile electronics," in *2010 Asia-Pacific Symposium on Electromagnetic Compatibility (APEMC)*, Beijing, 2010, pp. 247-250.

[20] Sub Committee SC 3 "Electrical and electronic equipment" Technical Committee ISO /TC 22 "Road Vehicles", *ISO 11452-5:1995 Road vehicles - Component test methods for electrical disturbances by narrowband radiated electromagnetic energy*.: International Standardization Organisation, 1995.

[21] H.A. Wheeler, "Transmission-Line Properties of Parallel Wide Strips by a Conformal-Mapping Approximation," *IEEE Transactions on Microwave Theory and Techniques*, vol. 12, no. 3, pp. 280-289, May 1964.

[22] G Guanella, "Novel Matching Systems for High Frequencies," *Brown-Boveri Review*, vol. 31, pp. 327-329, Sep 1944.

[23] C.L. Ruthroff, "Some Broad-Band Transformers," *Proc IRE*, vol. 47, pp. 1337-1342, Aug 1959.

[24] Jerry Sevick, *Transmission Line Transformers*, 4th ed. United States of America: Noble Publishing Corporation, 2001.

[25] Pablo Gómez-Jiménez, Pablo Otero, and Enrique Márquez-Sagura, "Analysis and Design Procedure of Transmission-Line Transformers," *IEEE MTT*, vol. 56, no. 1, pp. 163-171, Jan 2008.

[26] Kurt Andress, L.B. Cebik, Rudy Severns, and Frank Witt, "Coupling the Line to the Antenna," in *The ARRL Antenna Book*, R. Dean Straw, Ed. Newington, United States of America: ARRL The National association for amateur radio, 2000, ch. 25, pp. 26-15, 26-16.

[27] Bob van Donselaar. (2011, April) Ferriet, achtergronden en materiaal eigenschappen. [Online]. http://sharon.esrac.ele.tue.nl/~on9cvd/Achtergronden%20en%20materiaal%20eigenschappen.htm

[28] Bob van Donselaar. (2011, April) Transmissielijn trafo's inleidng en achtergrond. [Online]. http://sharon.esrac.ele.tue.nl/~on9cvd/Transmissielijn%20trafo,%20inleiding%20en%20achtergrond.htm

[29] Ferroxcube. (2009) Ferroxcube Data Handbook 2009. PDF Document.

[30] Fair-Rite Products Corp. (2010) Ferrite Components for the Electronics Industry Rev 10. pdf document.

[31] Gordon West, "LDG AT-1000 Pro Automatic Antenna Tuner," *CQ Magazine*, vol. 64, no. 11, pp. 32-34, November 2008, LDG AT-1000 Pro Automatic

Antenna Tuner.

[32] SGC. (2011, Aug.) SGC 235 Smartuner. [Online]. http://www.sgcworld.com/Publications/Brochures/SmartunerSpecChart.pdf

[33] MFJ Enterprises Inc. (2011, August) MFJ-998RT REMOTE AUTO TUNER, 1.5KW, 1.8-30 MHZ. [Online]. http://www.mfjenterprises.com/Product.php?productid=MFJ-998RT

[34] William R. Smythe, *Static and dynamic electricity*, 3rd ed. New York, United States of America: McGraw-Hill, 1968.

[35] David B. Davidson, *Computational Electromagnetics for RF and Microwave Engineering*. Cambridge, UK: Cambridge University Press, 2005.

[36] Pasternack Enterprises Inc. (2011, April) RG219U.pdf. [Online]. http://www.pasternack.com/Pdf/RG219U.pdf

[37] Heinz-Dietrich Brüns, Christian Schuster, and Herman Singer, "Numerical Electromagnetic Analysis for EMC Problems," *IEEE Trans. Electromagn. Compat.*, vol. 49, no. 2, pp. 253-262, May 2007.

[38] EMSS S.A. (2011, February) FEKO - EM Simulation software. [Online]. http://www.feko.info

[39] E.L. Bock, "Test Fixtures for RF Susceptibility Testing," *IEEE Trans. Electromagn. Compat.*, vol. EMC-15, no. 4, pp. 201-202, November 1973.

[40] Frank van Dam, , 2011, Private communications with Thales employees.

[41] M. Ehrenfried. (2011, May) The design of broadband voltage transformers. [Online]. http://g8jnj.webs.com/Balun%20construction.pdf

[42] Micrometals, Inc. (2011, May) Iron Powder Cores, Material Characteristics. [Online]. http://www.micrometals.com/materialchart.html#resonant

[43] Amidon, Inc. (2011, May) Power considerations (Iron Powder and Ferrite). [Online]. https://www.amidoncorp.com/specs/1-35.PDF

[44] Amidon, Inc. (2011, May) Power considerations (cont'). [Online]. https://www.amidoncorp.com/specs/1-36.PDF

[45] Ferroxcube. (2011, Nov.) Gluing ferrite parts. [Online]. http://www.ferroxcube.com/appl/info/gluing.pdf

[46] Carl Baum. (1966, June) Impedances and Field Distributions for Parallel Plate Transmission Line Simulators. PDF. [Online]. http://www.ece.unm.edu/summa/notes/note21.pdf

Appendices

Appendices are on the CD-ROM

A. **New method of impedance matching in radio-frequency circuits – G. Guanella**

B. **Würth Elektronik 7427015 core data sheet**

C. **Ferroxcube 4C65 core documentation for core sizes TX36 and TX102.**

D. **Fair rite type 68 material documentation**

E. **FEKO models for plate stripline antennas**

F. **FEKO models for wire stripline antennas**